

Title of thesis

Characterization of Physicochemical Properties and Process Design for Oil Removal Using <i>Ceiba pentandra</i> (L.) Gaertn. as a Natural Sorbent
--

I, ANISA UR RAHMAH

hereby allow my thesis to be placed at the Information Resource Center (IRC) of University Teknologi PETRONAS (UTP) with the following conditions:

1. The thesis becomes the property of UTP
2. The IRC of UTP may make copies of the thesis for academic purposes only.
3. This thesis is classified as

☐

Confidential

☒

Non-confidential

If this thesis is confidential, please state the reason:

The contents of the thesis will remain confidential for _____ years.

Remarks on disclosure:

Endorsed by

Anisa Ur Rahmah

AP. Dr. Mohd. Azmuddin Abdullah

Signature of Author

Signature of Supervisor

Asy-Syariefiyah, Kp. Ragadiem, RT.04/01

Desa Cinta, Karangtengah

Garut, Jawa Barat, Indonesia

Date: _____

Date: _____

UNIVERSITI TEKNOLOGI PETRONAS

Approval by Supervisors

The undersigned certify that have read, and recommend to The postgraduate Studies Programme for acceptance, a thesis entitled **“Characterization of Physicochemical Properties and Process Design for Oil Removal Using *Ceiba pentandra* (L.) Gaertn. as a Natural Sorbent”** submitted by **Anisa Ur Rahmah** for the fulfillment of the requirements for the DEGREE OF MASTER OF SCIENCE IN CHEMICAL ENGINEERING.

May, 2009

Signature: _____

Main Supervisor : AP. Dr. Mohd. Azmuddin Abdullah_____

Signature: _____

Co- Supervisor : AP. Dr. Zakaria Man_____

UNIVERSITI TEKNOLOGI PETRONAS

**Characterization of Physicochemical Properties and Process Design for Oil
Removal using *Ceiba pentandra* (L.) Gaertn. as a Natural Sorbent**

By

Anisa Ur Rahmah

A THESIS

SUBMITTED TO THE POSTGRADUATE STUDIES PROGRAMME AS A
REQUIREMENT FOR THE DEGREE OF MASTER OF SCIENCE IN
CHEMICAL ENGINEERING

Universiti Teknologi PETRONAS

May

2009

ACKNOWLEDGEMENT

First and foremost, I would like to give my sincere thanks to Allah S.W.T, the almighty god, the source of my life and hope for giving me the strength and wisdom to complete this thesis. Not to mention, many beautiful things that colored the life of my master program.

I am most grateful to my supervisors Assoc. Prof. Dr. Mohd. Azmuddin Abdullah and Assoc. Prof. Dr. Zakaria Man their guidance, inputs and encouragement during my master program. Their patience and encouragement has steered me to the right direction for many times

I would like to express my appreciation to Universiti Teknologi PETRONAS for the STIRF funding. I also would like to thank the technologist of Chemical Engineering Department, especially En. Firdaus, En. Jailani, En. Yussof, En. Fauzi, Azima and Kak Norhasyneeza for their assistance and exceptional cooperation during the laboratory works. And also my sincere appreciation to Chemical Engineering Department staffs headed by Dr. Shuhami Mahadzir for their constant support during my master study.

Special thanks to postgraduate office staffs, Pn. Norma , Pn. Kamaliah, and En. Fadhil and En. Kahar for their assistance during my study. My warmest thank to my postgraduate friends for their encouragement and friendship. At last and most important, I would like to thank my husband and family for their love, encouragement, and endless support which always being supply of strength in my life.

ABSTRACT

Ceiba pentandra (L.) Gaertn (Kapok) is a natural sorbent that exhibits excellent hydrophobic-oleophilic characteristics. The physicochemical properties of kapok fibre as oil sorbent were characterized. The effect of packing density and the experimental oil types on the oil sorption characteristics of kapok were studied in a batch system. Oil sorption capacity, percentage of dynamic oil retention, oil entrapment stability, packing height reduction, saturation time and kapok reusability were evaluated. Continuous packed-bed column was developed to examine the optimum conditions, in terms of flow rates and packing density for the diesel-water filtration. Chloroform and alkali treatment were employed to investigate the stability of hollow structure and waxy layer on the kapok surface and their roles in oil sorption.

Based on SEM, OM and FTIR analyses, kapok fibre was shown to be a lignocellulosic material with hydrophobic waxy coating that covered the hollow structures. The waxy coatings enhance the oil penetration inside the kapok structure and the presence of the hollow structure provide ample interstitial network for oil entrapment. Higher packing density showed lower sorption capacity, but higher percentage of dynamic oil retention, with 1% of oil drained out from the test cell at 0.08 g/cm^3 . The percentage of dynamic oil retention was in the decreasing order of: used engine oil, new engine oil and Diesel. At higher packing density and higher oil viscosities, kapok exhibited higher saturation but lower bed height reduction. Using diesel oil as the experimental liquid, only 30% of oil sorption capacity reduction was observed even after fifteen cycles of reuse at 0.04 g/cm^3 packing density. Oil entrapment inside the packing was stable even after 30 min of shaking inside a horizontal shaker, with more than 90% of diesel and used-engine oil retained inside the assembly of 0.08 g/cm^3 kapok.

A packed-bed column was constructed to study the performance of kapok filter for oily water filtration. Statistical analyses suggest that none of the factors significantly affected the percentage of COD reduction, but the interaction between packing density and flow rate significantly affected the percentage of turbidity reduction. However, about 99% COD reductions were observed for all kapok filters at

different packing densities and flow rate. About 97% turbidity reduction was observed for kapok at 0.08 g/cm^3 and 0.5 L/h flow rate. The excellent turbidity reduction could be due to the stronger interaction of kapok with oil which can break down oil-water emulsion.

After 8 hours of chloroform and alkali treatment, kapok fibres had lower oil sorption capacity, with 2.1 % and 26.3 % reduction, as compared to the raw kapok. SEM image analyses, in comparison to untreated kapok, showed no major structural difference after chloroform treatment, but major structural disruption to flattened-like structure was observed with alkali treatment. These results imply that kapok fibre had stable hollow structure and wax layer attachment on the kapok surface, and it takes extreme conditions as that employed with alkali treatment to make any significant changes. Based on these, the Malaysian kapok indeed has shown great potential as oil sorbent, in terms of high sorption and retention capacity, structural stability, high reusability and high COD and turbidity reduction capability.

Keywords: Kapok, hydrophobicity-oleophilicity, oil sorption, retention capacity, structural stability, reusability, COD, turbidity.

ABSTRAK

Ceiba pentandra (L.) Gaertn (Kapok) merupakan bahan penyerap semula jadi yang menunjukkan sifat hidrofobik-oleofilik yang baik sekali. Sifat fisik-kimia serabut kapok selaku penyerap minyak dicirikan. Kesan ketumpatan pemadatan dan jenis minyak uji pada sifat serapan minyak oleh kapok dipelajari dalam sistem sesekumpul. Muatan resapan minyak, peratusan penyimpanan minyak dinamik, kestabilan minyak terperangkap, pengurangan ketinggian pematat, masa perepuan, dan kemampuan diguna kembali merupakan pembolehubah yang dinilai. Turas *packed-bed* berkesinambungan dibina untuk menyelidiki keadaan terbaik, dalam batasan kadar aliran dan ketumpatan pemadatan untuk penyaringan diesel-air. Pengolahan kloroform dan garam alkali digunakan untuk menyelidiki kestabilan struktur berlubang dan penempelan lilin permukaan kapok.

Berdasarkan analisis SEM, OM, dan FTIR, serabut kapok merupakan satu bahan lignoselulos dengan struktur berlubang yang di tutupi pelapisan bersifat lilin. Pelapis lilin ini meningkatkan peresapan minyak dalam struktur kapok dan kehadiran struktur berlubang melengkapkan rangkaian pengisian kekosongan yang lebih luas untuk penahan minyak. Ketumpatan pemadatan yang lebih tinggi menghasilkan serapan yang lebih rendah tetapi dengan peratusan penyimpanan minyak dinamik yang lebih tinggi; sebanyak 1 % minyak dikeringkan dari 0.08 g/cm^3 sel pengujian. Peratusan penyimpanan minyak dinamik memiliki aturan menurun dengan minyak bekas enjin, minyak enjin baru, dan diesel. Pada ketumpatan pemadatan dan kepekatan minyak yang lebih tinggi, kapok mempunyai kerepuan yang lebih tinggi dengan pengurangan ketinggian dasar yang lebih rendah. Menggunakan minyak diesel sebagai cecair uji, hanya 30 % dari kapasiti serapan minyak pada 0.04 g/cm^3 ketumpatan pemadatan yang terceraap, bahkan selepas lima belas pusingan penggunaan kembali. Minyak yang terperangkap dalam pemadatan menjadi stabil selepas 30 minit goncangan dalam satu goncangan melintang, dengan lebih dari 90% diesel dan minyak bekas enjin tersimpan dalam 0.08 g/cm^3 kapok.

Satu kolum *packed-bed* didirikan untuk mempelajari prestasi tapisan kapok untuk menapis campuran air berminyak. Analisa statistik menunjukkan bahawa tiada

unsur yang nyata sekali mempengaruhi peratusan pengurangan COD, tetapi interaksi antara ketumpatan pemadatan dan kadar aliran nyata sekali mempengaruhi peratusan pengurangan kekeruhan. Namun, lebih kurang 99% pengurangan COD dicerap pada semua tapisan kapok, pada ketumpatan pemadatan dan kadar aliran yang berbeza. Lebih kurang 97% pengurangan kekeruhan dicerap pada kerapatan 0.08 g/cm^3 dan 0.5 L/j kadar aliran. Pengurangan kekeruhan yang sangat baik boleh jadi disebabkan interaksi yang lebih kuat antara kapok dan minyak, yang mana dapat mengurangkan emulsi air-minyak.

Selepas 8 jam perlakuan klorofom dan garam alkali, serabut kapok mempunyai serapan kapasiti serapan minyak yang lebih rendah, sebanyak 2.1% dan 26.3% dibandingkan dengan kapok yang tak mendapat perlakuan. Analisis gambar SEM, dibanding dengan kapok yang tak mendapat perlakuan, menunjukkan tiada perbezaan struktur berlubang setelah perlakuan klorofom namun gangguan struktur besar kepada struktur berbentuk pipih dengan perlakuan garam alkali. Keputusan ini bererti bahawa serabut kapok mempunyai struktur berlubang dan penempelan lapisan lilin yang stabil pada permukaan kapok, dan memerlukan keadaan yang ekstrim untuk membuat perubahan. Berdasarkan keputusan ini, serabut kapok sesungguhnya menunjukkan keupayaan besar sebagai penyerap, dalam batasan serapan dan kapasiti menahan minyak yang tinggi, kestabilan struktur, kemampuan digunakan kembali, keupayaan mengurangkan COD serta kekeruhan yang tinggi.

Kata Kunci: Kapok, hidrofobisiti-oleofilisiti, penyerapan minyak, kapasiti penahan minyak, kestabilan struktur, kemampuan diguna-kembali, COD, kekeruhan.

TABLE OF CONTENTS

ACKNOWLEDGEMENT	i
ABSTRACT.....	v
ABSTRAK.....	vii
TABLE OF CONTENTS.....	ix
LIST OF FIGURES	xi
LIST OF TABLES	xiii
ABBREVIATIONS	xiv
CHAPTER ONE: INTRODUCTION	1
CHAPTER TWO: LITERATURE REVIEW	8
2.1 Sorbent Application in Oil Spill Remediation	8
2.2 Characteristics of Oil Sorbent Material	9
2.3 Organic Synthetic Sorbent	11
2.3.1 Polypropylene	11
2.3.2 Polyurethane	13
2.4 Inorganic Mineral Sorbent	15
2.4.1 Expholiated Graphite (EG)	15
2.4.2 Expanded Perlite (EP).....	17
2.4.3 Zeolites.....	17
2.5 Organic Natural Sorbent	19
2.5.1 Peat.....	21
2.5.2 Asclepias syriaca (Milkweed).....	23
2.5.3 Kapok.....	23
2.6 Considerations for Field Application of Sorbent Materials.....	31
2.6.1 The characteristics of oil	31
2.6.2 Selection of sorbent materials	32
2.6.3 Engineering parameters	33
CHAPTER THREE: MATERIAL AND METHOD	35
3.1 Material.....	35
3.1.1 Kapok Raw Materials	35
3.1.2 Chemicals and Experimental Oils	35
3.2 Method	36
3.2.1 Research flowchart.....	36
3.2.2 Characterization of Kapok Physicochemical Properties.....	37
3.2.3 Characterization of Experimental Oils Properties	41
3.2.4 Investigation of Oil Sorption Characteristics of Kapok	43

3.2.5	Evaluation of kapok reusability	47
3.2.6	Evaluation of Kapok Column Process Design Parameters for Oily Water Filtration.....	48
3.2.7	The effect of chloroform and alkali treatment on kapok oil sorption characteristics.....	53
CHAPTER FOUR: CHARACTERIZATION OF THE PHYSICOCHEMICAL PROPERTIES OF CEIBA PENTANDRA (L.) GAERTN. AS OIL SORBENT.....		54
4.1	Characterization of Kapok Properties	54
4.2	Characterization of Experimental Oils Properties	60
4.3	Oil Sorption Experiments	63
4.3.1	Effect of packing density on oil sorption capacity.....	63
4.3.2	Effect of packing density on percentage dynamic of oil retention	67
4.3.3	Effect of packing density on saturation time and bed height drop	70
4.4	Evaluation of Kapok Reusability	73
4.5	Conclusions.....	74
CHAPTER FIVE: EVALUATION OF PACKED-BED COLUMN PROCESS DESIGN FOR OILY WATER FILTRATION.....		76
5.1	Profile of Oily Water Filtration at Different Packing Density and Flow Rate ...	76
5.2	Effect of Packing Density and Flow Rate on Chemical Oxygen Demand and Turbidity	80
5.3	Factorial Experimental Design and Statistical Analyses	88
5.4	Conclusions.....	90
CHAPTER SIX: CHLOROFORM AND ALKALI TREATMENT OF KAPOK		91
6.1	Comparison between Chloroform and Alkali Treatment on Chemical Constituent and Kapok Microstructure	92
6.1.1	Infrared spectra	92
6.1.2	Kapok microstructures and morphology.....	98
6.2	Comparison between Chloroform and Alkali Treatment on Oil Sorption Characteristics.....	98
6.2.1	Oil sorption capacity	98
6.2.2	Percentage of dynamic oil retention	101
6.3	Conclusions.....	103
CHAPTER SEVEN: CONCLUSIONS		104
7.1	Conclusions.....	104
7.2	Recommendations.....	105
REFERENCES		107

LIST OF FIGURES

Figure 1.1	Statistics of oil contamination in the seas worldwide [1]	2
Figure 2.1	SEM imaging of PP sorbent (a) stitch-bonded, (b) needle-punched 1 and (c) needle-punched 2 [45]	12
Figure 2.2	Image of polypropylene fiber by using SEM for (a) before [8] and ESEM for (b) after oil sorption [14]	12
Figure 2.3	OM image of PU foam with isocyanate to polyol molar ratio of (a) 0.6, (b) 0.7, (c) 0.8 and (d) 0.9 [47]	14
Figure 2.4	Morphology of worm-like particles with an exfoliating volume (a) before and (b) after kerosene sorption [49]	16
Figure 2.5	Expanded perlite, A_0 (a) before and (b) after oil sorption [32]	16
Figure 2.6	Scheme of plant cuticle layer [52]	20
Figure 2.7	Photomicrographs of microtome section of (a) <i>Sphagnum</i> -peat from Maine and (b) <i>Taxodium</i> - Okefenokee Swamp-peat from Georgia [54]	22
Figure 2.8	ESEM imaging of milkweed fiber [14]	22
Figure 2.9	Image of (a) kapok tree, (b) kapok leaf, (c) immature and (d) mature pod	25
Figure 2.10	Milkweed (MW) and cotton (COT) sorption properties after extraction and alkali scouring (\square : oil and \blacksquare : water) [59]	29
Figure 3.1	Research flowchart	36
Figure 3.2	Instrument for SEM analyses (a) Microscope and electron gun part (b) Sputter coater part	38
Figure 3.3	Instrument for (a) OM imaging and (b) Density measurement	38
Figure 3.4	Surface area analyzer	39
Figure 3.5	Instrument for FTIR analyses	39
Figure 3.6	Inter-Face Tension, IFT 700	41
Figure 3.7	Instrument for measurements of experimental oils (a) density and (b) viscosity	42
Figure 3.8	Cannon-Fenske Routine Viscometer	42
Figure 3.9	Experimental design for oil sorption and dynamic oil retention capacity	44
Figure 3.10	Experimental setup for investigating the effect of packing density on saturation time and bed height difference	45
Figure 3.11	Experimental design to test kapok reusability for sorption process	46
Figure 3.12	Experimental setup to test kapok reusability for desorption process	47
Figure 3.13	Experimental setup for oily water filtration of kapok	49
Figure 3.14	COD Thermoreactor DRB 200	51
Figure 3.15	Spectrophotometer HACH DR 5000 for COD absorbance measurement	51
Figure 3.16	Instrument for turbidity analyses (a) Turbidimeter 2100P, (b) cuvet	52
Figure 4.1	Infrared spectrum of raw kapok	57
Figure 4.2	SEM images of (a) single and (b) cluster of kapok fiber	58
Figure 4.3	Optical microscope image of kapok before oil sorption	58
Figure 4.4	Sensile drops technique for contact angle determination (a) high and (b) low contact angle value with r: droplet radius, θ : contact angle	61
Figure 4.5	Physical appearance of kapok (a) before and (b) after sorption	62
Figure 4.6	Image of kapok after oil sorption by using (a) OM and (b) SEM	62

Figure 4.7	Effect s of packing density on the amount of sorbed oil inside kapok assembly as expressed in (a) mass and (b) volume.....	66
Figure 4.8	Percentage of dynamic oil retention of (a) diesel oil, (b) new engine oil,	69
Figure 4.9	The percentage of oil released after applying sorbed kapok in a horizontal shaker at 150 rpm.....	71
Figure 4.10	Effect of packing density to saturation time	71
Figure 4.11	Oil sorption characteristics of kapok fibre after fifteen cycles (a) oil sorption capacity reduction, (b) packing height drop and (c) saturation time during fifteen sorption-desorption cycles	72
Figure 5.1	Liquid front movements at 0.08 g/cm ³ packing density and 0.5 L/h flow rate of oily water filtration	78
Figure 5.2	Liquid front movements of kapok filter at (a) 0.5 L/h, (b) 1.0 L/h, (c) 1.5 L/h flow rate and (d) 0.04 g/cm ³ , (e) 0.06 g/cm ³ , (f) 0.08 g/cm ³ packing density	79
Figure 5.3	COD vials color (a) before sample addition, (b) high organic content and (c) low organic content level.....	81
Figure 5.4	Effluent (a) before and (b) after filtration	81
Figure 5.5	Pareto charts for standardized effects of (a) COD and (b) COD reduction	84
Figure 5.6	Pareto charts for standardized effects of (a) turbidity and (b) turbidity reduction	85
Figure 5.7	Response surface contour plot with packing density and flow rate as independent variables for (a) COD and (b) COD reduction	86
Figure 5.8	Response surface contour plot with packing density and flow rate as independent variables for (a) turbidity and (b) turbidity reduction	87
Figure 6.1	FTIR spectrum of kapok (a) before, (b) after 4 hours, and (c) 8 hours of chloroform treatment	94
Figure 6.2	FTIR spectra of kapok (a) before, after (b) 4 hours and (c) 8 hours of alkali treatment.....	95
Figure 6.3	SEM image of (a) untreated and (b) chloroform-treated and (c) alkali-treated kapok	96
Figure 6.4	Kapok appearance (a) before and after (b) 4 hours and (c) 8 hours chloroform treatment, (d) 4 hours and (e) 8 hours alkali treatment.....	97
Figure 6.5	Typical structure of (a) untreated and (b) alkalinized cellulosic fiber.....	100
Figure 6.6	Oil retention profile kapok after (a) chloroform and (b) alkali treatment	102

LIST OF TABLES

Table 1.1	Major oil spill incident [1]	1
Table 1.2	Filtration methods for oily water separation [12]	4
Table 1.3	Regulations of water quality standard [10, 11]	4
Table 1.4	Commercially available synthetic and biosorbent for oil removal [24] ..	6
Table 2.1	Sorption Capacities of Sorbents	10
Table 2.2	Physical properties of raw kapok fibre [8]	24
Table 2.3	Chemical characteristics of kapok fibre [6]	27
Table 2.4	Alkaline nitrobenzene products of kapok cell walls [6]	27
Table 3.1	Experimental design for oily water filtration experiment	49
Table 4.1	Assignment of infrared absorption bands	56
Table 4.2	The physical properties of experimental oil	60
Table 4.3	The surface characteristics of kapok	60
Table 4.4	Oil sorption capacities of kapok at various packing densities for different experimental oils	65
Table 4.5	Void fraction of kapok at various packing densities	65
Table 5.1	COD value of effluent at different flow rate and packing density	82
Table 5.2	Turbidity value of effluent at different flow rate and packing density ...	82
Table 5.3	List of R^2 and polynomial equation for COD, COD reduction, turbidity and turbidity reduction	83
Table 6.1	Oil sorption capacity of chloroform and alkali-treated kapok at 0.04 g/cm ³ packing density	100

ABBREVIATIONS

COD	Chemical Oxygen Demand
EG	Expholiated Graphite
EP	Expanded Perlite
ESEM	Environmental Scanning Electron Microscopy
FTIR	Fourrier Transformed Infrared Spectroscopy
OM	Optical Microscopy
NTU	Nephelometric Turbidity Unit
PP	Polypropylene
PU	Polyurethane
SEM	Scanning Electron Microscopy

CHAPTER ONE

INTRODUCTION

Approximately 10 million tons of petroleum products and derivatives are used daily worldwide [1]. This means that the world environment is facing great risk of contamination from petroleum products especially during transportation, transfer and storage. Between 1974-1994, there are 175 major oil spills worldwide (Table 1.1). The exact number should actually be higher [1]. With the cost as high as \$20-200 per litre in USA and Canada just to cleanup the contaminated site, depending on the location and type of oil spilled, the whole strategies must be worked out to reduce social, economic and environmental impact from oil spills. Oil spills at sea may lead to the contamination of the water supply of the coastal zones and also the oily wastewaters form various industries [2].

Table 1.1 Major oil spill incident [1]

No.	Year	Month/Day	Ship/Incident	Country	Location	Tons (x10 ³)
1	1991	Jan 26	Gulf war	Kuwait	Sea Island	800
2	1979	Jun 5	IX TOC blown out	Mexico	Gulf of Mexico	470
3	1979	Jul 19	Atlantic Empress/Aegean Captain	Off Tobago	Caribbean Sea	300
4	1992	Mar 2	Oil well blown out	Uzbekistan	Fergana Valley	300
5	1993	Feb 4	Oil platform blown out	Iran	Nowruz Field	270
6	1983	Aug 6	Castillo de Beliver	South Africa	Saldanha Bay	260
7	1978	Mar 16	Amoco Cadiz	France	Brittany	235
8	1988	Nov 10	Odyssey	Off Canada	North Atlantic	145
9	1991	Apr 11	Haven	Italy	Genoa	140
10	1980	Aug 11	Oil well blown out	Libya	Inland	140
11	1967	Mar 18	Torrey Canyon	England	Land's End	130
12	1972	Dec 19	Sea Star	Oman	Gulf of Oman	125
13	1980	Feb 23	Irene's Serenade	Greece	Pylos	120
14	1981	Aug 20	Storgae tanks	Kuwait	Shuaybah	110
15	1971	Dec 7	Texaco Denmark	Belgium	North Sea	107

In terms of sources of oils contamination at sea, 50% of comes from the municipal/land and 26% from transportation and offshore production and exploration (Figure 1.1). Natural sources which contribute 11% of the total oil contaminant come from the many natural leakage or discharge from oil-bearing strata on the ocean floor. Another 13% is from re-precipitation of the polluted air into the land and ends up in the sea contributing until 13% [1]. While heavy hydrocarbons may result from lubricating of machinery, or leaking and spilling of crude oil transportation, light hydrocarbons and solvents are contaminants from industrial wastes from degreasing or extraction, cleaning, painting and coating operations. As shown in Figure 1.1, the oil spill accidents from the tankers only contribute less than 5% of the total oil pollution entering the sea. In actual fact, 50% of oil spilled into the sea actually comes from the oil and fuel runoff from the land-based sources, usually wastewater that is discharged directly into the sea [1]. Hence, the solution must not only look at the possibility of leakage from the tanker itself, but also more importantly how to prevent the oil from polluting the sea-front.

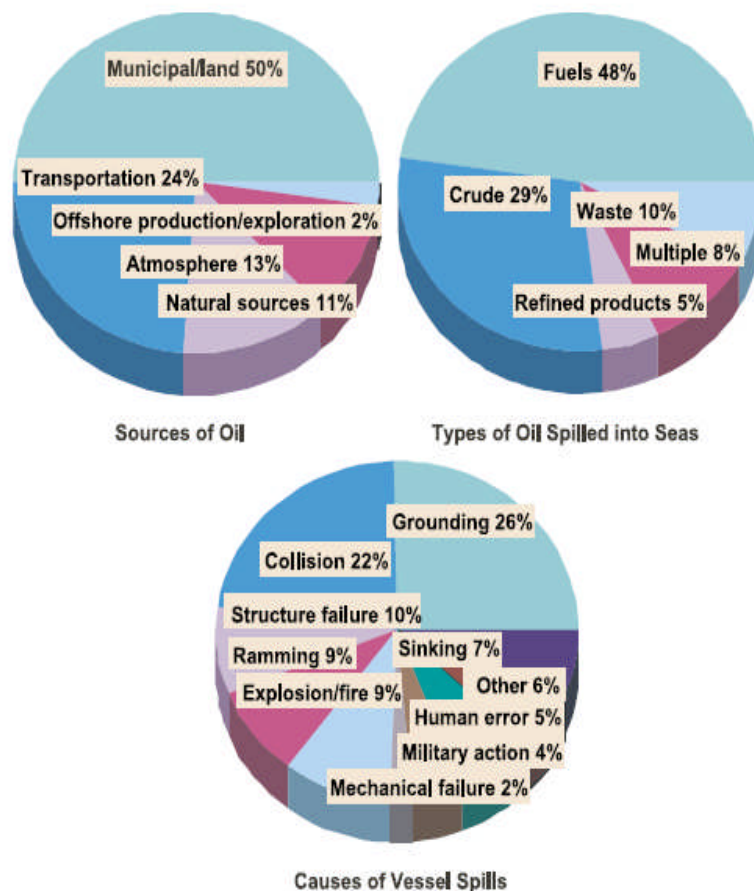


Figure 1.1 Statistics of oil contamination in the seas worldwide [1]

Generally, oily materials are liquid at room temperature, flammable, less dense, immiscible with water and tend to spread on the water surface. Oily materials are categorized based on properties. Physically, kerosene and diesel which belong to light hydrocarbon or solvents are less viscous and more volatile than heavy hydrocarbons, such as crude oil, fuel oil and asphalt. Some are classified as aliphatics or aromatics whose structures may contain acid, carbonyl or other functional groups and have elements other than carbon, hydrogen and oxygen, such as nitrogen and sulfur. Contamination of oily substances has detrimental effects on human health, environment and ecosystem, which include the killing of 95% of organism in the area of oil spill. The presence of wave and current in the coastal area could cause horizontal spreading and mixing of the hydrocarbons content with water. Natural bacterial remediation would affect the product with least toxicity, but the remaining compounds may remain more poisonous than before and stay for a long time [3].

Methods for contaminated site restoration from toxic chemicals have been developed based on chemical, biological and physical methods. Table 1.2 shows the different filtration method developed for oily water separation. No single method is completely effective for remediation of the oily water mixtures, but the use of oil sorbent has become commercially attractive and operationally effective. Hydrophobic-oleophilic type of sorbents may concentrate and transform liquid oil into semi-solid or solid phase, which can then be removed and handled in a convenient manner without significant oil draining out [3]. They can be applied to treat seawater, groundwater or wastewater which has been contaminated with oil [4-8]. Sorbents that exhibit high water repellent capacities are used for the separation of oily water and these hydrophobic properties have stimulated many research studies.

Wastewaters usually contain 10 to 10000 mg/L of oil and grease [9]. Due to the serious impact on the ecosystem, many government regulations stipulate that no oily waste to be discharged into the water streams. Summary of several parameters included in the regulations of water quality standard are listed in Table 1.3. Based on Malaysian Sewage and Industrial Effluent Regulations 1979, only 10 ppm of oil and grease content inside the water stream is allowed [10]. WHO (1984) and Canadian government (1971) also publish regulations for drinking water quality standard [11].

Table 1.2 Filtration methods for oily water separation [12]

Filtration method	Equipment	Phenomenon
Sedimentation	Plate sedimentation	Gravity
	Thickener	Gravity
Floatation	Flotation chamber	Gravity, surface tension
Centrifugal	Centrifuge	Centrifugal
	Screw centrifuge	Centrifugal
	Plate centrifuge	Centrifugal
	Hydrocyclon	Centrifugal
Screening and deep bed filtration	Sand/coal fibers	Size + gravity
	Rotary screen	Size + gravity
	Deep bed filter	Size + pressure
	Band filter	Size + pressure
	Frame filter	Size + pressure

Table 1.3 Regulations of water quality standard [10, 11]

Parameter	Unit	Malaysia	
		A	B
COD	mg/L	50	100
Suspended solids	mg/L	50	100
Oil and grease	mg/L	Not detectable	10
Turbidity	NTU	WHO	Canada
		5	1

A : for human consumption

B : for industrial consumption

Table 1.4 shows some of the commercially available sorbent for oil removal. The oil sorbent is categorized into three classes, namely synthetic organic sorbent, inorganic mineral sorbent and organic natural product [4]. Most of the commercially available hydrophobic-oleophilic sorbents are organic synthetic products such as polypropylene and polyurethane. Though the man-made fibers are good oil sorbents, they are non-degradable and also not naturally produced [4, 6, 8, 13]. As a result, organic and inorganic natural products, such as rice straw, corn cob, peat moss, wool, cotton, cotton grass, cattail fiber, rice husk, wood chips barks, bagasse, milkweed, *Salvinia* Sp., kenaf and *Ceiba pentandra* or kapok have become candidates of choice to replace the synthetic sorbents [2, 4-6, 8, 12-22]. However, some of the inorganic mineral sorbent has lower oil sorption capacity compared to synthetic sorbent and organic natural sorbent (Table 1.4). Difficulties for sorbent collecting and harvesting are also the disadvantages of several inorganic mineral sorbent such as rice husk and wood chips barks. For natural sorbents, they are more economical, environmentally-friendly and most of them are locally available. Natural sorbents made from corn cob, cellulose fiber, and vermiculite and wool fiber have all been marketed at competitive prices.

Ceiba pentandra (L.) Gaertn. or locally known as kapok is one of the natural sorbent that has good oil sorption capacity. This plant is cultivated in Southeast Asia, Malaysia, Sri Lanka, other parts of East Asia and Africa [23]. In Malaysia, *kekabu* is the local name for kapok. In Indonesia, it is an important product in Java island and the fibre is known as Java Cotton. The fibres are lustrous, yellowish brown in color, light in weight, inelastic and brittle for spinning. They are used in life preserving or water-safety equipment. The material could support as much as 30 times its own weight in water. Kapok is also used as stuffing material for pillows, mattresses as insulation for upholstery material and as a substitute for absorbent cotton in surgery. Due to its high flammability, its importance has decreased with the development of foam rubber, plastics and man-made fibers. The kapok seeds contain oil similar to cotton oil. The leaves and bark have medicinal values used by the ancient Chinese, and the trunk has been tested as resources of pulp for papermaking [23]. In Malaysia, only a limited application of kapok fibre has been developed, mainly as stuffing

material for beds and pillows. However, this limited application has also been devolved upon synthetic material, such as polyurethane.

Table 1.4 Commercially available synthetic and biosorbent for oil removal [24]

Product Name	Material	Company	Oil sorption capacity (g oil/g fiber)		
			Diesel fuel	Medium crude	Heavy crude
Instasorb	Cotton pads	Complete Environmental Services Inc., USA	17.4	35.5	44.8
Oclansorb	Wood	Hi-Poit Industries Ltd., Canada	6.4	9.2	13.8
Geo-Sorb	Organic peat	Jadon Environmental, USA	0.7	3.6	3.6
Jadon					
McHill	Wool	McHill Wool Processing, Canada	6.5	13.8	14.8
Sorbent					
Clay	Clay	Natural Select, USA	0.3	0.6	0.7
Oil sponge	Reclaimed cotton fibres	PHase III Inc., USA	1.1	2.0	2.0
Corn cobs	Corn cobs	Recovery I Inc, USA	0.7	1.5	1
Cellusorb	Wood fibre, clay, SiO ₂	Schaefer Associates, Ltd., USA	4.2	6.5	7
CAP	Heated-treated cork	Sevenson Env. Products, USA	4.4	7	7.3
EC100	Cotton	SpilKleen, Canada	10.6	20.7	17.5
Vermiculite	Vermiculite	Vermiculite Ltd., USA	3.3	5.3	6.2
Peat Sorb	Peat moss	Zorbit Technologies Inc, USA	3	5.7	6.4
EP100	Polypropylene	SpilKleen, Canada	13.3	33.1	29.9
Sorbent J	Polyurethane foam	U.S. Env. Pollution Control Co., USA	8.9	28.5	35.4

Kapok sorbents have been used in batch and continuous reactors for oil-water separation. Raw, chloroform and ethanol-treated kapok have been used for treating water contaminated with diesel, engine oil, crude oil and used engine oil [2, 6-8, 17-20]. Alkali treatment on kapok fibre has been reported but without further study on its oil sorption characteristics [25, 26]. Hori et al. (1993) have reported the detailed composition of kapok fibers originated from Vietnam and Philippines [6]. Compared to cotton, higher amount of waxy cutin on the kapok surface contribute towards its high water repellency [14]. Kapok fibers harvested from Philippines have been investigated for their properties and performance as oil sorbent for diesel,

hydraulic oil, engine oil and diesel-water mixture in batch and continuous systems [2, 7, 8, 17]. From all the studies on kapok fibre application for oil sorbent, some oil sorption characteristics such as the effect of packing density of kapok onto the saturation time, packing height reduction of kapok bed and the stability of oil entrapment on kapok structure have not been reported. The effect of packing density, kapok wall and diesel layer thickness on kapok performance for oily water filtration have been studied, but without including evaluation of the interaction between those factors [2, 7].

In this study, the physicochemical properties of kapok as oil sorbent were characterized. Several parameter variations such as packing density and the types of experimental oil which affect the oil sorption characteristics were studied in batch system. Oil sorption capacity, percentage of dynamic oil retention, oil entrapment stability, packing height reduction, saturation time and kapok reusability were the variables evaluated. Continuous packed-bed column was developed to examine the process design parameters, in terms of flow rates and packing density for the diesel-water filtration by applying statistical analyses. Chloroform and alkali treatment were employed to investigate the effects of solvent on the hydrophobic-oleophilic properties of kapok.

The objectives of this research were:

1. To characterize the physicochemical properties of raw kapok and the experimental oils
2. To determine the sorption parameters that would affect kapok performance in a batch system
3. To study the process design parameters such as flow rate and packing density for diesel-water in a continuous kapok packed-bed column
4. To study the effect of chloroform and alkali treatment on hydrophobic-oleophilic properties of kapok.

CHAPTER TWO

LITERATURE REVIEW

2.1 Sorbent Application in Oil Spill Remediation

The efficiency and effectiveness of sorbent application depend on the scale of contamination. Sorbent application includes several operations such as sorbent distribution, sorbent collection and harvesting, sorbent separation from contaminants, contamination storage and /or disposal, and oil sorbent reused and /or disposal [27]. For application in large area, blower may be used for dispersal before applying sorbent of different configuration and mode of application. In powder form, distribution and cleaning up after use may be problematic, whilst floating ability and difficulties to become waterlogged after oil sorption are essential for ease of sorbent collection. Centrifugations and mechanical squeezers are some available methods for sorbent separation from the contaminant. This separation may open up the possibility for another cycle of sorbent reuse. Barrel storage, burning or chemical treatment may be the final treatment of sorbent solidified-oil contaminant [27].

An example of clean up method was applied for oil spill incident in Sweden in 1970. The *in-situ* burning has become the only viable method for oil spill cleanup in the arctic area [1]. The Swedish authorities successfully burned the Bunker Oil Type C spillage in the ice. For minimum oil thickness of 2-3 mm, *in-situ* burning was chosen as the first response for oil spills, especially for large area. In one day, *in-situ* burning was capable of burning up to 5000 L/m² day. The second example was in 1989 involving Exxon Valdez is for oil spillage incident in Prince William Sound, Alaska. At that time, the majority of free-phase oil floated at the sea surface and the oil beach line. The cleanup effort was therefore focused on protecting the subsurface beach oil and pockets in the secluded bays for contaminating the adjacent were by applying polypropylene booms and pads [28]. These type or sorbents were used to protect the clean beach whilst the adjacent areas were remediated.

2.2 Characteristics of Oil Sorbent Material

The use of sorbent materials for oil removal is principally due to its ability to transform oil contaminant in the liquid phase to the solid or semi solid phase. Other characteristics that need to be fulfilled for oil sorbent include readily available, inexpensive, high oil sorption rate and oil sorption capacity, low water pickup, high oil retention capacity during transfer, high recovery of the sorbed oil using simple method, good reusability, excellent physical and chemical resistance against deformation, photo-degradation and chemical attacks [12, 21, 24].

Oil sorbent materials can be classified into three classes (Table 2.1), organic, inorganic and synthetic organic products [4, 8]. Organic sorbents include straw, corn cob, wood fibre, sawdust, cotton fibre, kapok fibre, wool fibre, kenaf fibre, *Salvinia* sp., rice husk, coconut husk, cattail fibre, bagasse and rubber powder [2, 4-8, 12, 13, 15-22, 29, 30]. Perlite, graphite, vermiculite, zeolites, bentonites, organo clay, fly ash, sand and diatomite are considered as mineral inorganic products [29, 31-40]. Based on the oil uptake of between 30-40 g oil/g fiber (Table 2.1), cotton, wool, milkweed and kapok show better performance than most other sorbent materials, apart from exfoliated graphite (83 g oil/g fiber) and polyurethane foam (100 g oil/g fiber). The major advantages of these natural sorbents may have over the inorganic and synthetic sorbents are that they are biodegradable, locally available and low prices of raw material.

Table.2.1 Sorption Capacities of Sorbents

Sorbent Materials	Oil Type	Oil Uptake (g oil/g fiber)	Form	Reference
<u>1. Organic Sorbents</u>				
Cotton	Diesel oil	30.6	Ground fiber	[41]
Kenaf bast	Diesel oil	7.2	Ground fiber	[41]
Kenaf core	Diesel oil	7.1	Ground fiber	[41]
Garlic peels	Crude oil	0.4	Sheets	[42]
Onion peels	Crude oil	0.5	Sheets	[42]
Natural wool	Motor oil	5.6	Fiber	[37]
Wool	Crude oil	31.8	Fiber	[14]
Milkweed	Crude oil	39.0	Fiber	[14]
Kapok	Crude oil	38.5	Fiber	[14]
Organo clay (Swy2)	Engine oil	1.6	Powder	[43]
Peat	Crude oil	7.7	Granule	[22]
Milled-wood	Diesel oil	2.1	Fiber	[43]
Salvinia sp.	Used-engine oil	0.9	Fiber	[18]
<u>2. Inorganic Sorbents</u>				
Sepiolite	Motor oil	0.2	Granule	[37]
Bentonite	Motor oil			[37]
Zeolite	Engine oil	0.9	Powder	[37]
Sand	Engine oil	0.3	Powder	[44]
Expanded Perlite	Heavy crude oil	3.3	Granule	[38]
Expholiated graphite	Crude oil	83.0	Powder	[34]
<u>3. Synthetic Sorbents</u>				
Polyurethane (PU)	Petrol oil	100.0	Foam	[4]
Polypropylene (PP)	Crude oil	14.0	Fiber	[45]
Viscose rayon (VR)	Crude oil	19.0	Fiber	[14]
Nylon 66	Crude oil	15.0	Fiber	[14]

2.3 Organic Synthetic Sorbent

The chemical structures of synthetic fibres and their functional groups provide sufficient information for determining the hydrophobicity-oleophilicity or hydrophilicity of the sorbents. Physical configurations such as the condition of the twist, crimp, surface roughness and fineness also contribute towards effective oil sorption parameters. Different types of oil sorbent configurations have been developed such as belts, chips, mops, pillows, powder, granular fibres and pellet materials, ropes, booms and sheets. These configurations facilitate easy spreading and recovery. Examples of common synthetic sorbents are polypropylene and polyurethane.

2.3.1 Polypropylene

Polypropylene (PP) with its monomer, $(-\text{CH}(\text{CH}_3)-\text{CH}-)_n$ is known for its hydrophobic properties. PP fibre is one of the commercialized oil sorbent (Table 1.4) and could perform as an oil sorbent due to its aliphatic chain monomer. Wei and co workers (2003) have evaluated different configurations of PP fibre; non-woven (stitch-bonded), needle-punched and melt-blown fibre, for oil spill recovery [45]. Non-woven PP sorbents are fibrous materials as shown in Figure 2.1, which are based on webs of the individual fibres. SEM image of individual of PP fibre is shown in Figure 2.2a. The formation of oil droplet on the PP surface can be observed as shown in Figure 2.2.b. The surface adsorption mechanism appears to be the main driving force for the high oil sorption capacity of PP and for its high sorption capacity. From Table 2.1, the oil sorption capacity of non-woven fibre is around 13.3 g oil/g fibre inside oil-marine water mixtures, as compared to 12.8 g oil/g fibre for needle-punched, and 10 g oil/g fibre for melt-blown. Each configuration has different porosity and fineness, and it is this construction that plays an important role in the retention capacity of the sorbent. Non-woven sorbent with high porosity has higher oil pickup but lower oil retention capacity. Needle-punched or melt-blown with finer structure has lower oil sorption but higher oil retention capacity. The network of small

pores inside these PP fibrous webs facilitate the oil pickup inside the sorbents and oil retention after sorption [8, 45].

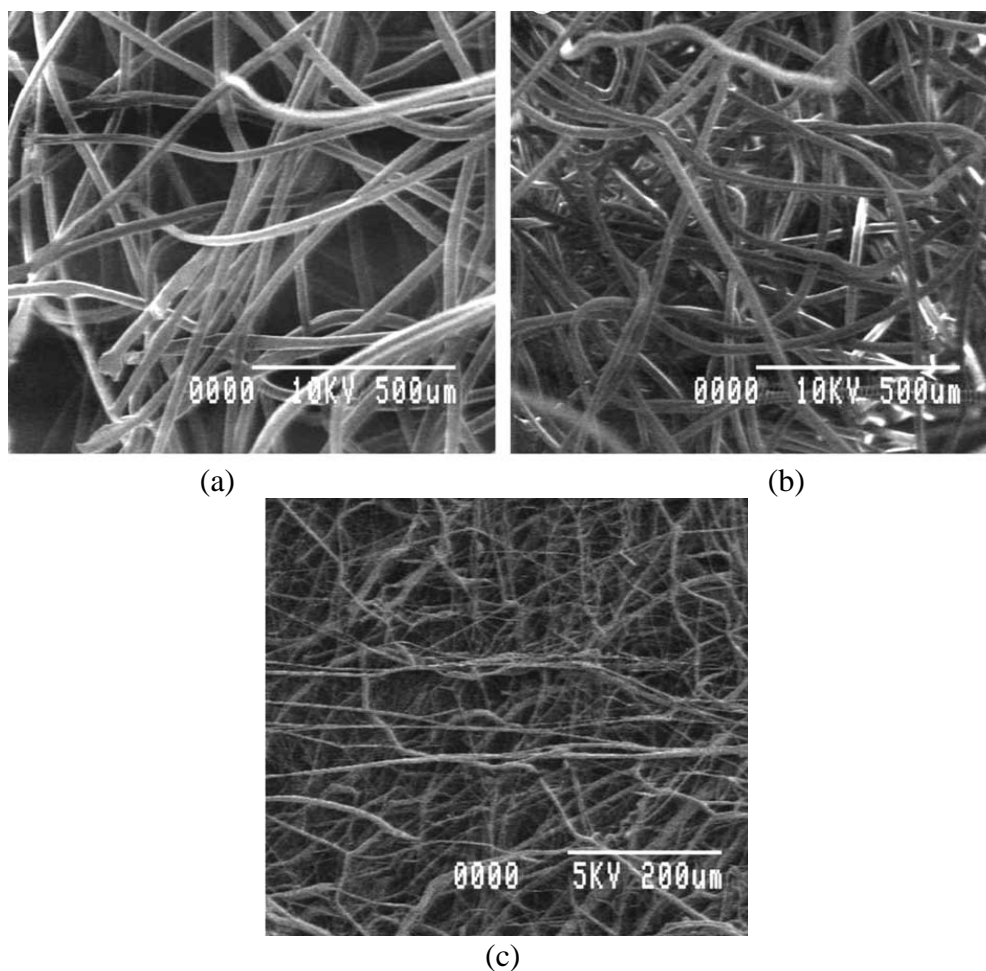


Figure 2.1 SEM imaging of PP sorbent (a) stich-bonded, (b) needle-punched 1 and (c) needle-punched 2 [45]

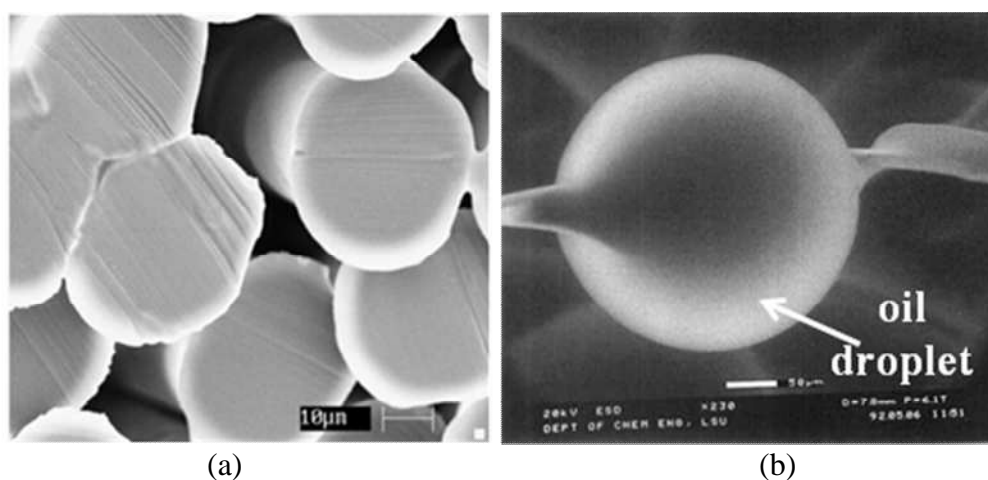
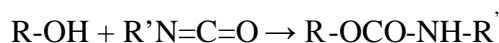


Figure 2.2 Image of polypropylene fiber by using SEM for (a) before [8] and ESEM for (b) after oil sorption [14]

2.3.2 Polyurethane

Polyurethane (PU) foam is one of the commercial synthetic sorbent with high oil sorption capacity as high as 100 g oil/g fiber (Table 2.1). The formation of PU foam is initiated by the generation of CO₂, while the amount of H₂O determines the density and hardness of PU foam. During PU synthesis, there are two stage of reactions [46]:

1. The polyaddition reaction of isocyanate with hydroxyl group of polyol to form polyurethane



2. The PU foam with open structure is formed as the CO₂ gas which released from the reaction of isocyanate with water through mixing



For oil spill application, the presence of open structure has contributed towards PU foam having the highest oil sorption capacity. To make open cell structure, the silicone-surfactant is sometimes added during preparation of PU foams [47]. The amount of open pore formation inside PU structure can be modified by varying the ratio of polyol and isocyanate, mixing time and gelling time [46]. Higher isocyanate and polyol ratio produce PU with larger pore structure (Figure 2.3). Higher open structure would produce PU foam with lower density, but the oil sorption capacity will be increased. When the cell size becomes large, organic solvent molecules can penetrate into foams more easily. Therefore, the absorbency increased with the cell size initially. But if the cell size is larger than a certain critical value, the once penetrated solvent molecules can come out of the cell easily due to the gravitational force. Hence, the absorbency will decrease after a certain value of isocyanate to polyol molar ratio. The presence of open pore for oil entrapment area in the modified PU allows the fibre to absorb oil, even until 100 times its weight [47]. Ample interstitial spaces for oil to be trapped are available within PU fiber.

Mechanical entrapments of oil inside synthetic fibre pore structure become major mechanism behind their oil sorption capabilities.

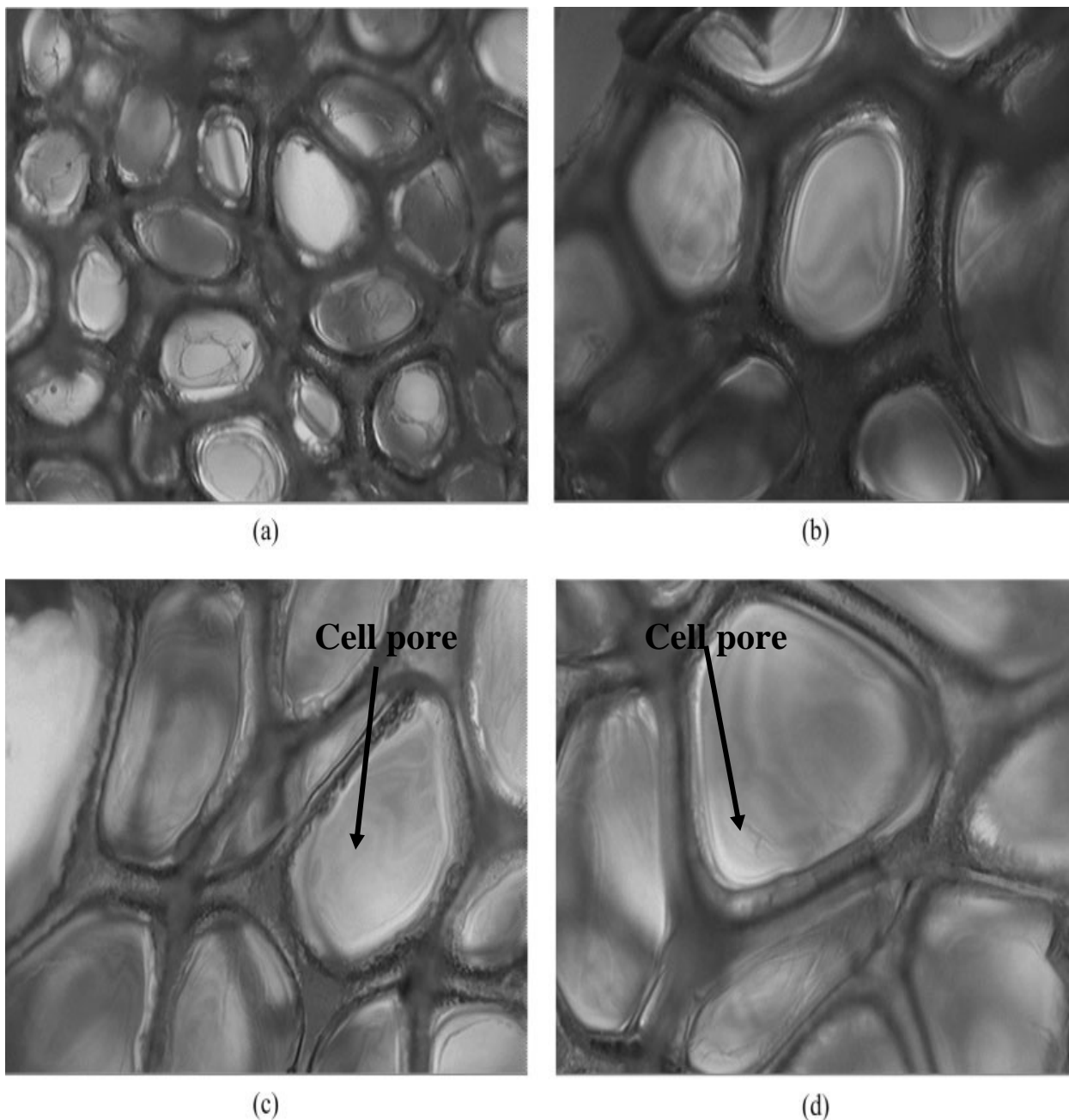


Figure 2.3 OM image of PU foam with isocyanate to polyol molar ratio of (a) 0.6, (b) 0.7, (c) 0.8 and (d) 0.9 [47]

2.4 Inorganic Mineral Sorbent

Inorganic sorbent could be prepared by extracting from the natural source (raw perlite, graphite, natural zeolite), or by applying applied a pretreatment to a natural raw material (expholiated graphite, expanded perlite) or by synthesizing it from the natural material (synthetic zeolites).

2.4.1 Expholiated Graphite (EG)

Commercially available EG materials for oil sorption are prepared form the intercalation of natural graphite with sulfuric acid [48]. Bulk density and pore volume are the major factors influencing the oil sorption characteristics of carbon-based sorbents. Higher values of the two factors could result in higher oil sorption capacity of EG. There are three types of EG pores; large spaces, inter-particle pores and intra particle pores. The inter-particle pores are formed among the entangled worm-like particles and cleavage-like pores on the surface of the worm-like particle. among the entangled worm like particles of EG among the entangled worm like particles of EG, large pores of 600 μm in size assumed to be inter-particle pores could have been the reason for the large sorption capacity for heavy oils. Intra-particle pores inside and cleavage-like pores on the surface of worm-like particles are assumed to assist in the capillary pumping of heavy oil. The hydrophobic-oleophilic nature of the EG surface could also be important factor governing heavy oil sorption.

The disappearance of brown color from oil-water mixtures is used to characterize the performance of the EG. When soaked in heavy oil-water mixture, 83 g of oil has been reported to be sorbed within 2 min [39]. Four EG samples with volume ranging from 102.6 to 267.7 mL/g have been reportedly synthesized [49]. The volume of worm-like particles increases almost linearly with the EG volume. The average volume shrinkage of each worm-like particle is less than 1% and its oil sorption behavior is not affected by the oil viscosity differences implying the conserved volume of EG after sorption. By increasing EG volume, the amount of oil entrapment inside EG pores and among the worm-like particles are also increased. For

oil with light viscosity, such as kerosene, most oil is trapped inside in the worm-like particle whereas for oil with high viscosity oil higher amount of oil was trapped in the space among worm-like particle (Figure 2.4).

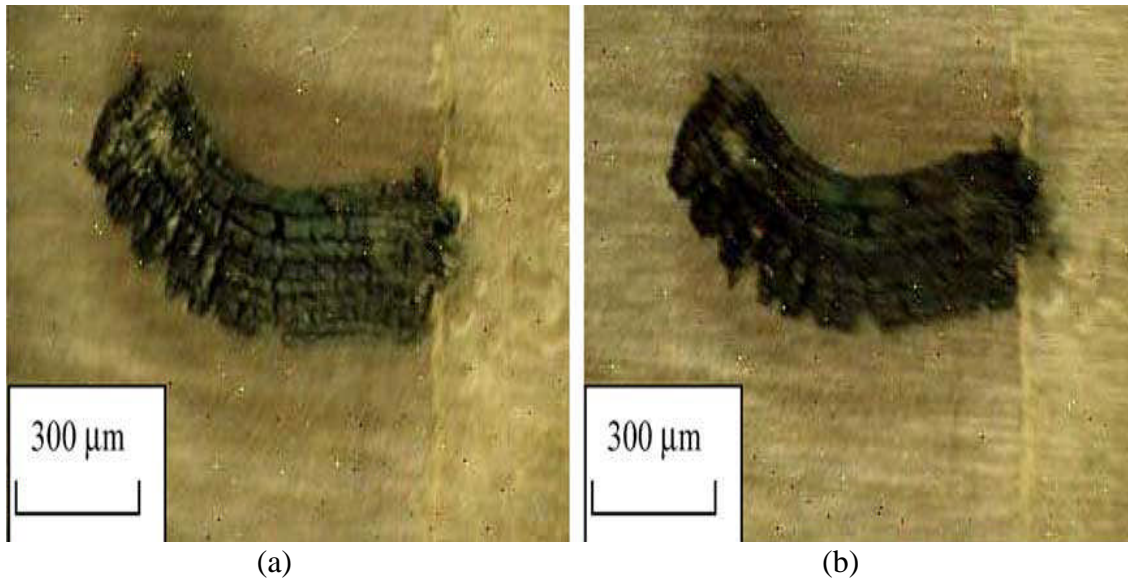


Figure 2.4 Morphology of worm-like particles with an exfoliating volume (a) before and (b) after kerosene sorption [49]

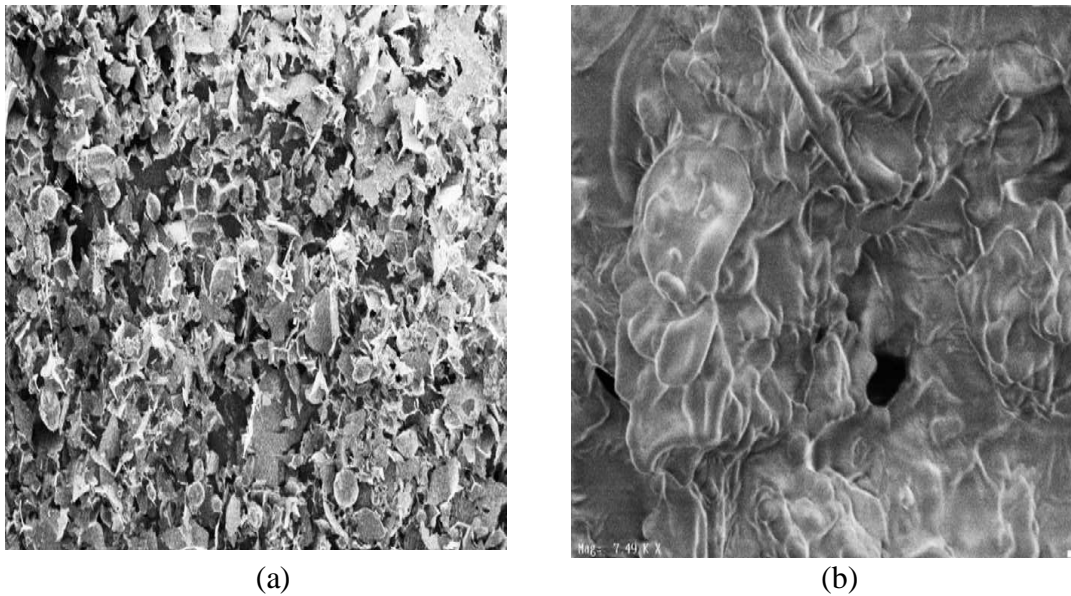


Figure 2.5 Expanded perlite, A_0 (a) before and (b) after oil sorption [32]

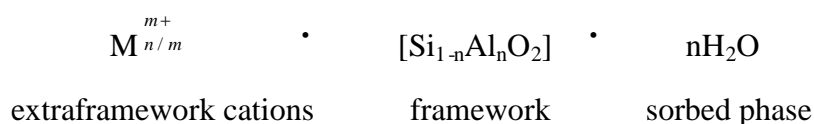
2.4.2 Expanded Perlite (EP)

Raw perlite is a glassy volcanic rock containing between 2 and 6 % of water. EP is produced by heating rapidly the raw perlite at 700-1200°C. The thermal treatment expands the perlite from five to eight times its original volume. As shown in Figure 2.5.a, EP is composed of tiny irregular and randomly-placed shreds. The advantages of EP include its ability to float on the water surface, environmentally-friendly, high porosity, high adsorption capacity and also high resistance against thermal and chemical treatments [32]. The combinations of these properties lead to increased use of EP in many industrial field, including combating oil spills.

In a study examining the capacities of three EPs from the Milos Island in Greece to absorb oil, EP has of 3.3 g oil/g sorbent [38]. This suggests that EP is a potential material for oily water treatment, especially due to its local abundancy and biodegradability. SEM imaging of EPs originated from Mahabad Province in Iran (Figure 2.5), confirms the presence of pore inside EP structure which provides the available space for oil to be trapped within [32] with oil sorption capacities ranging from 7.5-3.2 g oil/g sorbent. EP with the highest oil sorption capacity has the highest porosity.

2.4.3 Zeolites

Zeolites are minerals that belong to the aluminosilicate groups of microporous solids known as “molecular sieves”. The term describes particular ability of zeolites to selectively sort molecules by size exclusion with the pore size unit is 0.2-0.9 nm [4]. The materials have regular pore structures of molecular dimensions with diameter of the tunnel opening would control the size of molecules that could be trapped within its structure [37]. The zeolite composition can be summarized as having three main components:



The microporous crystalline aluminosilicate part consists of TO_4 tetrahedra ($T = \text{Si}, \text{Al}$) with oxygen atom as the connector of the neighbouring tetrahedral. Silicon atom present as SiO_4 which has neutral charge. The incorporation of Al^{3+} causes the network to become negatively charged. Therefore, extraframework cations are added to neutralize the overall structure which are exchangeable and increased the ion-exchange capability of zeolites [50]. Typically, the water present during the synthesis which occupies the internal zeolites internal voids. The sorbed phase and organic non-framework cations can be removed by thermal treatment/oxidation, making the intracrystalline space available. The fact that zeolites retain the structural integrity upon loss of water makes them different from other porous hydrates such as CaSO_4 [50]. Hydrophobic zeolites are commonly synthesized either by direct synthesis or by thermochemical framework modification of hydrophilic zeolites through modification of hydrophilic dealumination procedure such as steaming, treatment with mineral or organic acid, or chelating agents, reaction with tetrachloride and treatment with silicon hexafluoride [4]. Surface properties could be modified by silylating agent to produce hydrophobic zeolites.

Zeolites have been used in the treatment of water contaminated with motor oil [37]. Activation before sorption is carried out where zeolites are mechanically cleaned from visible impurities, ground and sieved to obtain 0.5mm-size fraction. A solution of 10 g/L zeolites produced is allowed to settle for 24 h in distilled water. This is followed by filtration or supernatant suspension and finally the drying of solid zeolites in the drying oven. Zeolites have significantly low oil sorption capacity at 170 mg of oil/g of zeolites. The sorption behavior is very much influenced by pH. About 10% increment for oil sorption efficiency at pH 10, while 18 % efficiency is reported at pH 5. There are, no detailed information on the natural zeolites used in this oil sorption experiment [37]. However, compared to carbon sorbent, zeolites have lower organic compound sorption capacity.

2.5 Organic Natural Sorbent

One attractive feature of organic sorbent for oil spill remediation is its hydrophobic-oleophilic properties. These are determined by factors such as the chemical constituent of the sorbent, amount of the surface wax, the physical configuration of the fiber, such as hollow lumen, twist, crimp, surface roughness and its pore nature [14, 51]. Plant fibre consists of cellulosic and non-cellulosic constituent. Cellulose, hemicellulose and lignin are common constituents contributing towards hydrophobic properties of plant surface, which regulate the moisture uptakes of natural fibers.

Cuticle is a boundary that covers the plant surface. This surface layer provides important roles in the physiology and autoecology of the plant, while serving the first contact area for plant interactions with the surroundings [52]. The most common structural model to describe cuticle membrane is the bilayered model. As shown in Figure 2.6 where the two layers are separated by the difference in ontogeny, ultra structure and chemical composition [52]. Cuticle proper layer which is generally made up of ester bond compound, serves as the border with the outer epidermal cell wall. The cell wall polysaccharides lie in the cuticle layer. Intracuticular waxes are located at the outer layer of the cuticle and covered with thin film of epicuticular waxes. The cuticle layers consist of important lipophilic fraction, namely cutin and waxes. Cutin is a polyester-type biopolymer that resides in the cuticle matrix. The main component of cutin layers are the two families of hydroxyl and hydroxyepoxy fatty acids which are derived from common cellular fatty acids, as well as C_{16} saturated and C_{18} unsaturated fatty acids [52]. For cuticular waxes, present in the lipophilic fraction of the cuticle, the major constituents are n-alkanes (chain length C_{21} - C_{35}) and smaller proportions of iso and anteiso homologues, primary alcohols (C_{22} - C_{40}), fatty acids (C_{20} - C_{24}), aldehydes (C_{24} - C_{36}), ketones (C_{21} - C_{35}), β -diketones (C_{22} - C_{36}) and n-alkyl esters (C_{36} - C_{60}) resulting from the combination of long chain primary alcohols and fatty acids. The amount of each of the constituent is unique for each plant.

The non-cellulosic constituents of the fibre are located principally in the cuticle, in the primary cell wall and in the lumen. The non-cellulosic constituents include proteins, amino acids, other nitrogen compounds, wax, pectin substances, organic acids, sugar, inorganic salts, and very small amount of pigments. These non cellulosic materials can be removed by selective solvents. The wax constituent can be removed selectively with non-polar solvents, such as hexane and chloroform or non selectively heated in a 1% sodium hydroxide solution [53]. Hot non-polar solvents and other water inorganic solvents remove wax but no other impurities. Hot ethanol removes wax, inorganic salts (metals), sugars, amino acids and low molecular weight peptides, and proteins. Most of the non-polymeric constituents such as sugars, amino acids, organic acids and inorganic salts may be removed with water. The remaining pectins and high molecular weight proteins are removable by heating in a 1% sodium hydroxide solution with appropriate enzyme treatments. All of the non-cellulosic materials can be removed almost completely by boiling the fibre in hot, dilute, aqueous sodium hydroxide, followed by washing thoroughly with water [53].

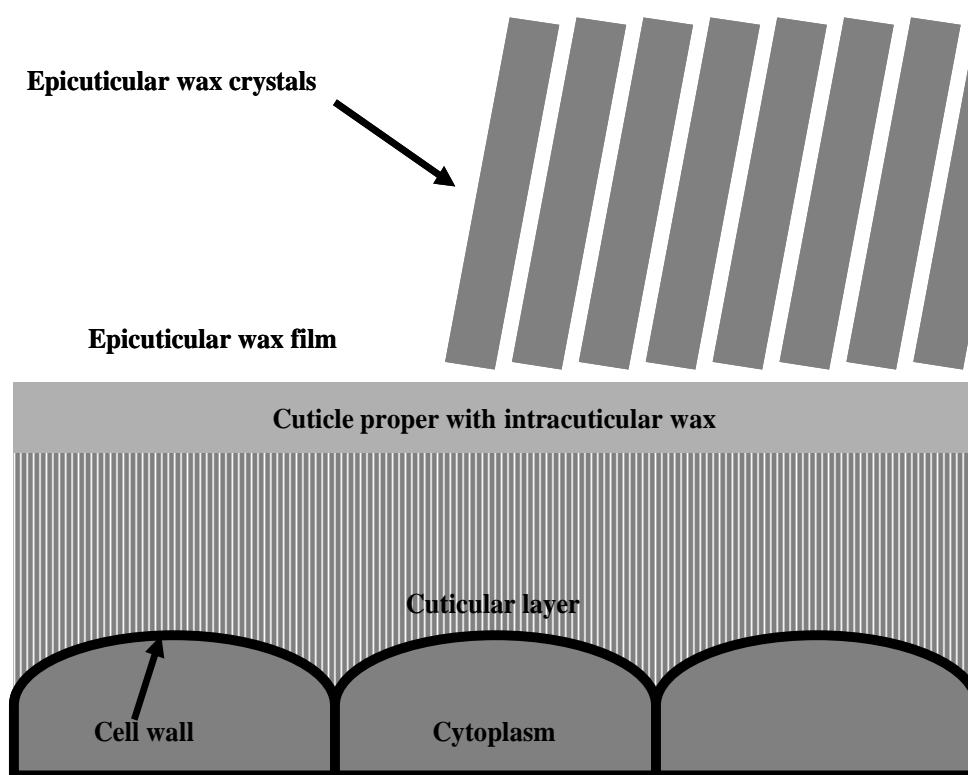


Figure 2.6 Scheme of plant cuticle layer [52]

2.5.1 Peat

Peat is an inexpensive natural product that can be used for hydrocarbon removal from the water stream. The possible correlation between peat composition and its capability to extract hydrocarbon from water has been proposed [54]. The “Irish” peat and H₂SO₄-treated “Michigan” peats have been found more effective to separate oil from bilge water of oil tankers than the synthetic sorbents [55]. *Sphagnum* peat, granulated bag-peat and cotton grass-peat are all capable of removing 88-99 % of oil from water at the rates of 5-13 m³/h at concentrations of about 0.9 mg/L. Horticular-peat is capable of absorbing 7.5-7.8 times of its dry weight different types of oil such as crude oil, refinery effluent, mineral oil and cutting oil from water emulsion [22, 56]. Peat may be mixed with lime, clay, diatomaceous earth or alkaline substances to form an absorbent mat or filter for oil sorbent [54].

Figure 2.7 shows the photomicrographs of microtome section of *Sphagnum*-peat and *Taxodium*-peat from Okefenokee Swamp. The microtome section of *Sphagnum*-peat (Figure 2.7a) appears to be dominated by well preserved tissues (fibres), light in color and high in porosity, whereas micrograph for Okefenokee *Taxodium*-peat (Figure 2.7b) shows the low amount of fibres content.

However, the Okefenokee *Taxodium*-peat, the one that has low fibre content (17.5%), low birefringence organics (20%), high ash content (13%), high guaiacyl lignin pyrolysis products (27.3%) and high furan pyrolysis products (6.3%), has been found to absorb the highest amount of hydrocarbon with the highest hydrocarbon capacity. The functional base-structure similarity between peat-lignin and hydrocarbon studied is suggested as the reason behind the high adsorptive capability of peat. This interaction is similar to the compound partition in the stationary phase in the chromatography. The hydrocarbon would attach to the aromatic group on the lignin surface, and the cross-linking side chains of lignin would provide sufficient space for the hydrocarbon to be trapped in.

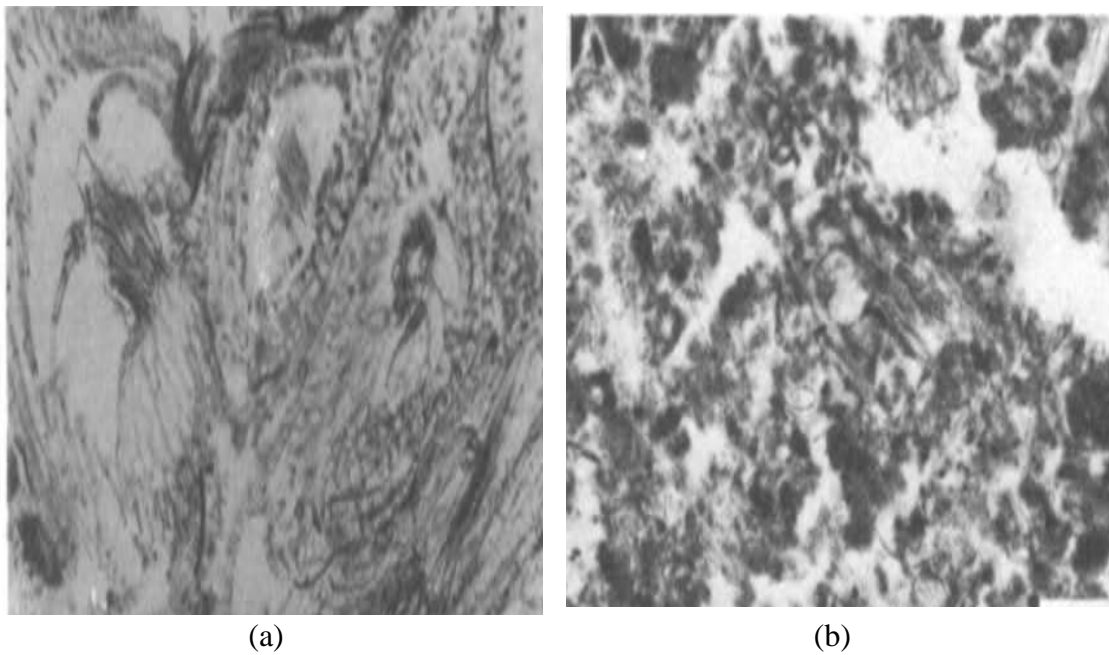


Figure 2.7 Photomicrographs of microtome section of (a) *Sphagnum*-peat from Maine and (b) *Taxodium*- Okefenokee Swamp-peat from Georgia [54]



Figure 2.8 ESEM imaging of milkweed fiber [14]

2.5.2 *Asclepias syriaca* (Milkweed)

Asclepias syriaca or *A. incarnate* is commonly known as milkweed floss or butterfly weed. The two species belonging to *Asclepiadaceae* family are found in North America. The fibers are lustrous, buoyant and yellowish-white in color. The diameter of individual fibre is about 20-50 μm . Milkweed has the fibre structures which are similar to a cylinder rod as shown in Figure 2.8. The rod-like structure consists of a hollow space in the middle of the fibre (Figure 2.8) known as hollow lumen structure. It is a seed fiber where the fibre inside the seedpods are detached and mechanically processed for further use. Milkweed floss has found application in water-safety equipment that will float on the water surface supporting upto 30 times its own weight. It is also used as upholstery padding and insulating material [57].

2.5.3 Kapok

Ceiba pentandra (L.) Gaertn. or kapok, from *Bombaceae* family, is commonly named after certain countries, highland or lowland [23]. Kapok tree can grow from 60-70 m tall with a spreading crown, huge trunk and large palm-shaped leaves having 5-9 leaves, of 20 cm length. The mature tree bears hundreds of pods (Figure 2.9), up to 15 cm long, filled with fibrous seeds. Its mature pods are either cut open or gathered when they fall, and broken with mallets. The seed and fibre are removed by hand and stirred in a basket, whilst the seeds fall on the ground may leave the fibres free. The seeds can be processed to obtain oil for soap manufacturing, and the residue used as fertilizer or cattle feed. Kapok is a moisture resistant, quick-drying, resilient and buoyant fibre. Individual fibres are 0.8-3.2 cm long, averaging 1.8 cm in length, with diameter 30 to 36 μm [23].

2.5.3.1 The physical properties of kapok

Based on SEM and OM analyses, significant amount of oil penetrates the hollow lumen inside kapok fibre while high surface tension of kapok fibre surface

against air at 7.2×10^{-4} N/cm at 21°C inhibit water from penetrating the hollow tubes [4, 6, 8, 13, 14, 18]. The oil sorption capacity of kapok, milkweed and cotton are attributed to the presence of large and non-collapsing hollow lumens that enable oil sorption through capillary action and provide ample interstitial space for oil entrapment. Higher amount of wax content are reported in kapok and milkweed as compared to cotton. The greater wax content promotes the interactions between oil and sorbent through hydrophobic and Van der Waals forces [14]. The oil sorption capacities of several natural fibers such as wool, kapok, milkweed and cotton have been studied [4, 6, 8, 13, 14, 18]. The sorption capacities of kapok and milkweed for crude oil are not significantly different (Table 2.1) but the natural fibres are better than synthetic fibres [14]. The lower contact angle for experimental oils (Table 2.3) as compared to water may proof the waxy layer on the kapok surface [8]. Lower surface tension values of experimental oils also confirm that they are the wetting liquid for kapok surface, enabling them to penetrate the kapok structure.

Table 2.2 Physical properties of raw kapok fibre [8]

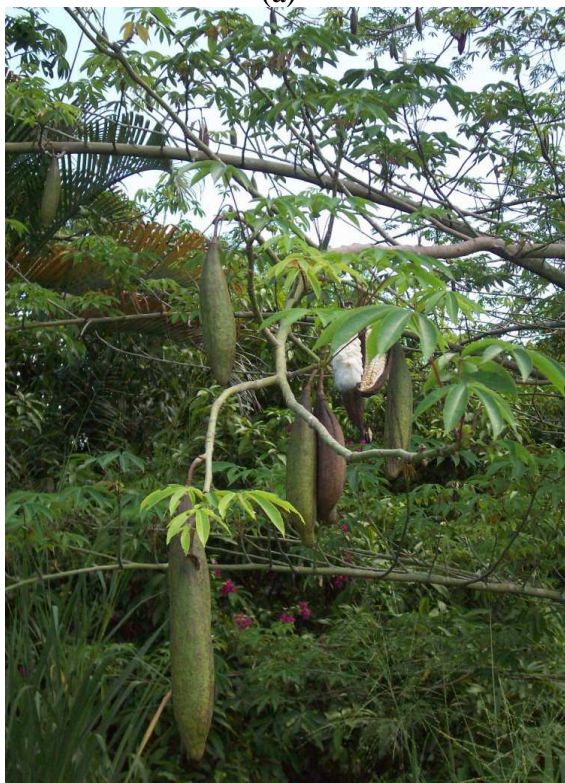
Physical properties	Dimension	
Internal diameter	$14.5 \pm 2.4 \mu\text{m}$	
External diameter	$16.5 \pm 2.4 \mu\text{m}$	
Density	1.31 g/cm^3	
Contact angle (degree)	Liquids	Contact angle
	Water	117
	Diesel	13
	Hydraulic oil	21
	Engine oil	27
Surface tension (MNm^{-1})	Liquids	Surface tension at 21°C
	Water	72.00 ± 0.01
	Diesel	26.29 ± 0.01
	Hydraulic oil	31.14 ± 0.01
	Engine oil	23.28 ± 0.01



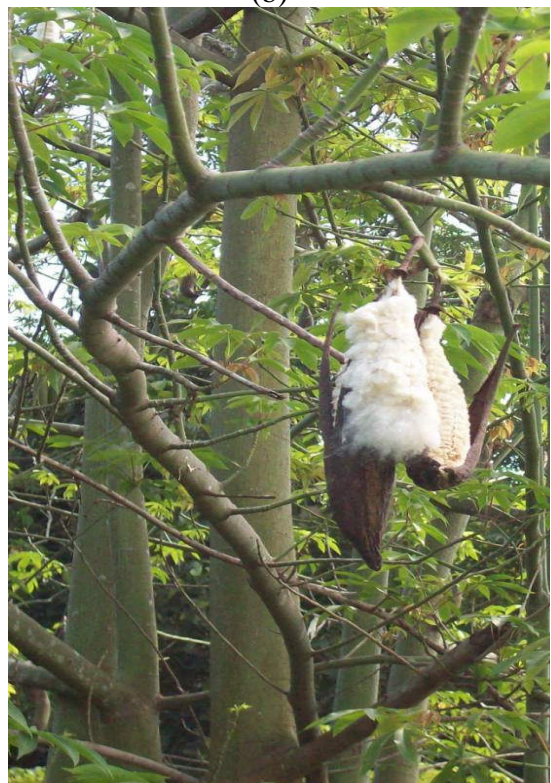
(a)



(b)



(c)



(d)

Figure 2.9 Image of (a) kapok tree, (b) kapok leaf, (c) immature and (d) mature pod

2.5.3.2 The chemical properties of kapok

The kapok fibre has been earlier characterized as comprising of 64% cellulose, 13% lignin and 23% of pentosan [19]. The chemical constituents inside kapok fibre originated from the Philipines and Vietnam have also been reported [6]. Table 2.4 summarizes the chemical characteristics of the two different kapok fibres. Most of non-cellulosic polysaccharide in plant cell walls appear to be substituted by acetyl group between 2-4% in kapok. A comparable acetyl content at 13 and 12.5 % for Philipines and Vietnam kapok, respectively. While kapok from Philipines show higher ash and lignin content, Vietnam kapok exhibits higher total neutral sugars.

The alkaline nitrobenzene products derived from kapok cell walls describe the aromatic composition of lignin component in the kapok cell walls as shown in Table 2.5. Wood lignins mainly consist of three basic building blocks of guaiacyl, syringyl and p-hydroxyphenyl [58]. Lignin can be isolated using different methods. By hydrolyzing the polysaccharide with H_2SO_4 72% (w/w), Klason-Lignin extract can be obtained. For kapok lignins from Philipines and Vietnam, the molar ratio of syringyl nuclei to guaiacyl nuclei (S/V), which is the ratio between syringaldehyde to vanillin are 3.67 and 3.90, respectively. These are higher than the amount of lignin in typical angiosperm woods walls. The degree of substitutions of these acetyl groups on the xylosyl residue are 1.43 and 1.38 for kapok fibres originated from Philipines and Vietnam, respectively. These values are calculated based on the assumption that all acetyl groups are attached to xylan molecules of kapok cell walls.

Table 2.3 Chemical characteristics of kapok fibre [6]

Substances	Content (% of ODM)	
	Philippines	Vietnam
Ash	0.8	0.5
Lignins		
Klason lignin	17.4	15.4
Acid-soluble lignin	4.1	3.8
Total	21.5	19.2
AcBr lignin	20.8	18.8
Neutral sugars		
Rhamnose	0.4	0.5
Arabinose	0.3	0.2
Xylose	21.9	22.8
Mannose	0.8	0.6
Galactose	0.4	0.3
Glucose	35.1	38.5
Total	58.9	62.9
Acetyl group	13.0	12.5

Table 2.4 Alkaline nitrobenzene products of kapok cell walls [6]

Product	Philippines	Vietnam
Oxidation product		
p-Hydroxybenzaldehyde	0.3	0.2
Vanillin	5.1	4.8
Syringaldehyde	21.3	22.2
p-Hydroxybenzoic acid	0.0	0.0
Vanilic acid	0.3	0.4
Syringic acid	2.4	2.1
Total yield (% of total lignin)	29.5	29.7
phhydroxypheugl/guaiacyl	0.06	0.04
Syringl/guaiacyl	3.67	3.90

2.5.3.3 Modification of kapok chemical constituent

Physicochemical properties of plant wax determine the plant wettability, optical appearance, water repellency and its solubility among organics and polar solvents. Wax content of kapok (about 3%) is higher than cotton (0.4-0.8 %). Higher waxy content promotes stronger interaction between the oil and kapok by lowering the surface tension between kapok surface and the sorbed oil. Once the surface tension between two solid-liquid interfaces is lowered, no energy barrier exists to prevent the liquid from penetrating the solid structure and therefore enhances the oil sorption capacity and its water repellent capacity [14].

Extractions with different types of solvents are carried out for the kapok fibre preparations before chemical composition determination. The high hydrophobicity and oil absorptivity could not be exactly due to the extractable components of the kapok fibre. The fibre extracted with diethyl ether, followed by alcohol-benzene, has shown similar performance to the original fibre. However, no clear correlations between the chemical composition and the oil sorption characteristics are proposed [6]. FTIR analyses on the solvent-treated fibres show that the absorbance of several well-pronounced peaks associated with the presence of plant wax are reduced [2].

In comparison with kapok fibre, scouring and extraction of milkweed and cotton fibre also have been carried out using 1,1,2-trichloroethane and NaOH for wax removal [59]. The oil and water sorption characteristics are investigated after each treatment, and the report suggests that no reduction in oil sorption capacities for diesel and light crude oil samples are observed. Soxhlet extraction of cotton wax surface using 1,1,2-trichloroethylene also produces the same result with only marginal reduction in oil sorption capacity [13, 59]. With milkweed fibre after alkali scouring, the fibres become hard and pulplike product, resulting in less oil and water sorption capacities. For cotton, alkali scouring has increased the water sorption capacity by ten folds due to the removal of natural wax. The overall milkweed and cotton sorption properties after extraction and scouring are shown in Figure 2.10.

Chloroform and ethanol treatment are applied on kapok fiber [2]. Treated-kapok performance is evaluated using deep-bed filtration for oily water containing 2.5% diesel-water mixture through several parameters, such as breakthrough time, filtration rate, filtrate quality and the oil retention capacity. Both treated and untreated kapok shows excellent oil water separation/filtration characteristics. The filtrate quality parameters, turbidity and percent oil removal, are also unaffected. The oil removal efficiencies of treated-kapok are consistently exceeding 99%. However, treated-kapok shows premature oil breakthrough and lower oil retention. Hence, the solvent treatments using chloroform and ethanol could impair the hydrophobicity-oleophilicity of kapok fiber.

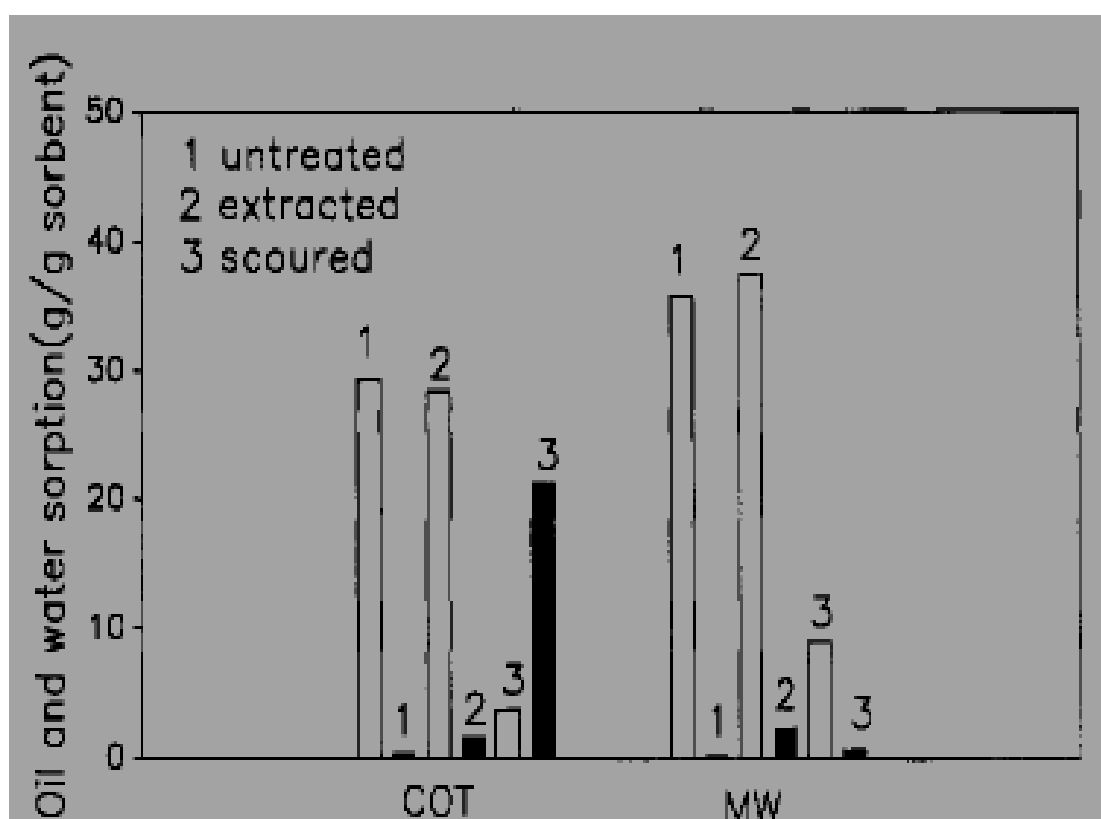


Figure 2.10 Milkweed (MW) and cotton (COT) sorption properties after extraction and alkali scouring (□: oil and ■: water) [59]

2.5.3.4 Kapok fibre as oil sorbent

The evaluation of kapok fibre originated from Thailand has been carried out based on the effect of the packing density on oil sorption capacities, percentage of dynamic oil retentions and the reusability and its selectivity for the oil-water mixtures [8]. More than 83% of the absorbed oil can be recovered by centrifugation of the densely-packed kapok assembly. At the lowest packing density, 13% reduction of oil sorption capacity is obtained but the reduction could be much lesser for higher kapok packing density. Application of kapok for oil-water mixture separation is successful with only invisible oil slick remains on the water surface [8]. Without any pretreatment, kapok fibres exhibit excellent buoyancy and water repellency and also high selectivity for different types of oil, with higher sorption and retention capacity than PP fibre. PP has smaller effective pore due to unavailability of hollow structure, but remain consistent after 6 times of reuse. Successful reuse of any sorbent requires continuous sorption-desorption cycle. Desorption test has been conducted on six fibres to evaluate the oil retention capability of sorbents, namely kapok, cattail, *Salvinia* sp., woodchip, rice husk, coconut husk, and bagasse [18]. Similar trends are observed in all the six fibres with the oil concentration of the effluent relatively high at the beginning but decrease rapidly during the first 5 min of the test. The desorption trend for kapok fibre is reportedly similar to polyester fibre where oil is rapidly desorbed within the first 3 min, followed by slow desorption.

The kapok feasibility as oil sorbent in the form of mat and belt has been investigated [19]. A bag of unbleached cotton is also packed with 100 g of kapok and quilted in the shape of mat to investigate their oil sorption properties. This kapok-cotton mat is capable of sorbing oil 20 times its own weight whilst PP fibre mixed with kapok has resulted in 25 g oil/g mat sorption capacity. Kapok fibre packed inside a column to simulate a recovery well model has also been constructed to perform a lab scale feasibility study for groundwater cleanup using diesel-water mixture [7]. The kapok wall fibre allows the oil permeation into its structure instead of water. Hence, water repellency and oil permeability are the two parameters proposed for in situ oil/water separation system for selective liquid filtration of the oil-contaminated groundwater. By increasing packing density, the intrinsic permeability values of

kapok column are decreased drastically following almost a linear correlation. However, significant deformation of the loosely packed kapok is observed which causes uneven flow pattern through the kapok column. Higher packing density 70 g/L is chosen where the permeation rates increase almost linearly with the increasing thickness of diesel layer but with decreasing thickness of kapok wall. Thinner wall is proposed to allow higher permeation rate because of the existence of greater hydraulic gradient. The kapok wall could maintain a substantial portion of its initial oil recovery rate even after several cycles of reuse. Selectivity of kapok wall is indicated by the phenomenon where no capillary migration of water rises along the kapok wall.

2.6 Considerations for Field Application of Sorbent Materials

For field application of sorbent materials, several factors need to be considered, such as, oil characteristics, the properties of selected sorbent material and also the engineering parameters for the operational setup.

2.6.1 The characteristics of oil

The liquid to be considered as the sorbent wetting liquid must have low surface tension and contact angle. Diesel oil is an example of wetting liquid for kapok sorbent since it has low value contact angle and surface tension (Table 2.2). As the energy barrier being overcome, the liquid can penetrate easily the sorbent inner structure. On the other hand, water has high surface tension and contact angle with kapok surface which inhibit its penetration. Viscosity and density are two other important parameters that determine the sorbent oil sorption characteristics. Oil has lower density than water which makes it float on the water surface. For oil spill application, the ability of sorbent to float on the water surface is a must-have property. Density also influences the oil sorption capacity whereby oil with low density will result in low oil sorption capacity of the fibre [8]. Viscosity is the flow resistance of oil inside the sorbent [60]. Crude oil is a mixture of various hydrocarbons, ranging from low to high molecular weight compounds. During oil spill, low molecular

weight compound with lower viscosity will evaporate, leaving the more viscous components which are more difficult to absorb [59]. Oil with lower viscosity will flow at a faster rate as compared to the more viscous one. Hence, oil with lower viscosity drains out at a faster rate and reaches equilibrium sooner than the oil with higher viscosity. The sorbent maximum sorption capacity should therefore be achieved much quicker [8].

2.6.2 Selection of sorbent materials

As mentioned before, chemical nature of sorbent, such as the presence of surface wax and the molecular arrangement determine the oil sorption characteristics of sorbent. The fibre physical configurations such as the presence of hollow lumen, twist, crimp, surface roughness, porosity and fineness are also correlated to the oleophilic-hydrophobic characteristic of sorbent. The chemical nature and the physical configuration become a combined factor that determines the hydrophobic-oleophilic characters of sorbent material. Surface tension, contact angle, density and viscosity are parameters that characterized the sorbent-oil interaction.

Several studies have been carried out on the correlation between the chemical nature of sorbent and its sorption ability. Cattail fibre has excellent oil sorption capacity due to the capillary action and the spike core which confers its water repellency property [18]. Water can wet the cattail fibre once the spike core has been removed. The high oil sorption capacity of kapok fibre has been attributed to its hydrophobic nature from the wax covering surface and capillary action through hollow lumen. The presence of the wax surface facilitates the oil attachment, and the oil becomes trapped within the kapok lumen structure through capillary action. After wax removal with solvent extraction and alkalization, milkweed and cotton still retain high oil sorption capacity, comparable to polypropylene fibre [59]. In the case of viscose rayon, although it is hydrophilic, the presence of twist, crimp and rough surface inside its structure, have provided ample space for oil deposits. The presence of crimp structure increases sorbent porosity which yields higher surface area. The high oil sorption capacity of rayon proves that physical configuration could equally

play important role as chemical nature of the sorbent [14]. With increasing surface roughness and dull physical appearance of cellulose acetate and viscose rayon as a result of delustering with titanium dioxide, no difference in oil sorption capacity with the unmodified ones has been reported [13].

Different chemical content of sorbent could influence the oil sorption capacity. In a study, peat from different location including the Okefenokee *Taxodium*-peat, Minnesota hemic peat, Loxahatchee sawgrass peat, Loxahatchee *Nymphaea* -peat from Florida, *Nymphaea* peat from the Okefenokee swamp and *Spaghnum* peat from Maine, has been tested for hydrocarbon sorption [54]. The results show that the Okefenokee *Taxodium*-peat has the highest hydrocarbon capacity attributable to its low fiber content (17.5%), low birefringence organics (20%), high ash content (13%), high guaiacyl lignin pyrolysis products (27.3%) and high furan pyrolysis products (6.3%). The cross linking between the aromatic group of peat-lignin with hydrocarbon has provided sufficient space for the hydrocarbon to be trapped within.

For better oil sorption performance, sorbent pretreatment is sometimes necessary. These include cleaning from the visible impurities such as dust and lump [8], or grinding and sieving of zeolites to get the desired size fraction [37]. Water presoaking of cotton wad for five minutes has reduced its oil sorption capacity suggesting that this presoaking is not a preferable pretreatment. However, once soaked inside the oil bath, there appears to be a process to detach water from the cotton surface. This is assisted by the presence of natural wax on the cotton surface, which facilitate the water detachment and therefore maintain its oil sorption capacity though somewhat reduced by 2-5% [13].

2.6.3 Engineering parameters

The possible interactions between sorbent and sorbate are reversible Van der Waals interactions or irreversible stronger interaction, like direct electron transfer. The strength of this interaction explains the difficulties of sorbent regeneration for further reuse. Sorbent nature selectivity is primarily due to the high accessibility and

the strong surface interaction over certain component in a feed mixture. Several criteria are required to select the best sorbent for removing the specific contaminant [61]:

1. Sorbent capacity that tells how much contaminant is sorbed per unit quantity of sorbent. Highly porous material with high surface area and compatible interaction is usually chosen.
2. The purity requirement of the fluid phase indicates the amount of materials need to be removed.
3. Sorbent selectivity which follows several mechanism:
 - i. Selective binding to the surface
 - ii. Excluding certain component based on its geometry
 - iii. Differences in diffusion rates from the sorbate to the sorbent surface which facilitate by the intra-particle diffusion
4. Method chosen for sorbent regeneration to recover the sorbate inside the sorbent structure. This regeneration or desorption will reduce the sorbent replacement cost, extent the life duration of sorbent and minimize the amount of waste disposal.
5. The sorbent bed volume design which includes the portion of the bed which is not completely saturated when the sorption step is stopped as well as the one that provides sufficient void space inside the bed. The size and bed dimensions influences the mass transfer rate and overall the sorption process.
6. Sorbent deactivation would occur once the sorbent establishes strong interaction with other component beside sorbate which leads to the reduction of lifetime and sorption capacity.
7. Operational cost in choosing the sorbent with the best performance. This cost parameter can be reduced by using less expensive sorbent with the one that can be easily recovered.

CHAPTER THREE

MATERIAL AND METHOD

3.1 Material

3.1.1 Kapok Raw Materials

The kapok used in this study was a product of Malaysia. The kapok was obtained from villager in Bota Kanan district with the price of RM20 (in ringgit Malaysia) for every 1 kg. Before the kapok fibres were used in any studies, all the visible dust and lumps had been removed manually. The kapok fibers were dry (moisture content <1%), light, fluffy, and pale yellow in appearance.

3.1.2 Chemicals and Experimental Oils

Three types of experimental oils were used in this experiment, namely diesel (Petronas D2, Petronas Sdn Bhd.), new-engine oil (Petronas Synthium, Petronas Sdn.Bhd.) and used-engine oil. Diesel oil was used without further purification. Diesel represents low-viscosity oil such as light crude oil, and cooking oil. This oil was investigated in favour of the crude oils or lightweight hydrocarbon oils because it is less volatile and has better compositional uniformity, which minimizes transient change in its chemical and physical characteristics during experiments. New engine oil and used engine oil represent medium and heavy hydrocarbons. The used-engine oil samples were obtained from the local automobile workshop in Tronoh, Perak. Diesel was dyed using Oil red O (Sigma-Aldrich, Germany). Chloroform (Systherm, UK) and NaOH (R&N Chemicals, USA) used as solvent for kapok treatment, were of analytical grade.

3.2 Method

3.2.1 Research flowchart

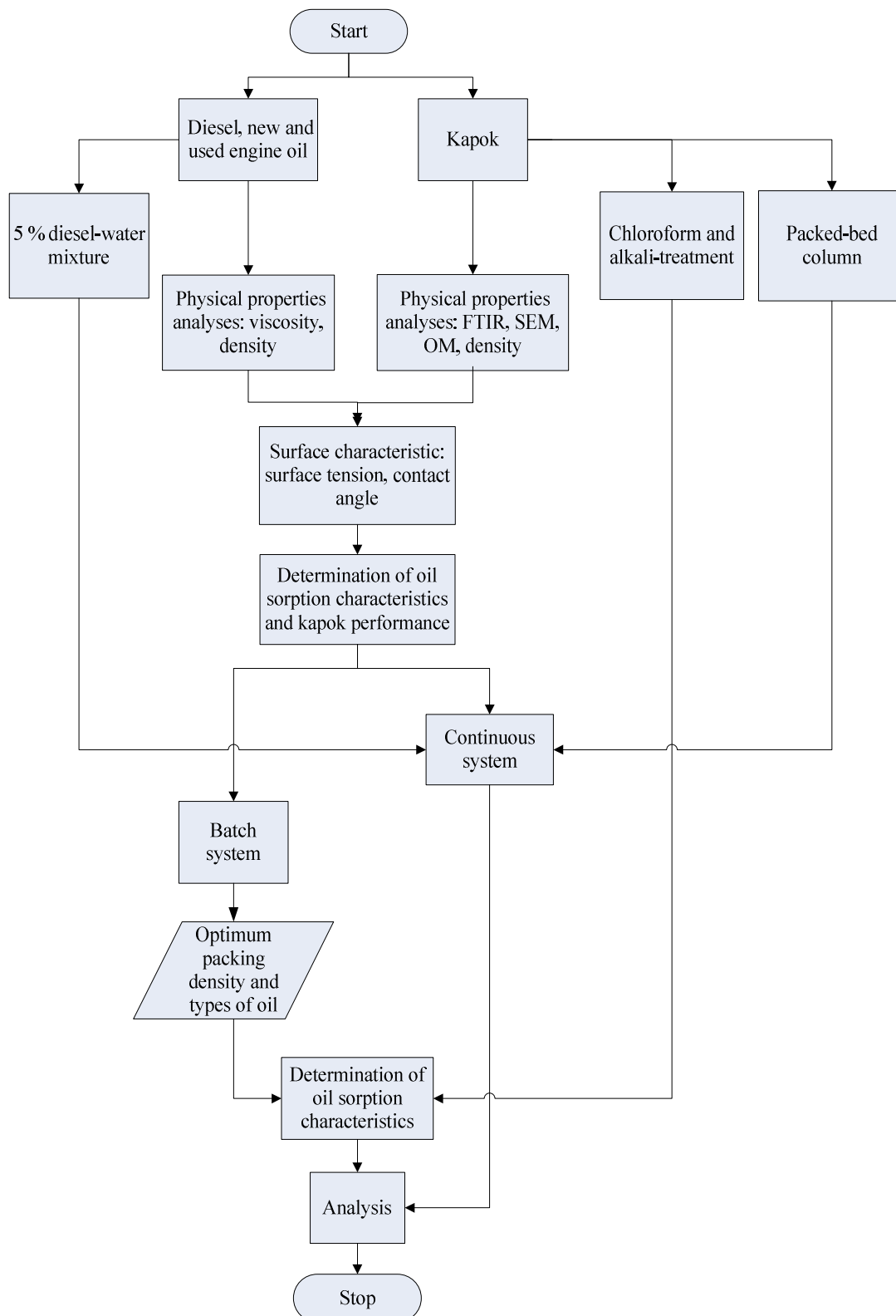


Figure 3.1 Research flowchart

3.2.2 Characterization of Kapok Physicochemical Properties

Kapok physical characteristics as oil sorbent were characterized based on morphology and density. Kapok morphology was analyzed by Scanning Electron Microscopy (SEM, LEO 1430P VPSEM) and Optical Microscopy (Nikon Eclipse ME 600, Japan).

For SEM analyses, the samples were mounted on round stainless steel sample holders with double-sided conductive adhesive tape. To provide a conductive coating that enhances the images under SEM, the samples were sputter-coated using a sputter coater (Polaron SC 764) with Gold (Figure 3.2). SEM images were examined using accelerating voltage at 15 kV. The diameter of kapok fibre was measured using a measuring tool bar inside the SEM instrument computer program.

For OM analyses, small amount of kapok fiber sample for was placed on a glass plate sample holder and observed under halogen lamp. The image was captured using software attached to the OM instrument (Figure 3.3.a). Around 0.5 g of kapok was placed inside the sample cell. Nitrogen was used as the purging gas using a flow mode. Twenty runs were carried out for each density measurement (Figure 3.3.b). Kapok density was measured using Ultrapycnometer 1000 (Quantochrome, USA).

Surface area of kapok fibre was measured using Flowsorbs II 2300 (Micromeritics, USA) as shown in Figure 3.5. About 0.0288 and 0.0029 g of kapok fibre were placed inside the test cell and degass for 30 min before the experiment started. This measurement was based on N₂ gas adsorption at 77 K using a single point BET which involves the continuous flow of a mixture of an adsorptive and carrier gas at atmospheric pressure.

Infrared spectrum of raw kapok was analyzed using Spectrum One FTIR (Perkin Elmer, USA) as shown in Figure 3.5. Kapok fibre, at 2 mg weight, was mixed with 200 mg of KBr and compressed into a pellet by using a hydraulic pump. Two scans were carried out at 400 until 3000 cm⁻¹ wavelength, at resolution of 4 cm⁻¹.

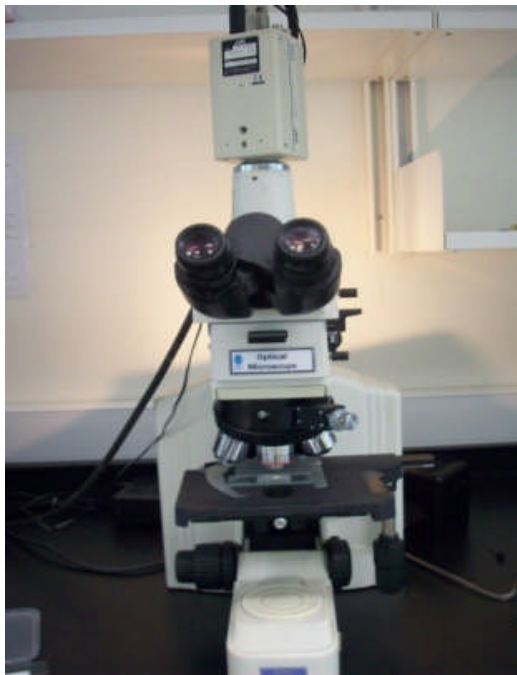


(a)



(b)

Figure 3.2 Instrument for SEM analyses (a) Microscope and electron gun part (b) Sputter coater part



(a)



(b)

Figure 3.3 Instrument for (a) OM imaging and (b) Density measurement



Figure 3.4 Surface area analyzer



Figure 3.5 Instrument for FTIR analyses

Interactions between solid and liquid in the adsorption properties were characterized based on contact angle value and surface tension. Static and dynamic contact angle between extracted kapok walls with the experimental oil, and surface tension were measured using Interfacial Tension, IFT 700 (Vinci Technologies, France) as shown in Figure 3.6. The instrument is equipped with CCD camera to capture image and video of the solid-liquid interface. The contact angle was determined by processing the video frames captured during the measurement.

The value of surface tension is calculated from the drop shape of the image recorded by CCD camera, using the Laplace equation:

$$\Delta p = \frac{2\gamma}{r} \cos \theta \quad (\text{Equation 1})$$

where:

Δp = pressure difference between gas and liquid phase (bar)

γ = surface tension (MN/m)

θ = contact angle ($^{\circ}$)

r = droplet radius (mm)

For both contact angle and surface tension measurement, 1 g of fibre was soaked inside 100 mL of chloroform for 4 hours. The fibres were separated from the liquid by vacuum suction. The extracted liquid was evaporated onto the surface of the test plate inside the viewing cell chamber of IFT 700. One drop of experimental oils was placed on the kapok surface by using hand pump filling system. The measurement was started immediately after the oil drop was captured by the CCD camera.

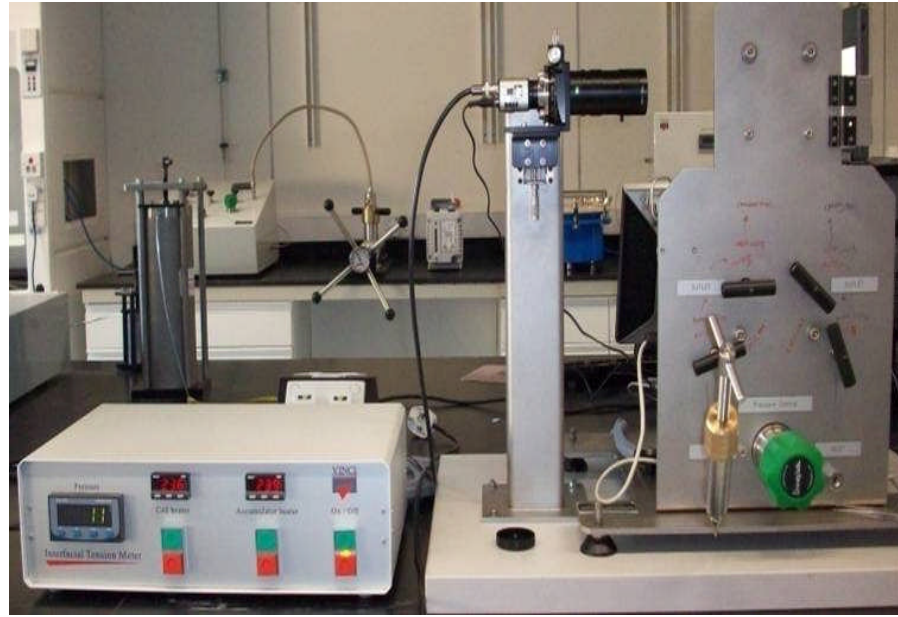


Figure 3.6 Inter-Face Tension, IFT 700

3.2.3 Characterization of Experimental Oils Properties

In addition to surface tension and contact angle, experimental oils (Diesel, Used and New engine oil) were also characterized based on density and viscosity using the instruments as shown in Figure 3.7. Density measurement was carried out using DMA 5000 Density Meter (Anton Paar, Austria). Viscosity of Used and New Engine oil was measured using CAP 2000+ Viscometer (Figure 3.7.a) (Brookfield Engineering Laboratories, Inc., USA).

The viscosity of diesel oil was measured using Cannon-Fenske Routine type for transparent liquid (No.100/N856, Cannon Instrument Co., USA). The measurement was conducted at 25°C. The temperature was maintained during viscosity measurement using waterbath (Labline, USA). Diesel oil was filled inside the viscometer through opening A (Figure 3.8). The oil sample was sucked via rubber bulb suction until above point C. After disconnecting the rubber bulb, the oil sample would flow to point B. The efflux time was recorded from the oil hitting point C until reached point B. To obtain kinematic viscosity (mm^2/s or centistokes, cSt), the efflux time was multiplied by the viscometer constant (0.15 mm^2/s or cSt). For unit

conversion to centiPoise (cP), the viscosity in cSt was multiplied by the density of the oil sample.



(a)



(b)

Figure 3.7 Instrument for measurements of experimental oils (a) density and (b) viscosity

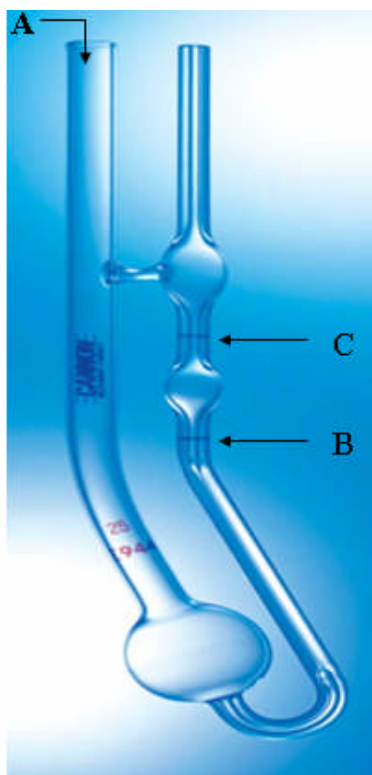


Figure 3.8 Cannon-Fenske Routine Viscometer

3.2.4 Investigation of Oil Sorption Characteristics of Kapok

3.2.4.1 Effect of packing density on oil sorption and dynamic oil retention capacity

The procedure for determining oil sorption capacity generally followed the method F726-99 (ASTM, 1998c) [62]. Loosed-form kapok was packed inside 87.5 cm³ wire-mesh basket and immersed inside an oil bath until it reached the equilibrium stage (Figure 3.9). Several packing densities were tested: 0.02; 0.04; 0.06 and 0.08 g/cm³. The cells were soaked inside 500 mL beaker glass (Pyrex, Germany) filled with 400 mL of experimental oil. Oil that has lower viscosity reached faster equilibrium stage. The test cell were soaked 30 min inside diesel oil, 60 min for fresh and 90 min for used engine oil. The oil-saturated test cells were then lifted and the oil was left out dripping out from the test cell above the oil baths. The transient weight of oil bath were recorded using a balance for each minute of dripping for 30 minutes. The experimental procedure was carried out in 3 times replications and the results were calculated based on mean values. The oil sorption capacity was calculated as shown in Equation 2.

$$\text{Oil sorption capacity} = \frac{(S_I - S_F)}{S_A} \quad (\text{Equation 2})$$

Where:

S_I = the weight of the oil before sorption inside the oil bath (g)

S_F = the weight of oil inside the beaker at 1 min dripping (g)

S_A = dry weight of kapok (g)

The percentage of dynamic oil retention was calculated as follows:

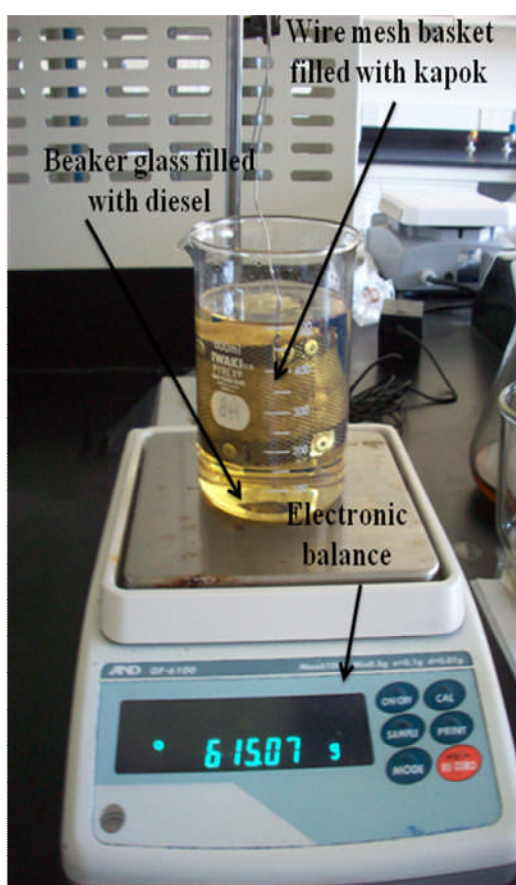
$$\text{Percentage of dynamic oil retention} = \frac{W_t}{W_{t=1}} \times 100\% \quad (\text{Equation 3})$$

Where:

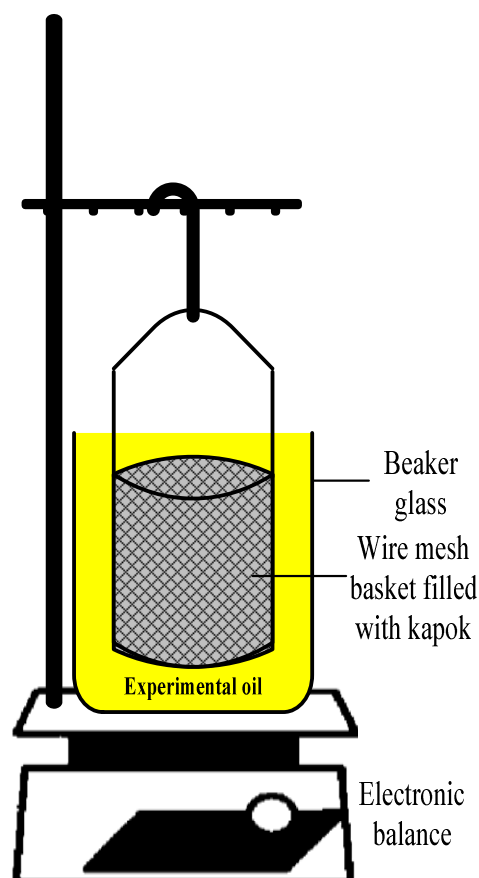
$W_{t=1}$: Weight of oil bath (g) at 1 min dripping

$W_{t=i}$: Weight of oil bath (g) at t min dripping, i = 2, 3, 4, ...

To check the stability of oil entrapment inside kapok assembly after oil sorption, an external force via horizontal shaking was applied. After 30 min of oil dripping, the kapok-filled wire mesh basket, for each packing density, was placed inside a horizontal shaker at 150 rpm for 30 min. Only kapok that have been soaked inside diesel and used engine oils investigated. They were chosen due to their significant difference in viscosity. Weight difference of the test cell was recorded.



(a)



(b)

Figure 3.9 Experimental design for oil sorption and dynamic oil retention capacity

3.2.4.2 Effect of packing density on saturation time and bed height drop

Plastic syringe of 35 mL volume was fabricated as a column to study the effect of packing density on saturation time and bed height difference (Figure 3.10). Kapok was packed in a 20 mL volume of the designated column to give packing densities of 0.02; 0.04; 0.06 and 0.08 g/cm³. Experimental oil of 20 mL volume was poured into the column until saturated. The saturation point was noted from the appearance of the first oil droplet from the column tip. The saturation time is calculated from the time the oil was poured into the column until the saturation point. Bed height difference was measured from the initial bed height until the height after no remaining oil was observed dripping out of the column.

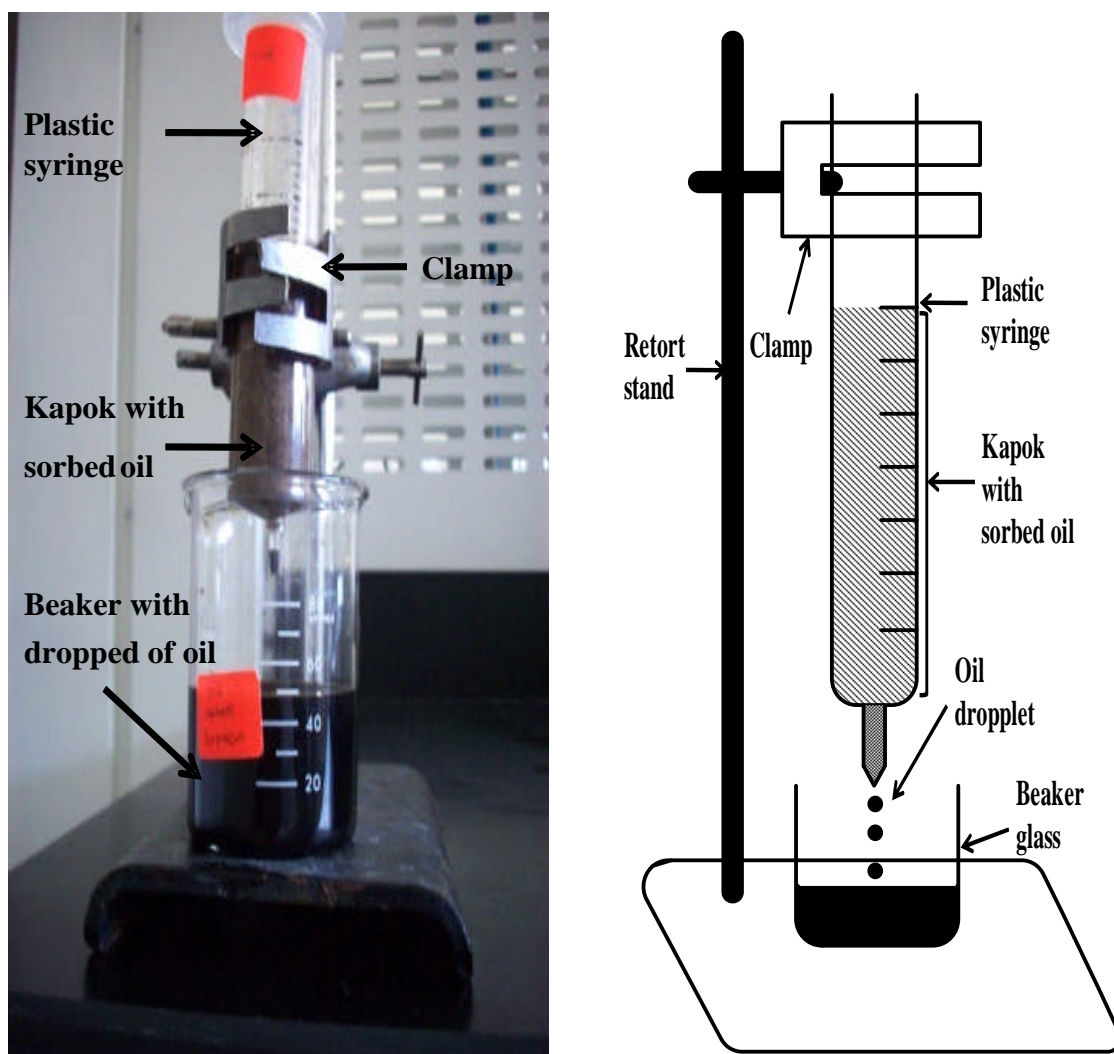


Figure 3.10 Experimental setup for investigating the effect of packing density on saturation time and bed height difference

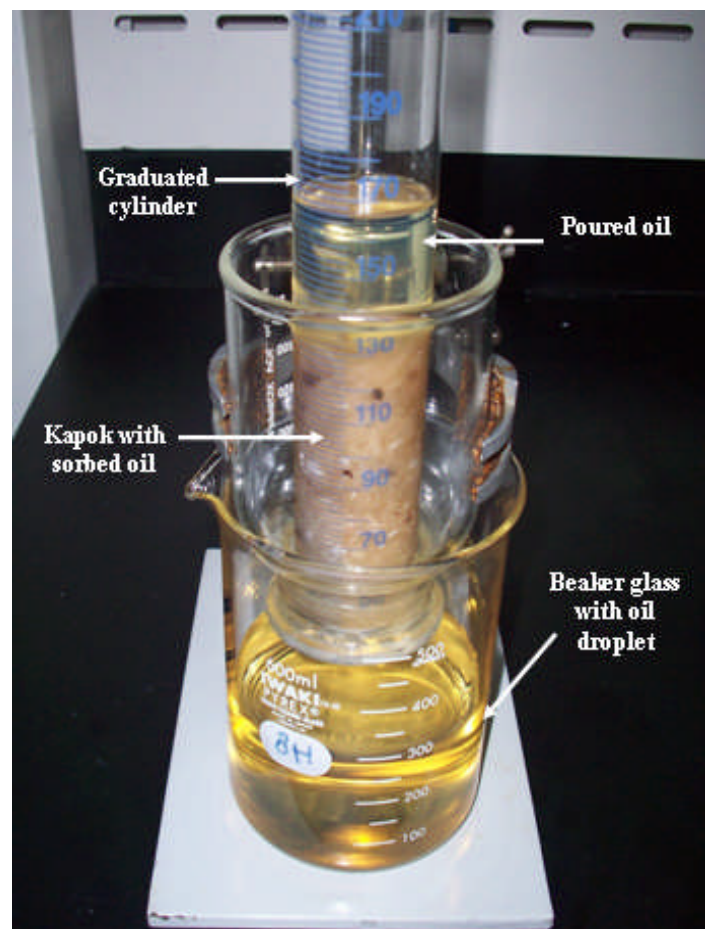


Figure 3.11 Experimental design to test kapok reusability for sorption process

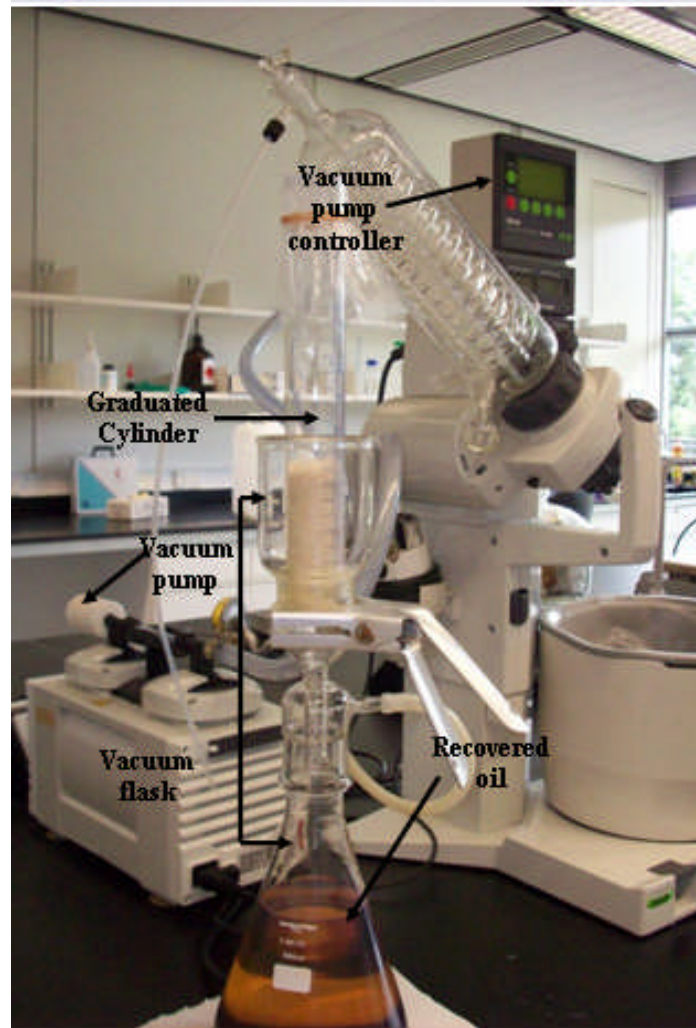


Figure 3.12 Experimental setup to test kapok reusability for desorption process

3.2.5 Evaluation of kapok reusability

The kapok reusability was tested using a 250 mL graduated glass column packed with kapok at 0.04 g/cm^3 in 100 mL volume (Figure 3.11). Diesel oil of 100 mL volume, was poured into the column until saturation point. Free dripping of oil was allowed for 15 min duration before applying a pressure difference via vacuum pump (BUCHI Vacuum Controller V-800, Germany) at 525 mbar every 10 minutes interval for 3 times. The weight of the glass column filled with kapok and the amount of oil pumped out was measured in each cycle. Saturation time and bed height difference were also observed after each cyclic sorption-desorption cycle. The desorption experimental setup is shown in Figure 3.12.

3.2.6 Evaluation of Kapok Column Process Design Parameters for Oily Water Filtration

3.2.6.1 Experimental setup

Customized column made from acrylic of 2 cm diameter and 15 cm length was developed as a kapok fibre packed-bed column. Wire mesh of 1 mm opening was used as the perforated disk and placed in the two column ends. Rubber stopper with tubing joint sealed the two ends. The overall experimental setup is shown in Figure 3.13. Blender (Philips, UK) mixing for 15 minutes at high speed was used to produce diesel-water mixture with 5 % (w/w) concentration and total weight of 475 g was used in each set of experiment. The mixture was blended at high speed for 15 minutes in a blender (Philips, UK) to produce a homogenous mixture.

Two parameters were studied to evaluate the kapok performance for oily water filtration, packing density and flow rate (Table 3.1). Two-way factorial design was developed as shown in Table 3.1. Before column loading, the diesel-water mixture was agitated with stirrer at 500 rpm (Heidolph, Germany). This is to ensure a well-mixed diesel-water mixture. The liquid feed of diesel-water mixtures were drawn from inlet tank out into the column by a dosing pump (Grundfos, Denmark). The experiment deemed started when the first drop of liquid feed entered the column. Filtrate samples were collected every two minutes, starting from the water breakthrough. The breakthrough time was monitored when a visible blob of oil free-phase appeared in the outlet stream corresponding to the end of the filtration process. [2, 7].

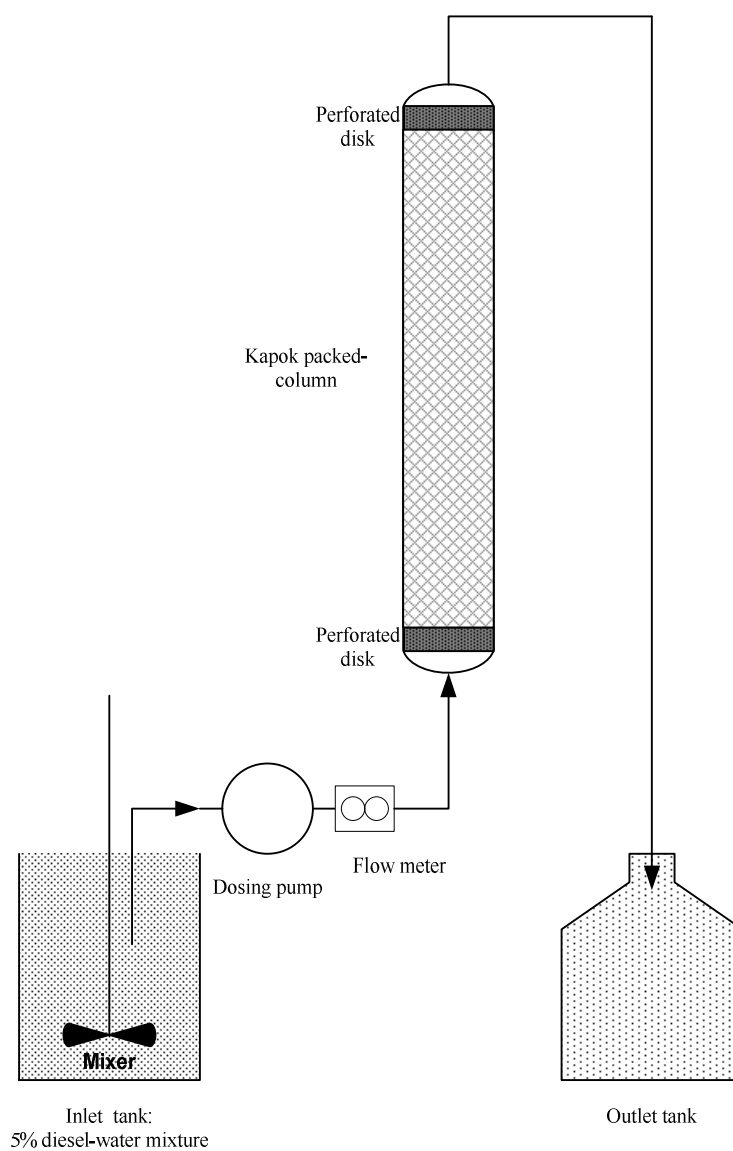


Figure 3.13 Experimental setup for oily water filtration of kapok

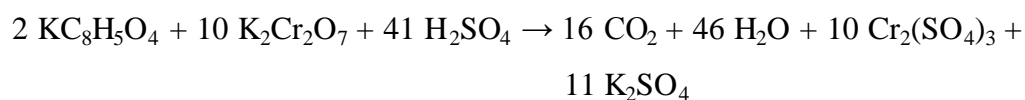
Table 3.1 Experimental design for oily water filtration experiment

Run	Packing density (g/cm ³)	Flow rate (L/h)	Packing density	Flow rate
1	0.04	1.0	-	0
2	0.04	0.5	-	-
3	0.08	1.5	+	+
4	0.08	1.0	+	0
5	0.06	0.5	0	-
6	0.04	1.5	-	+
7	0.06	1.0	0	0
8	0.08	0.5	+	-
9	0.06	1.5	0	+

Chemical Oxygen Demand (COD) Analyses

By definition, COD is “ a measure of the oxygen equivalent of the organic matter content of a sample that is susceptible to oxidation by a strong chemical oxidant” [63]. By using a strong chemical oxidant in an acid solution and heat, the organic carbon can be oxidized into CO₂ and H₂O. The amount of oil content inside the sample effluent was quantified by means of COD. To measure the COD values (mg/L), combination of several reagents as mentioned below are required:

1. Potassium dichromate in a 50% sulfuric acid solution as the oxidizing agent. The amount of oxygen used will be equivalent to the amount of organic matter oxidized. The color of the dichromate ions is orange-brown and will be changed into green solution when it is oxidized into chromic ion, which will increase as the COD concentration increases. The oxidizing reaction is given as:



2. Silver compound as a catalyst to enhance the oxidizing of special class of organic compound, such as straight-chain aliphatic.
3. Mercuric compound addition is used to overcome the interference from oxidation of chloride ions. The presence of chloride ions will reduce the performance of silver compound as a catalyst by forming insoluble compound, silver chloride. By adding the mercuric sulfate, chloride ions will be masked by this reagent.



Figure 3.14 COD Thermoreactor DRB 200



Figure 3.15 Spectrophotometer HACH DR 5000 for COD absorbance measurement

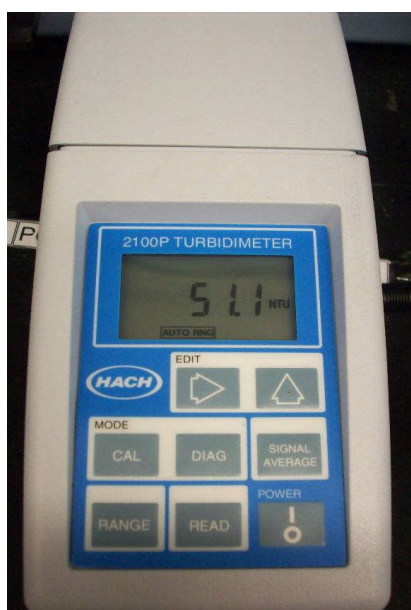
The COD vials, supplied by HACH, USA, come complete with the concoction of the three combinations as described above. Sample of 50 μL with 1950 μL of water were added into the COD vials using a micropipette (Eppendorf, Germany). Low range COD vials were used. After mixing, two hours heating of the vial in a 150°C reactor (DRB 200 HACH, USA) (Figure 3.14) was carried out. After the heating step, the vial was cooled at room temperature. The COD values (ppm)

were measured by colorimetric method in a spectrophotometer at 420 nm (Spectrophotometer DR 5000, HACH, USA) (Figure 3.15).

Turbidity Analyses

Turbidity measurement is based on the behavior of the suspended matter inside the sample irradiated with light. Generally, the suspended matter will scatter or absorb the light radiation. Light that emerges from the sample will be directed to a photometer that quantifies the light absorbed. There are two types of turbidimeter, the Jackson turbidimeter which is based on the absorption principal and the Nephelo turbidimeter which is based on the light scattering from the sample with Nephelometric Turbidity Unit (NTU) for its unit [64]. Light source illuminates the sample and the photometric detectors are connected whilst a reader quantifies the intensity of the scattered light at 90° angles to the path of the incident light [64, 65].

The turbidity of about 5 mL samples measurements were carried out by using DR 2100 P Turbidimeter (HACH, USA) (Figure 3.16.a) inside a cuvette (Figure 3.16.b). The turbidity of the sample before and after filtration process was measured, using water as a blank solution.



(a)



(b)

Figure 3.16 Instrument for turbidity analyses (a) Turbidimeter 2100P, (b) cuvet

3.2.6.2 Statistical analyses

The statistical analyses were performed using Statgraphic® Plus Professional Version 5 (2005), Rockville, USA. Three levels of experimental factors - low, high and medium, were applied in this design (Table 3.1). The COD, percentage of COD reduction, turbidity and percentage of turbidity reduction are the evaluated response. Pareto charts and contour surface response were constructed to find out the interaction that has significant effect on the kapok packed-bed performance. Regression analysis data on COD, COD reduction, turbidity and turbidity reduction follows a second-order polynomial equation as described by Equation (4). The true values of the unknown parameters are represented by the β_o , β_i , β_{ii} , and β_{ij} coefficients.

$$y = \beta_o + \sum_{i=1}^k \beta_i x_i + \sum_{i=1}^k \beta_{ii} x_i^2 + \sum_{i < j} \sum \beta_{ij} x_i x_j + \varepsilon \quad (\text{Equation 4})$$

3.2.7 The effect of chloroform and alkali treatment on kapok oil sorption characteristics

Soxhlet extraction using chloroform and alkalization using 1% (w/w) NaOH were chosen were carried out to identify the major factors contributing towards the kapok hydrophobic-oleophilic properties and the stability of kapok waxy surface. Kapok with 5 g of weight was added into either 200 mL of chloroform or 125 mL of NaOH. Reflux method was used for the alkalization treatment. The duration of extraction for both chloroform and alkali treatment were 4 and 8 hours.

Extracted liquid and kapok was separated using vacuum suction (BUCHI, Germany) for 10 minutes. Kapok was then dried inside drying oven (Mettler, Germany) at 61°C for 24 hours. The functional group of the treated-kapok was analyzed using FTIR spectrophotometer as described in Section 3.2.2. The oil sorption capacity and percentage of dynamic oil retention of extracted kapok were determined using the procedure as described in section 3.2.4.3. Packing density of 0.04 g/cm³ and diesel oil was tested in this study.

CHAPTER FOUR

CHARACTERIZATION OF THE PHYSICOCHEMICAL PROPERTIES OF KAPOK AS OIL SORBENT

The addition of absorbents to oil spill areas facilitates a change from liquid to semi-solid phase which followed by further final sorbent disposal or recycled by oil drawn out from the sorbent structure. From environmentally engineering point of view, natural absorbent materials are attractive because of the possibility of collection, complete removal of the oil from the oil spill site, and the sorbent easy disposal with least environmental hazard. Ideally, oil sorbent must both be hydrophobic and oleophilic. Besides that, other characteristics that must be fulfilled for oil sorbent material include high sorption capacity, high uptake rate, capability to retain oil inside its structure, ease of recoverability, and high reusability rate [4, 8, 38].

Physicochemical properties of natural sorbent and the experimental oils need to be characterized to assist in the design strategies for field application. Contact angle and surface tension are important parameters to evaluate the interactions between sorbent-adsorbate for oily water treatment. The design parameters for operational and economic consideration include the oil sorption capacity, percentage of dynamic oil retention, saturation time, packing height drop and the reusability of the sorbent. These characteristics in essence describe the nature of each sorbent and should correlate with their hydrophobic-oleophilic properties.

4.1 Characterization of Kapok Properties

Functional group analyses of kapok fibre before and after treatment were carried out by radiating the kapok sample mixed with KBr pellet with the infra red light. Infra red radiation is absorbed by organic molecule and used it as energy for molecular vibration. When the infrared energy radiant matches the vibration energy, the absorption occurs. Typical infrared spectrum is plot of percentage transmittance or

absorbance against wavelength number (cm^{-1}). Percentage transmittance is the ratio between final intensity with the initial intensity after radiation on the organic compound. Percentage transmittance is the ratio between final intensity to the initial intensity, after irradiation of the organic compound.

Kapok is a lignocellulosic material whose surface is covered by hydrophobic waxy coating [66]. The chemical composition of kapok harvested from the Philippines and Southern Vietnam analyzed by Hori and co workers (2000) suggest the presence of the following component: cellulose (35% dry fibre), xylan (22%) and lignin (21.5%). Kapok fibre is also characterized by high amount of acetyl group content (13%). Functional group analysis using FTIR spectrophotometer could give general information about the constituents of the kapok fibre.

The infrared spectrum of raw kapok used in this study is shown in Figure 4.1. Table 4.1 shows the assignment of infrared bands for typical plant [26, 67]. At 2918 cm^{-1} , a well-pronounced trough was observed which corresponds to the asymmetric and symmetric aliphatic CH_2 and CH_3 stretching. This can be associated with the presence of plant wax, which generally consists of n-alkanes, smaller portion of alcohols, fatty acids, aldehydes, ketones and n-alkyl esters [2, 68]. The bands around 1736 , and 1242 cm^{-1} were due to the presence of carbonyl group ($\text{C}=\text{O}$) in the ester bonds [2]. The $\text{C}=\text{O}$ stretching vibrations are believed to be associated with the aliphatic aldehydes, esters and ketones of kapok wax. Intensive band around 1510 cm^{-1} corresponds to C-O stretching in lignin. The band at 1050 cm^{-1} is within the region of carbohydrate or polysaccharides [2].

The FTIR spectra as shown in Figure 4.1 indicate all the components of kapok as a lignocellulosic material with hydrophobic waxy coating, similar to that reported previously [2, 6, 8]. The chemical composition of kapok harvested from the Philippines and Southern Vietnam analyzed by Hori and co workers (2000) further suggest the presence of the following components: cellulose (35% dry fibre), xylan (22%) and lignin (21.5%). Kapok fibre is also characterized by high amount of acetyl group content (13%). An infrared spectrum pattern of cotton similarly suggests the band for CH stretching of CH_2 and CH_3 as observed at 2891 cm^{-1} . An infrared

spectrum pattern of cotton comparable to our study, is reported [67]. The band for CH stretching of CH₂ and CH₃ is observed at 2891 cm⁻¹. The presence of carbonyl C=O stretching of ester and C-O stretching of acetyl group bands are monitored, at 1745 and 1234 cm⁻¹ respectively. Both of these bands are associated with the presence of plant wax. At 1017 cm⁻¹, C-O stretching band corresponding to the presence of cellulose, hemicellulose and lignin is also observed. Cotton is also a lignocellulosic material with hydrophobic waxy coating. The presence of waxy coating on the cotton surface has caused untreated cotton difficult to be spun.

Table 4.1 Assignment of infrared absorption bands

Frequency (cm ⁻¹)	Assignment
2918	CH stretching of CH ₂ and CH ₃ group
1750	Carbonyl C=O stretching of ester
1643	H-O-H of absorbed water
1604	C=C stretching
1508	C-H bending of aromatic group
1425	OH and CH ₂ bending
1375	C-H bond in -O(C=O)-CH ₃ group
1330	CH ₃ bending or OH in-plane bending
1247	C-O stretching of acetyl group
1161	C-O-C anti symmetric bridge stretching in cellulose and hemicellulose
898	B-glucosidic linkages between the sugar units in hemicelluloses and celluloses
669	OH out-of-plane bending and/or atmospheric CO ₂ (deformation vibration) contamination

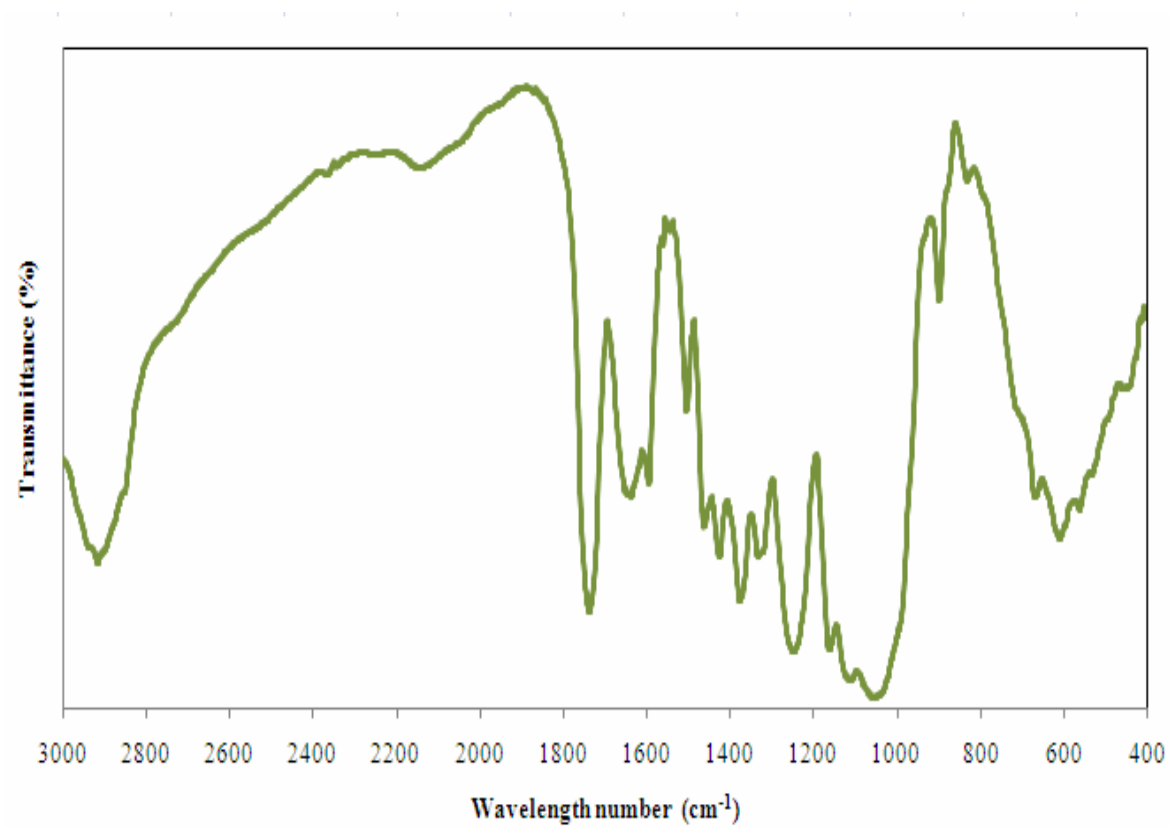
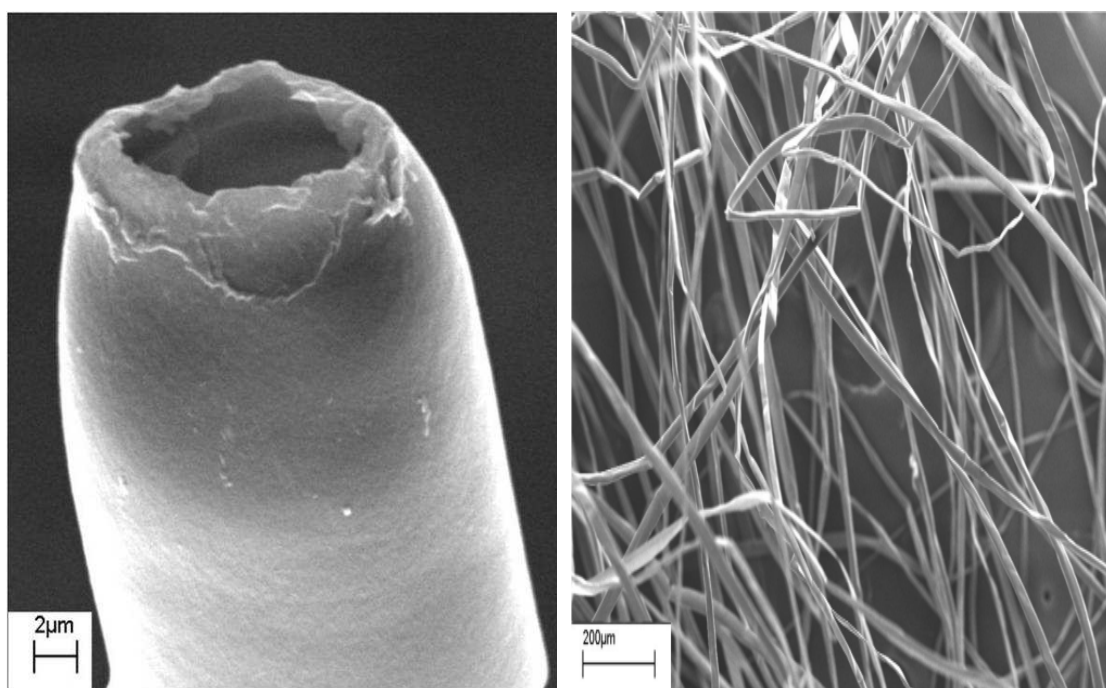


Figure 4.1 Infrared spectrum of raw kapok



(a) (b)
Figure 4.2 SEM images of (a) single and (b) cluster of kapok fiber



Figure 4.3 Optical microscope image of kapok before oil sorption

Kapok microstructures as analyzed by SEM (Figure 4.2) exhibit hollow tubular structures (or lumen) with average external diameter of $21.5 \pm 6.5 \mu\text{m}$. OM image (Figure 4.3) shows transparent channel of kapok. As shown in Table 2.3, kapok originated from Thailand has smaller average external diameter of $16.5 \pm 2.4 \mu\text{m}$ as compared to kapok originated from Malaysia in this study. Raw kapok fibres show smooth surfaces, with density of 1.3 g/cm^3 . The network of hollow structure could provide ample interspatial area for oil to be retained and trapped within the kapok assembly. Clusters of kapok fibre show rod-like structure with similar fineness correlating well to the configuration of each fibre. This architecture of fibre network also provides uniform distribution of absorbed oil inside the kapok fibre. As shown in Figure 2.9, milkweed floss also has similar structure as kapok fiber [14], and it has been suggested to provide sufficient space for oil entrapment.

Surface area analyses of kapok fibre were conducted using a single point BET method utilizing N_2 gas adsorption. The surface area of kapok fibre with two different weights were measured for repetition. Based on the BET analyses, the kapok fibres have specific surface area of $35.81 \text{ m}^2/\text{g}$. During the N_2 gas adsorption, the entire kapok fibre surface was vacuum dried or degassed. This degassing process led to the removal of the intramolecular water molecules which followed by the collapsing cellulose chains and difficult to be replaced by N_2 molecules [69]. Hence the analyses only include the external surface of kapok fibre, where in this case only the wax surface without including the hollow structure and the interfibre pores. As a result, the value of the specific surface area does not represent its true value. This low value of specific surface area does not explain the high oil sorption capacity of kapok fibre which concludes that other mechanism must be responsible. Choi and co workers suggest that the space inside or between fibre is generally responsible for most of the sorbent capacity [14]. The oil adsorption mechanism based on the fiber capillaries of kapok fibre will be discussed in sub chapter 4.3. BET analyses of cotton fibre also obtained a similar results which its specific surface area does not represent the true values [70]. The same result for cotton also occurred due to the BET method only measured the external surface area of cotton. Hence, the interfibre capillaries also proposed as the main adsorption mechanism of cotton sorbent.

4.2 Characterization of Experimental Oils Properties

Table 4.2 shows experimental oil characteristics based on density, viscosity, surface tension and contact angle. Diesel showed both lower density and viscosity than fresh and used engine oil, but used engine oil is the most viscous. All the three experimental oils had lower density than water, causing the oil to float on water surface. The oil density value could influence the oil sorption characteristic where oil with higher density could result in the sorbent having higher oil sorption capacity. Viscosity on the other hand determines the flow resistance of the oils inside the sorbent structure. Oil with lower viscosity flows at a faster rate than the more viscous one resulting in shorter sorbent soaking time. Oil with the lower viscosity therefore drains out at a faster rate and the sorbent system reaches equilibrium sooner than the system having oil with higher viscosity.

Table 4.2 The physical properties of experimental oil

Experimental Liquid	Density at 25°C (g/cm ³)	Viscosity at 25°C (cP)
Water	1.001	0.8
Diesel	0.839	6.5
New engine oil	0.865	165.7
Used engine oil	0.883	260.8

Table 4.3 The surface characteristics of kapok

Experimental Liquid	Surface tension (MNm ⁻¹)	Contact angle (degree)
Water	66.0	102.0
Diesel	12.8	24.9
New engine oil	23.5	21.4
Used engine oil	19.3	36.8

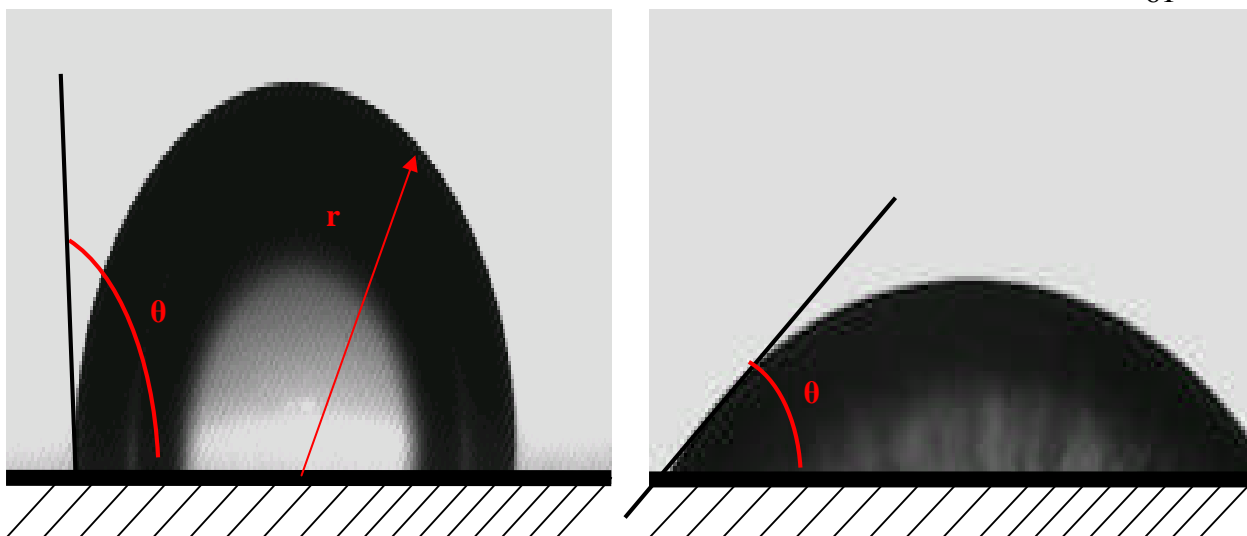


Figure 4.4 Sensile drops technique for contact angle determination (a) high and (b) low contact angle value with r : droplet radius, θ : contact angle

Solid-liquid phase interactions between sorbents and experimental oils were quantified based on contact angle. Sensile drops technique was applied for the contact angle determination using IFT 700 instrument. The captured image from the IFT instrument is shown in Figure 4.4. Liquid forms a droplet on the surface of the sorbent, and is not considered as the wetting liquid when the $\theta > 90^\circ$. At $\theta < 90^\circ$, a liquid tends to spread onto the surface of the sorbent and serves as the wetting liquid. As shown in Table 4.2, the three experimental oils can be classified as the wetting liquid for the kapok sorbent as $\theta < 90^\circ$. While diesel has the lowest surface tension, water on the other hand shows high surface tension at $66 \text{ MN}^{-1}\text{m}$ with $\theta < 90^\circ$. Surface tension is the resultant intermolecular force when one fluid exerts on another surface or liquid. Low value of surface tension suggests that oil could penetrate the kapok tubular structure and remain trapped within the solid sorbent. Water is prevented from penetrating the kapok fibre structure due to high surface tension. Waxy kapok surface is therefore a water repellent (hydrophobic) and an oil attractant (oleophilic), resulting from this complex interactions between oil and kapok properties.

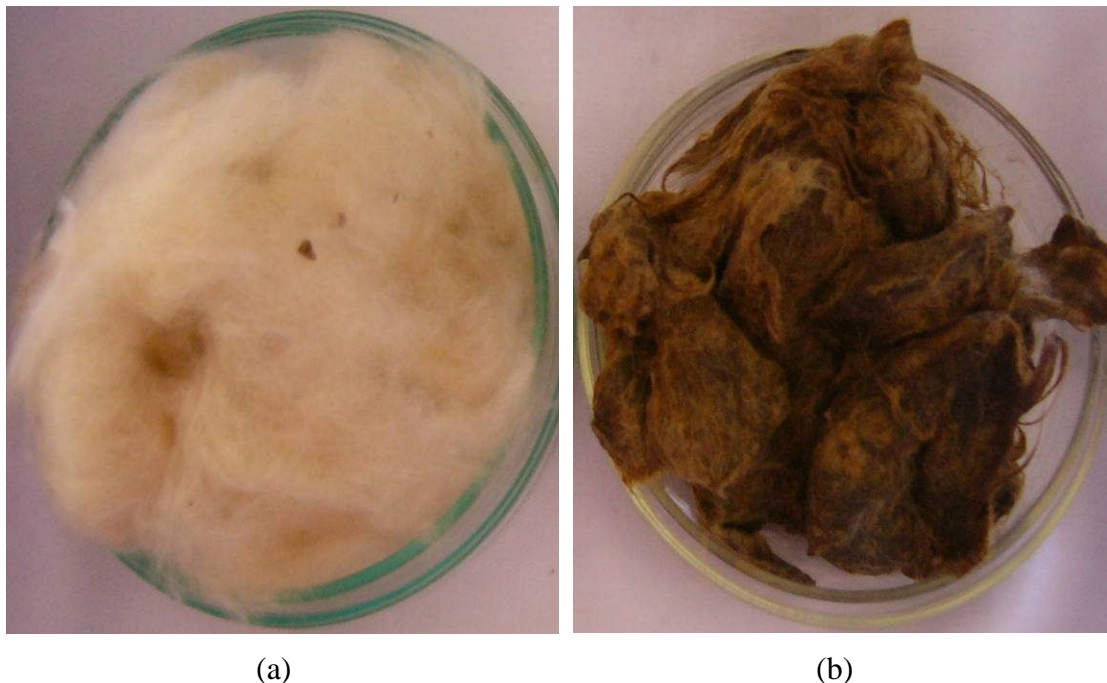


Figure 4.5 Physical appearance of kapok (a) before and (b) after sorption

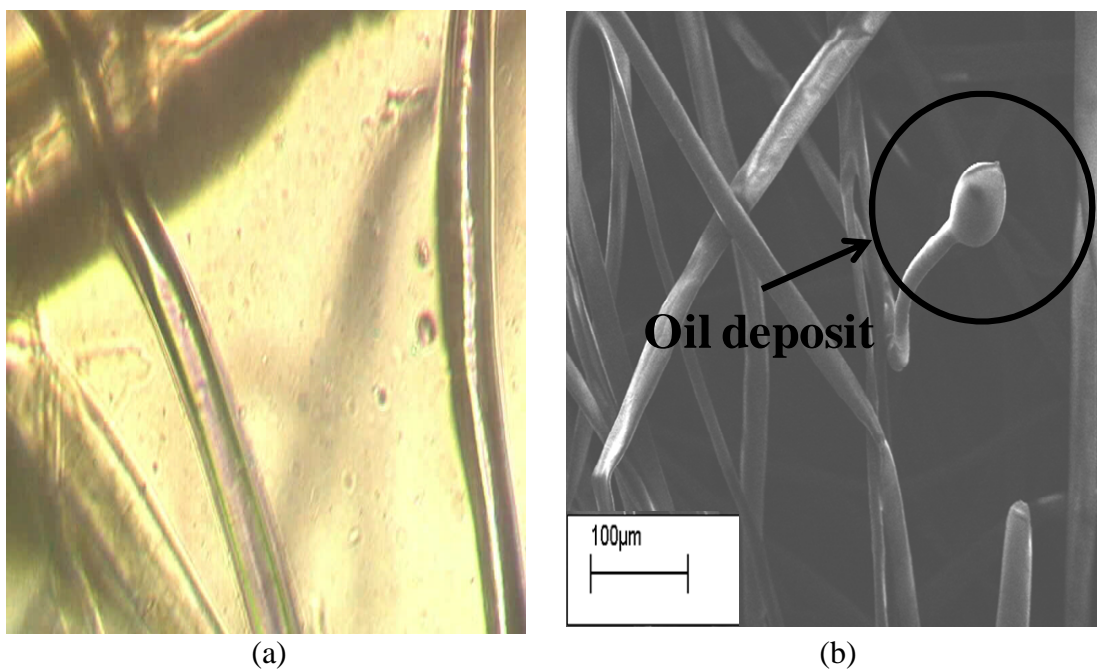


Figure 4.6 Image of kapok after oil sorption by using (a) OM and (b) SEM

4.3 Oil Sorption Experiments

4.3.1 Effect of packing density on oil sorption capacity

Transparent channels were observed before the oil sorption inside kapok assembly (Figure 4.3). After two weeks sorbed with oil and then allowed the oil to drip out, the colour and physical appearance of kapok fibre changed (Figure 4.5). The used engine oil changed the colour from transparent white into yellowish-brown. However, the kapok tubular structure appeared to remain intact as confirmed by OM and SEM observation (Figure 4.6a,b). The colour change may suggest the oil entrapment inside the hollow structure indicating the ability of experimental oil to penetrate the kapok tubular structure and overcome the surface tension. The conserved structure could be the reason behind the excellent oil sorption capacity of kapok.

The capacity of kapok to retain the absorbed oil during the transfer and handling operation is important parameters for sorbent evaluation. Table 4.4 shows the oil sorption of kapok at various packing density. At 0.02 g/cm^3 , kapok showed highest sorption capacity of engine and used-engine oil at 47.4 and 50.8 g oil/g sorbent, respectively, while diesel has the lowest capacity at 36.7 g oil/g sorbent. By increasing the packing density two-fold to 0.04 g/cm^3 , the oil capacity was reduced by almost two-fold. At 0.08 g/cm^3 , there was an almost four-fold reduction. Hence, the higher the packing density, the lower the oil sorption capacity will be. Although the amount of oil sorbed per unit mass decreases with increasing density, the mass and volume of sorbed oil for each different packing density is actually not significantly different (Figure 4.7). There is a probability that there is a maximum capacity in which kapok fibre can trap oil within its structure.

The higher sorption capacity of oils than diesel is a result of engine oil being heavier than diesel within the same unit volume. The order of increasing oil sorption capacity is actually based on the density value [8]. It appears that the higher the packing density, the less loosely packed it becomes, the harder the oil can absorb through. It suggests for the availability of lumen network with the inter fibre pores

located in the kapok microstructure, for kapok to be effective as oil sorbent. In addition, by increasing the value of packing density four fold, void fraction (percentage ratio of kapok fibre volume to wire mesh basket volume, at specific packing density) is not increased linearly, but reduced by 5 % as shown in Table 4.5. At 0.02 g/cm^3 , due to the loosely-packed fibre together with the hollow structure, void fraction may be mainly as a consequence of inter fibre pores. In contrast, at 0.08 g/cm^3 , due to a more compact architecture, and lesser amount of inter fibre pores, the void fraction may instead be contributed more by the presence of hollow structure.

High sorption capacity of kapok is also a result of hydrophobic waxy coating on the kapok surface. The waxy coatings increase the kapok compatibility with the experimental oils based on their characteristic similarities (hydrocarbon group). At the initial stage of oil absorption onto the kapok surface, the hydrophobic interactions and Van der Waals forces could play important role between the experimental oils and waxy surface coating. Chemical compatibility between oil and kapok wax surface provides minimum energy barrier for oil to penetrate inside the fibre tubular structure through minimum surface tension and contact angle. After minimum energy barrier is overcome, void fraction availability would predominantly affect the oil sorption capacity of the fibre at specified packing density. The presence of effective space inside the kapok assembly determines the oil sorption capacity. Higher amount of effective space will increase the oil sorption capacity of the kapok assembly which is achievable at low kapok packing density.

Table 4.4 Oil sorption capacities of kapok at various packing densities for different experimental oils

Packing density (g/cm ³)	Oil sorption capacity (g oil/g sorbent)		
	Diesel oil	Used engine oil	New engine oil
0.02	36.7	50.8	47.4
0.04	20.8	25.4	25.1
0.06	13.9	16.8	15.9
0.08	10.8	12.2	12.1

Table 4.5 Void fraction of kapok at various packing densities

Packing density (g/cm ³)	Void Fraction (%)
0.02	98.5
0.04	96.9
0.06	95.4
0.08	93.9

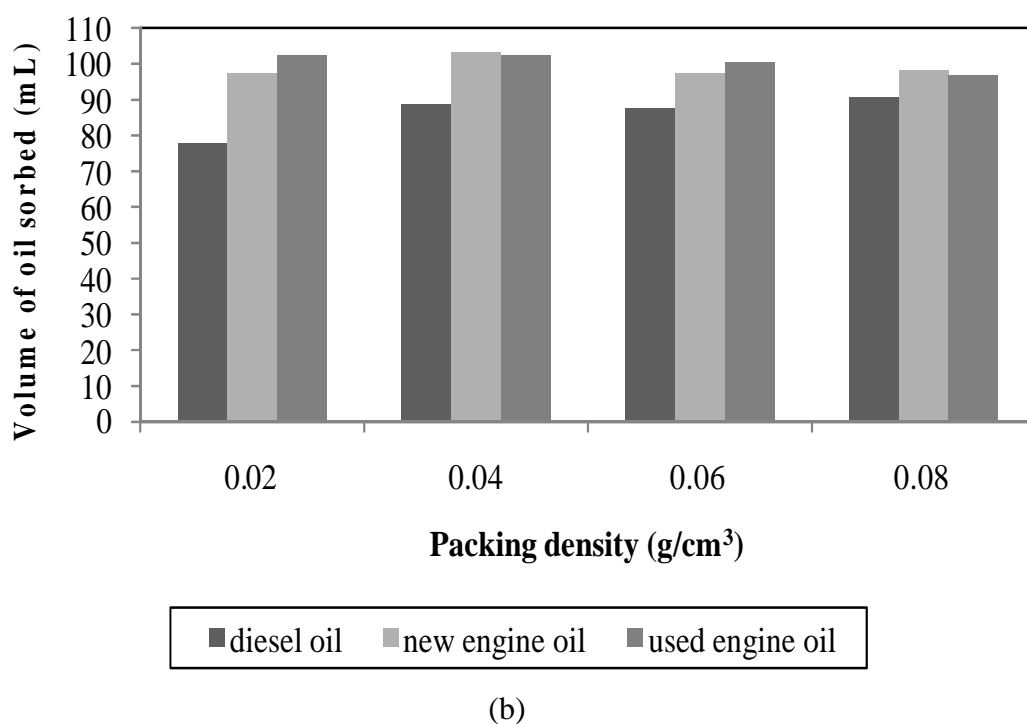
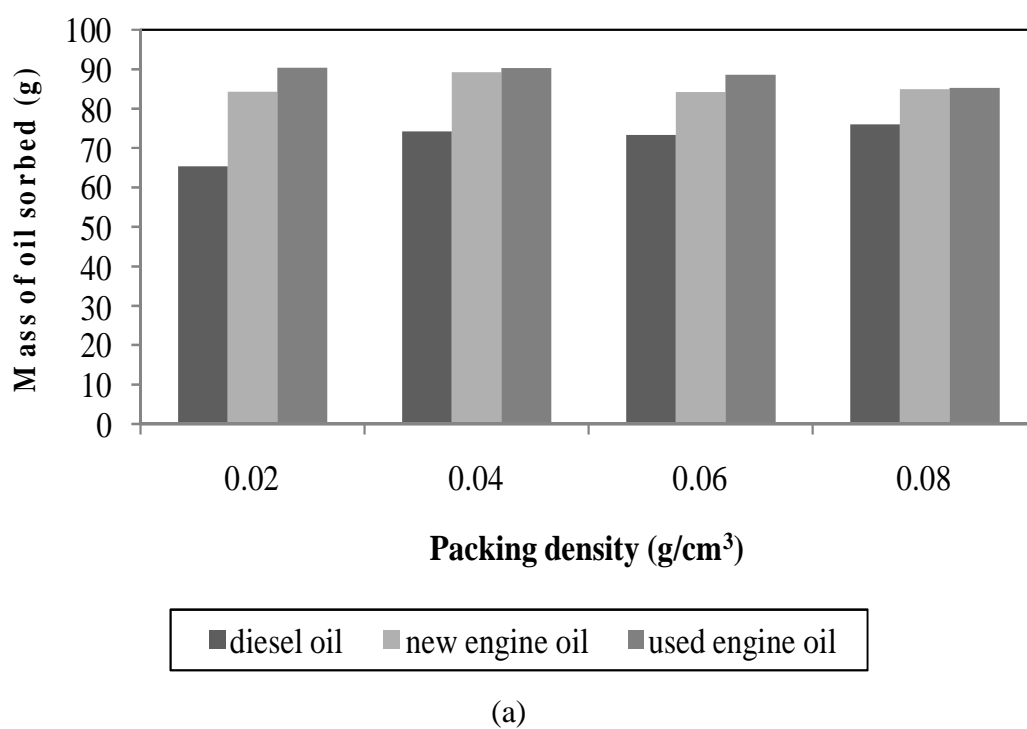


Figure 4.7 Effect s of packing density on the amount of sorbed oil inside kapok assembly as expressed in (a) mass and (b) volume

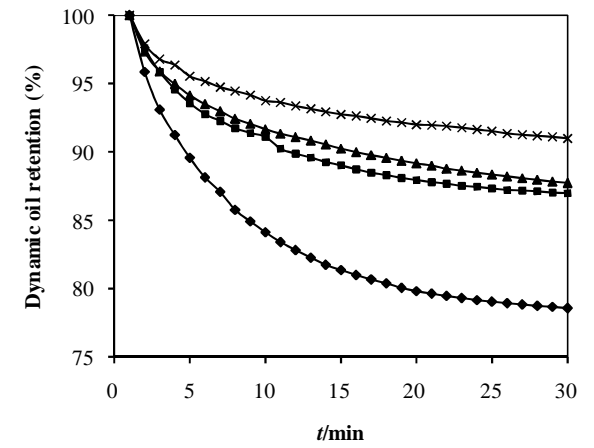
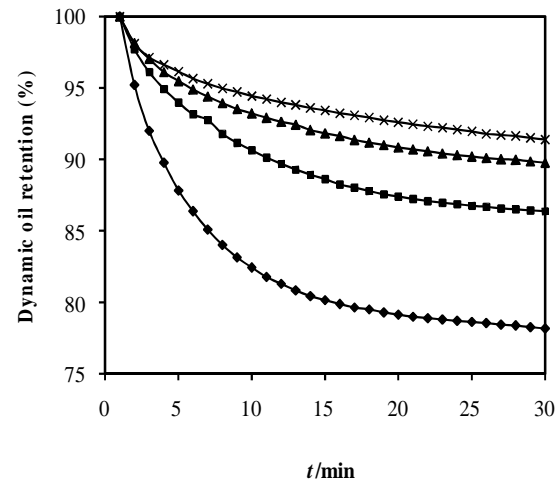
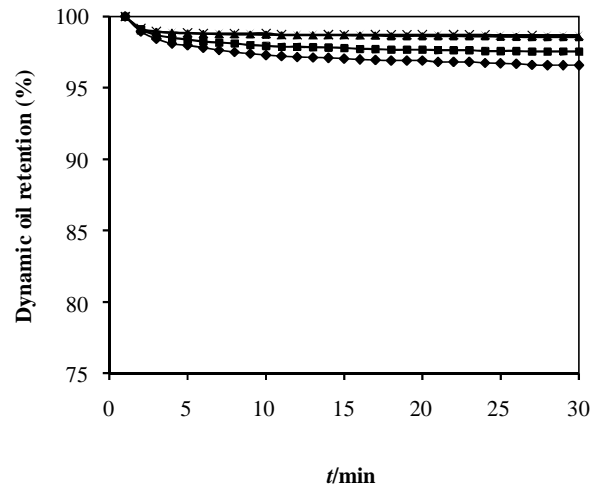
4.3.2 Effect of packing density on percentage dynamic of oil retention

The oil properties such as contact angle, surface tension, density and viscosity, together with fibre oleophilicity, determine the oil sorption and retention capacity of kapok assembly. The capability to retain oil within its structure is one of the important parameters for sorbent evaluation. The dynamic oil retention of kapok at various packing density over time interval was measured. This was done by allowing oil to drip from the test cell for a specified duration. For diesel oil (Figure 4.8a), the amount of oil readily dripped out at any packing density was lesser than new and used engine oil. Between, 96-99 % of diesel oil still retained. There appears to be a correlation between the percentage of oil retention and packing density within 0.02-0.08 g/cm³ packing density. With new and used engine oil (Figure 4.8b,c), only 78% of the absorbed oil remained at 0.02 g/cm³ density, and more than 90 % of oil retained at 0.08 g/cm³ packing density.

At lower packing density, higher amount of oil would drip out from the kapok assembly as compared to the more packed assembly. Similar result has been reported by Lim and Huang [8]. The draining process happens due to instantaneous dripping of oil from kapok assemblies in the wire mesh-test cell, and the oil draining out from the extra-lumen liquids. The draining occurs as the capillary pressure is insufficient to hold the weight of the oils. Capillary pressure is a function of surface tension, capillary diameter and contact angle between solid-liquid interfaces. With packed-assembly, the stabilization force comes from the capillary pressure inside the tubular structure. Loosely-packed kapok has the tendency to allow higher percentage of oil dripping out due to the larger inter-fibre distances that destabilize the liquid bridges between the fibres [13]. Most heavy oils trapped inside the inter fibre pores are stabilized by liquid bridges, developed within the structures. The dripping out of oil is further assisted by its heavy nature, although the viscosity is higher than diesel. With the lowest viscosity, diesel drains out at a faster rate, but this also helps the system to reach equilibrium sooner with the tendency for diesel to remain within the kapok assembly.

To check the stability of oil entrapment inside kapok assembly, an external force was applied in the form of horizontal shaker at 150 rpm for 30 minutes. For diesel and used engine oil at 0.02 g/cm^3 packing density, 66% and 82% of sorbed oil were retained (Figure 4.9), respectively. At $0.04\text{-}0.08 \text{ g/cm}^3$ packing density, the amount of oil released was not significantly different with more than 90% remained stable within the entrapment. As discussed earlier, lower packing density has lower amount of inter fibre pores together with high hollow lumen network. Within a loosely-packed kapok, the liquid-liquid bridges are the predominant forces that hold up the oil within the assembly, as the oil is mainly entrapped inside the kapok fibre pores. The large inter fibre distance could have resulted in the highest percentage of oil dripping out with horizontal shaking, as it could easily destabilize the liquid bridges between fibers, thus reducing the capability of kapok assembly to retain the oil [13].

At higher packing density, the inter fibre liquid bridges are sufficient enough to hold up the sorbed oil within its structure, hence increasing the kapok assembly resistance against external forces from the horizontal shaker. The stability of the liquid bridges formed at the contact area between wax fibers and oils within the range of the stabilization capability of the liquid bridges is a direct consequence of the natural compatibility between wax surface and the experimental oil. The chemical interactions are in the form of Van der Waals forces and hydrophobic interactions coupled with the complex interaction between the availability of void fraction and the oleophilicity of kapok fibres. The capillary pressure becomes the predominant force that holds up the oil within the kapok assembly. The liquid hold up capacity affected by capillary pressure is more stable than the liquid bridges. Based on this, 0.04 g/cm^3 packing density may be suitable for sorbent development as it ensures stable oil entrapment inside the kapok assembly. In field application, this could mean ease of handling and transportation of the sorbed material for further treatment.



(a) (b) (c)

Figure 4.8 Percentage of dynamic oil retention of (a) diesel oil, (b) new engine oil, (c) used engine oil at packing density of (♦) 0.02 g/cm^3 , (■) 0.04 g/cm^3 , (▲) 0.06 g/cm^3 and (x) 0.08 g/cm^3 .

4.3.3 Effect of packing density on saturation time and bed height drop

Apart from sorption and retention capacity, saturation time and bed height drop are two important parameters to evaluate the effect of packing density on kapok performance. Saturation time measurement starts from the time the oil was fed into the column until the saturation point. Bed height difference was measured from the initial bed height until the height after no remaining oil was observed dripping out of the column. As shown in Figure 4.10, the saturation time increased as the packing density and viscosity of the experimental oil increased. In densely-packed kapok, the significant reduction of oil flow was mainly due to the constriction of channel flow sizes, resulting in longer saturation time. The rate of oil penetration into a capillary movement is inversely proportional to the oil viscosity [71]. Viscosity of used engine oil is 52 times higher than diesel and twice higher than new engine oil. The high viscosity of used engine oil actually reduces the rate of absorption within the internal capillary movement [14]. This result in longer saturation time as observed with new and used engine oil. The bed height drop increased slightly with higher packing density and viscosity of experimental oil. At 0.02 g/cm^3 packing density, 15% of bed height drop was observed with both new and used engine oil. However no significant bed height drop was observed at 0.04 g/cm^3 packing density. This lower percentage of bed height drop was primarily due to a more packed-density and the reduced amount of inter-fibre pores, thus limiting the space for reduction of kapok packing height.

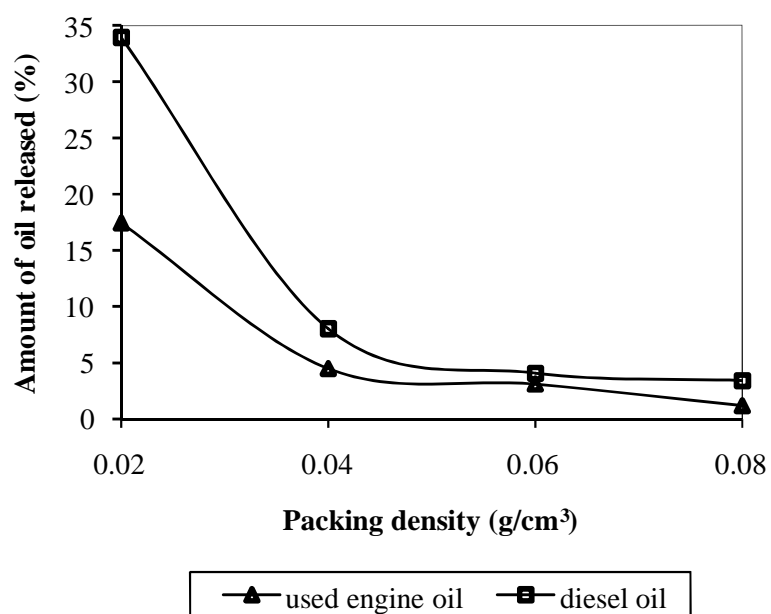


Figure 4.9 The percentage of oil released after applying sorbed kapok in a horizontal shaker at 150 rpm

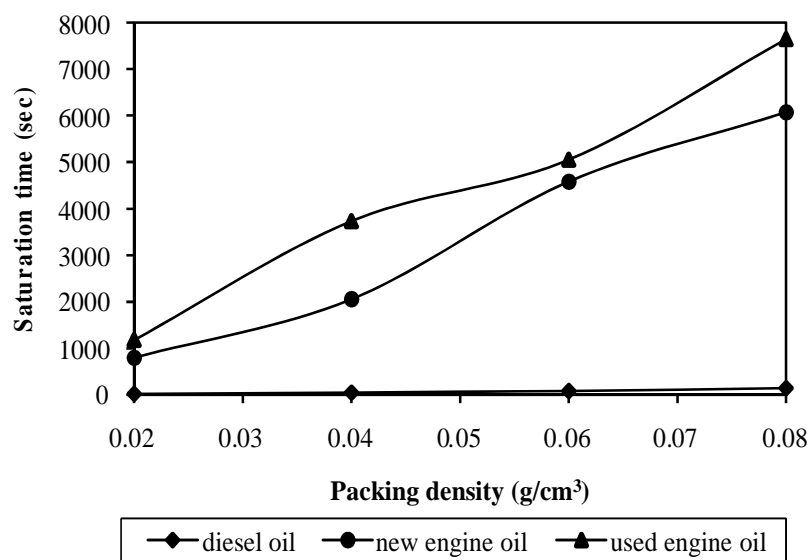
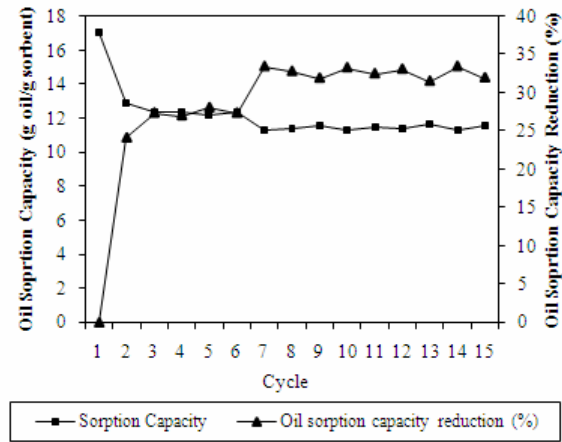
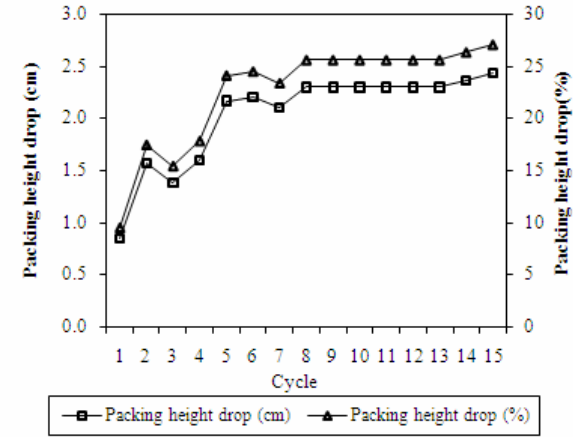


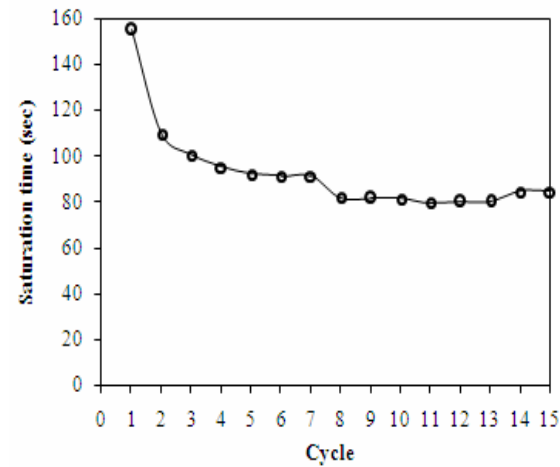
Figure 4.10 Effect of packing density to saturation time



(a)



(b)



(c)

Figure 4.11 Oil sorption characteristics of kapok fibre after fifteen cycles (a) oil sorption capacity reduction, (b) packing height drop and (c) saturation time during fifteen sorption-desorption cycles

4.4 Evaluation of Kapok Reusability

Kapok reusability experiment evaluates kapok durability over prolonged usage, without significant reduction in performance due to tearing, crushing or any mechanical deformation [8]. In this study, diesel oil and 0.04 g/cm^3 packing density were chosen as experimental conditions. Having the lowest viscosity, diesel should take the least time to flow down the column. Kapok was packed in a customized column with 100 mL working volume of kapok fibre. Upon completing each desorption process, test cell was weighed to monitor the oil sorption capacity and the packing height. Saturation time for each of the cycle was recorded, when the first oil droplet appeared from the test cell.

Figure 4.11a shows that the capacity was 17 g oil/g sorbent in the first cycle and dropped to 13 g oil/g sorbent in the second cycle, with 77% of oil recovered from the test cell. From the second cycle until the fifteenth cycle, no significant changes in oil sorption capacity were observed. The significant reduction observed in the second cycle has also been reported by Lim and Huang [8]. The sudden drop in sorption capacity from first and second cycle could be due to irreversible deformation as 20-23% oil remain trapped inside kapok lumens. The continuous deformation due to this remaining oil in the kapok assembly, affected the capacity of kapok to absorb more oil in the subsequent cycle [8, 14]. The inter-fibre distance could have been contracted after the sorbed oil being drained out. Full recovery of the effective pore may not be achieved once the test cell was soaked inside the oil bath. This effective pore reduction coincides well with the packing height reduction after oil desorption (Figure 4.11b). After 15 cycles, the bed height was reduced by almost 25%. Saturation time of the test cell dropped from 160 seconds to approximately 90 seconds after the second cycle, and remained constant until the fifteenth cycles (4.11c). The fast saturation time (80-160 sec) is a result of diesel having all the properties to penetrate easily into the fibre microstructure. For comparison, the saturation time for new and used engine oils at 0.04 g/cm^3 , are between 2000-4000 seconds (Figure 4.10).

In this study, sorbed oil inside kapok assembly was recovered using vacuum pump at 525 mbar. Reusability of natural fiber has been investigated by Lim and Huang (2007) by centrifugation at 3000 rpm, and Choi and co-workers (1992) by mechanical pressing with two roller at 50 psi [8, 14]. Higher energy may be needed to draw out the oil entrapped inside kapok hollow structure instead of just from the inter fiber pores. The oil entrapment inside kapok hollow structure is more stable than inter fiber pores. Unrecovered oil trapped inside kapok lumens reduce the oil sorption capacity, thus reducing the capacity for oil uptake in the second cycle. In a study with cotton fibre, more than 90% of oil is recovered using the squeezed-roller at its maximum pressure, and after the second cycle, 84% of oil sorption capacity can still be obtained [14]. The disadvantage of this method is the disruption of initially natural occurrence of fibre network, and the possibility for continued use in the longer cycles.

4.5 Conclusions

Ceiba pentandra (L.) Gaertn (Kapok) as a natural sorbent exhibits high hydrophobic-oleophilic characteristics, which are attributable to its waxy surfaces and hollow lumens. SEM and OM imaging confirmed the presence of hollow lumens inside kapok structure. Infrared spectrum showed that raw kapok is a lignocellulosic materials with hydrophobic waxy coating. Low values of surface tension and contact angle of kapok surface with oils suggested that the oils were the wetting liquid of kapok surface. Higher packing density resulted in lower sorption capacity, but higher percentage of dynamic oil retention, with only 1% of oil drained out from the test cell at 0.08 g/cm³. The percentage of dynamic oil retention was in the decreasing order of: used engine oil, new engine oil and diesel. At higher packing density and higher oil viscosities, kapok exhibited higher saturation time but lower bed height reduction. Using diesel oil as the experimental liquid at 0.04 g/cm³ packing density, only 30% of oil sorption capacity reduction was observed even after fifteen cycles of reuse. Oil entrapment inside the 0.08 g/cm³ packing density, was stable after 30 min of shaking inside a horizontal shaker, with more than 90% of diesel and used-engine oil retained inside the assembly. The overall sorption characteristics of kapok imply that kapok

fibre is a potential cellulosic-material for oil removal with high oil sorption and retention characteristics and stable for prolonged use.

CHAPTER FIVE

EVALUATION OF KAPOK PACKED-BED COLUMN PROCESS DESIGN FOR OILY WATER FILTRATION

5.1 Profile of Oily Water Filtration at Different Packing Density and Flow Rate

Filtration technique by utilizing a fibrous bed deep filtration is a chosen method for separating immiscible liquid from polluted wastewater due to its good performance and simplicity in operation. By using proper filter material, initial and operating cost can be reduced [17]. In this study, oily water mixture sample was used to give better insight into kapok packed-bed column process design parameters and the fibre selectivity. In addition, the optimum working performance can be investigated. The diesel oil was dyed using Oil Red O to enable the visual observation of kapok filter during filtration stage. The packing densities used were 0.04, 0.06 and 0.08 g/cm³. Oil permeability and water repellency are two important factors that determine the performance of kapok filter for oily-water filtration and selectivity. The high selectivity of kapok filter towards oil-water can best be explained in terms of interfacial interactions between kapok filter and oil/water mixtures.

As shown in Figure 5.1, several authors [7, 17] have divided the dynamics of the interaction between the oily-water mixtures and the kapok sorbent during separation inside the column into four stages:- 1) Infiltration, 2) Separation, 3) Displacement, and 4) Equilibrium. In the filtration stage, separation started with the infiltration of oily water mixtures inside the kapok filter bed. When the liquid enters the column, the liquid interacts with the column and kapok filter. These interactions result in two different shapes of liquid curvature inside the column. The adhesive tendency of the two fluids with the solid surface determines the curvature shape. Liquid with stronger affinity with the solid surface takes the concave shape, while the liquid with the lower affinity is on the convex side.

In our study, the concave water front was first observed during the initial stage and this was followed by the convex diesel front. Kapok surface is covered with hydrophobic wax, causing the oil to have lower contact angle value than water. Oil therefore is the wetting liquid for kapok, instead of water. However, the stronger interaction between glass column and water as compared to kapok created the concave front of water and the convex advancing front of diesel. The different resistance between the glass column and kapok towards both liquids were only affected during the initial stage. With the continuous flow channel, water may flow along the same channel. Therefore, the tortuosity and the flow channel geometry should be the main factors that govern the water flow rate.

During separation stage, water and oil flowed as two separate liquid fronts. The water front was increasing more rapidly than oil front. This different advancement rate was most likely caused by the combination of viscosity and the different resistance in interactions with the solid phase as described earlier. Strong interactions between oil and kapok fiber will lower the oil advancing front rise inside kapok column based on Van der Waals forces and hydrophobic interactions. In this stage, the oil droplet in the effluent was believed to coalesce with the entrapped oil drops until a certain thickness of oil plume formed. The displacement stage started when the water front appeared at the filter column outlet, and ended with the appearance of oil droplet in the filter outlet. This was also the beginning of the equilibrium stage where no additional oil can be retained inside kapok structure since maximum coalescence capacity was achieved.

The distinct separation of water rise and oil-rise curve, as shown in Figure 5.2, supported earlier discussion on different rate of advancement of liquid fronts. The effect of flow rate was more pronounced than packing density. Low water-rise flow rate showed the lower advancement rate than the high oil-rise flow rate. When the oily water mixtures entered the kapok column, the initial concentration of oil inside the filter will be at minimum value. During initial stage (infiltration), the oily water mixtures only reached the lower height of kapok column which produced only a small area of mass transfer zone (MTZ). The upward flow rate direction led the MTZ movement until maximum column height. The oil sorption occurred until the sorbent

reached its maximum capacity and the oil-water concentration inside kapok column reached equilibrium. At equilibrium stage, the oil sorption no longer took place due to the kapok fibre saturation, which was followed by oil breakthrough. By varying the flow conditions, the mass transfer characteristics of the column changes and lead to the different breakthrough curve as has been demonstrated in other study [61].

Lower packing density caused the reduction of the interactions between oil and kapok surface leading to the faster water breakthrough time. Water penetrates at a higher rate manifested in faster duration of each stage of the liquid movements (infiltration, separation, displacement and equilibrium). At higher packing density longer residence time of oily water mixtures inside kapok column led to the longer saturation time and longer duration of each stage of the liquid movement. Larger volume of oily water mixtures can be filtered with higher packing density. However, higher liquid flow rate created premature interaction between kapok and oily water mixtures which can be observed from the small area of separation stage. This led to lower kapok performance to retain oil and to allow water to pass through (Figure 5.2d,e,f).

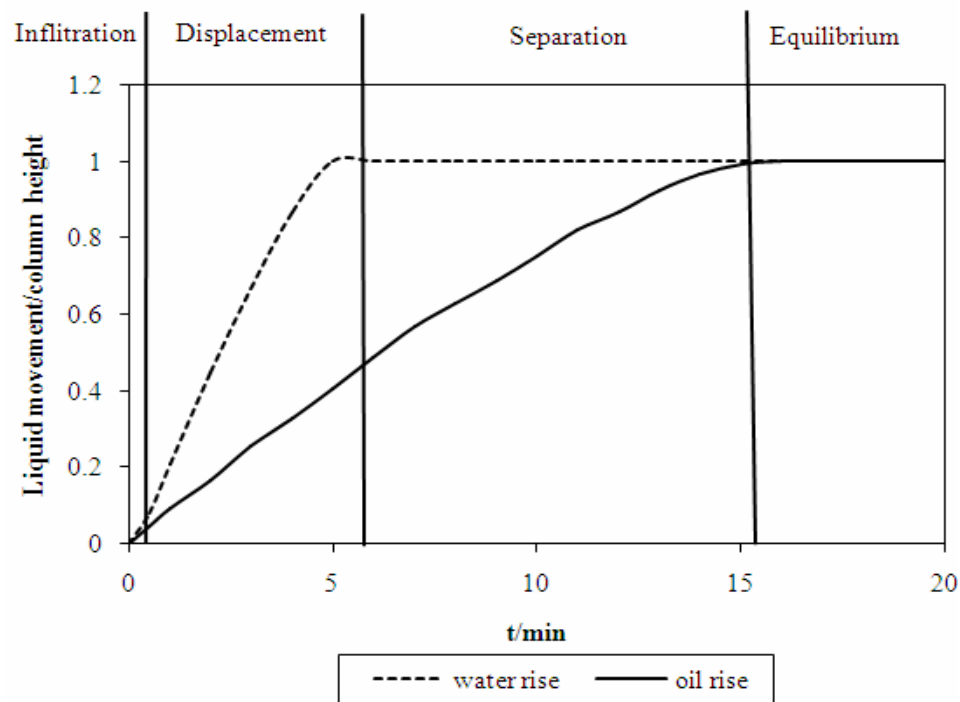


Figure 5.1 Liquid front movements at 0.08 g/cm³ packing density and 0.5 L/h flow rate of oily water filtration

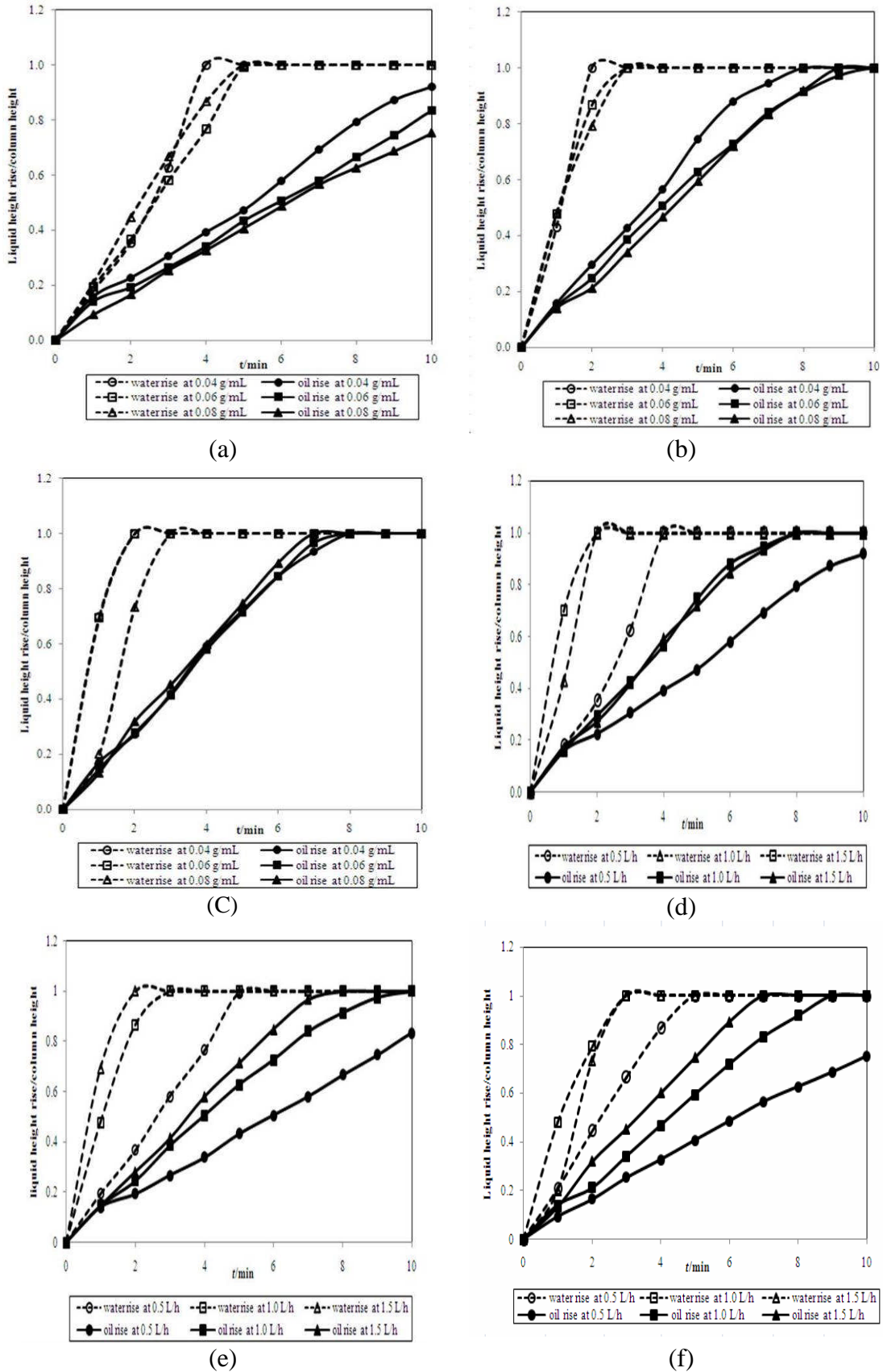


Figure 5.2 Liquid front movements of kapok filter at (a) 0.5 L/h, (b) 1.0 L/h, (c) 1.5 L/h flow rate and (d) 0.04 g/cm³, (e) 0.06 g/cm³, (f) 0.08 g/cm³ packing density

5.2 Effect of Packing Density and Flow Rate on Chemical Oxygen Demand and Turbidity

Kapok performance for oily water filtration was further evaluated based on Chemical oxygen demand (COD) and turbidity. Both methods were chosen due to ease of handling during preparation and measurement, and faster response time for on-site analyses. COD method utilizes the oxidation of the organic content inside water sample using potassium dichromate with silver catalyst and mercuric compound to overcome the interference, such as chloride ions. For turbidity, the nephelometry method was employed. The light source illuminates the sample, and the photometric detector connected with a read-out device quantifies the intensity of the scattered light at 90° angles to the path of the incident light. The light that emerges from the sample will be directed to a photometer that measures the light absorbed, and the amount of the suspended solids inside effluent sample can be quantified. The sample collections were done from the moment the water droplet appeared at the column outlet. Two minutes after water breakthrough, effluent samples were collected.

Before oxidation of organic content, the color of COD solution vial is light yellow (Figure 5.3a). High level of organic content turned the COD vials light green and show insignificant difference at low organic content (Figures 5.3b,c). The capability of kapok to break the oil-water emulsion is one of the added values of kapok as oil sorbent. Table 5.1 and 5.2 display that the COD reduction was more than 99 % and the turbidity reduction was 87-97 % at various flow rate and packing density. Low level of COD and turbidity were attributed to the reduced amount of diesel inside oily-water mixtures. This proved the excellent selectivity of kapok for oil over water. Figure 5.4a shows the physical appearance of the 5% diesel-water mixtures sample before filtration process. After diesel-water mixing, some of the diesel droplets form suspension inside water, resulting in a colloidal-like suspension at the bottom layer of the mixtures. Some amount of oils floated at the surface. The colloidal-like suspension was used for turbidity measurement and considered as the initial value of turbidity before filtration. Physical appearance of samples after the filtration process is shown in Figure 5.4b.

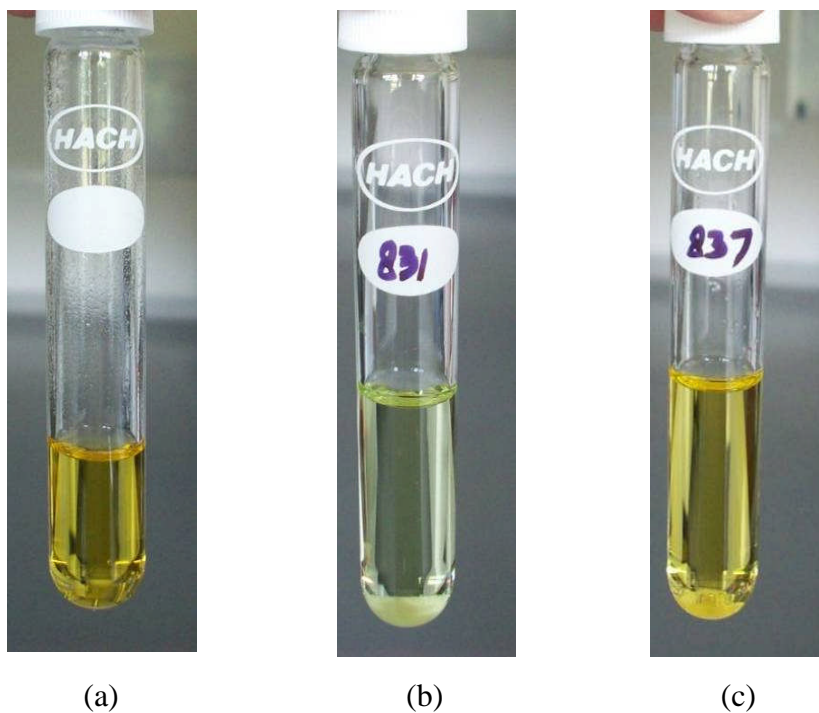


Figure 5.3 COD vials color (a) before sample addition, (b) high organic content and (c) low organic content level

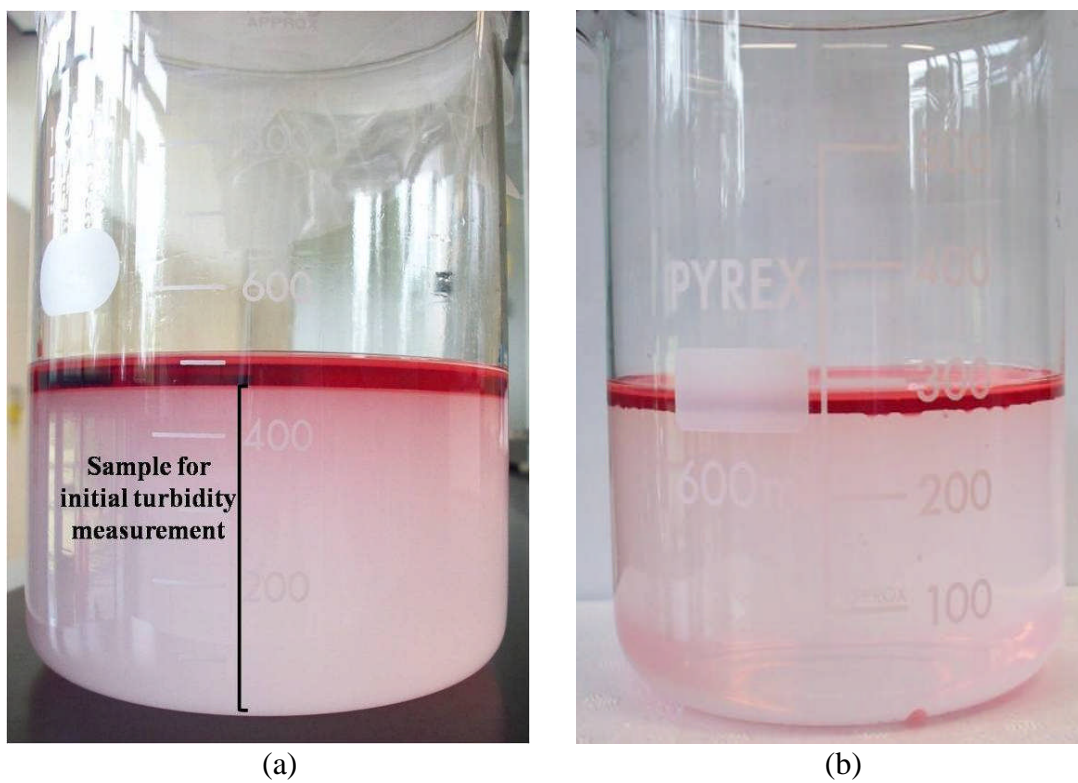


Figure 5.4 Effluent (a) before and (b) after filtration

Table 5.1 COD value of effluent at different flow rate and packing density

Packing density (g/cm ³)	Flow Rate (mL/h)	COD (ppm)	%
			Reduction COD
0.04	0.5	520	99.0
	1	440	99.2
	1.5	313	99.4
0.06	0.5	360	99.3
	1	426	99.2
	1.5	270	99.5
0.08	0.5	190	99.6
	1	400	99.2
	1.5	240	99.5
Initial COD (ppm)		52632	

Table 5.2 Turbidity value of effluent at different flow rate and packing density

Packing density (g/cm ³)	Flow Rate (L/h)	Turbidity (NTU)	%
			Reduction Turbidity
0.04	0.5	252	89.3
	1	138	94.2
	1.5	232	90.2
0.06	0.5	185	92.2
	1	304	87.1
	1.5	136	94.3
0.08	0.5	70	97.0
	1	185	92.2
	1.5	153	93.5
Initial Turbidity (NTU)		2357	

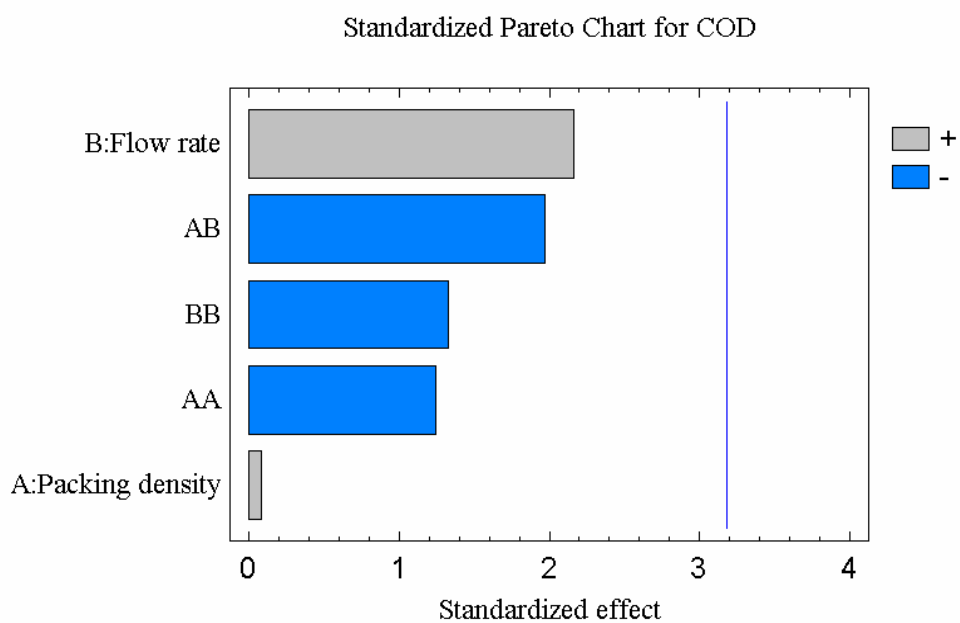
Table 5.3 List of R^2 and polynomial equation for COD, COD reduction, turbidity and turbidity reduction

Response $f(x_i, x_2)$	R^2	Second order polynomial equation
COD (ppm)	0.80	$f(x_i, x_2) = -1074.69 + 28425.0x_i + 1189.25 x_2 - 171458 x_i^2 - 7712.5 x_i x_2 - 294.33 x_2^2$
COD reduction (%)	0.81	$f(x_i, x_2) = 101.89 - 52.5 x_i - 2.08 x_2 + 333.33 x_i^2 + 12.5 x_i x_2 + 0.53 x_2^2$
Turbidity (NTU)	0.96	$f(x_i, x_2) = -373.78 + 10725.0 x_i + 383.02 x_2 - 26625.0 x_i^2 - 7822.5 x_i x_2 + 88.4 x_2^2$
Turbidity reduction (%)	0.96	$f(x_i, x_2) = 101.894 - 52.5 x_i - 2.08 x_2 + 333.33 x_i^2 + 12.5 x_i x_2 + 0.53 x_2^2$

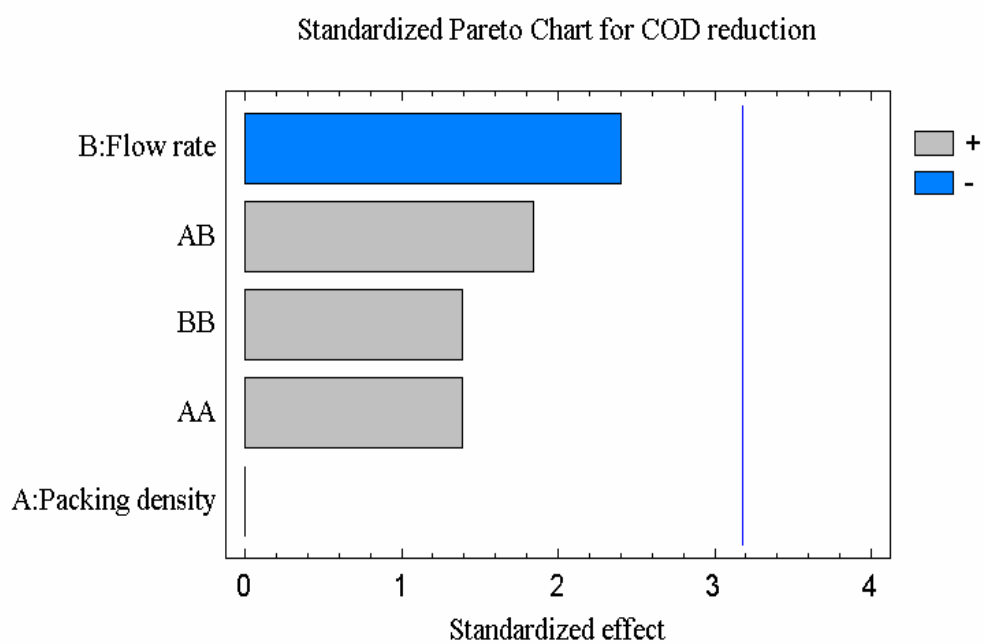
with :

x_i : packing density and

x_2 : flow rate

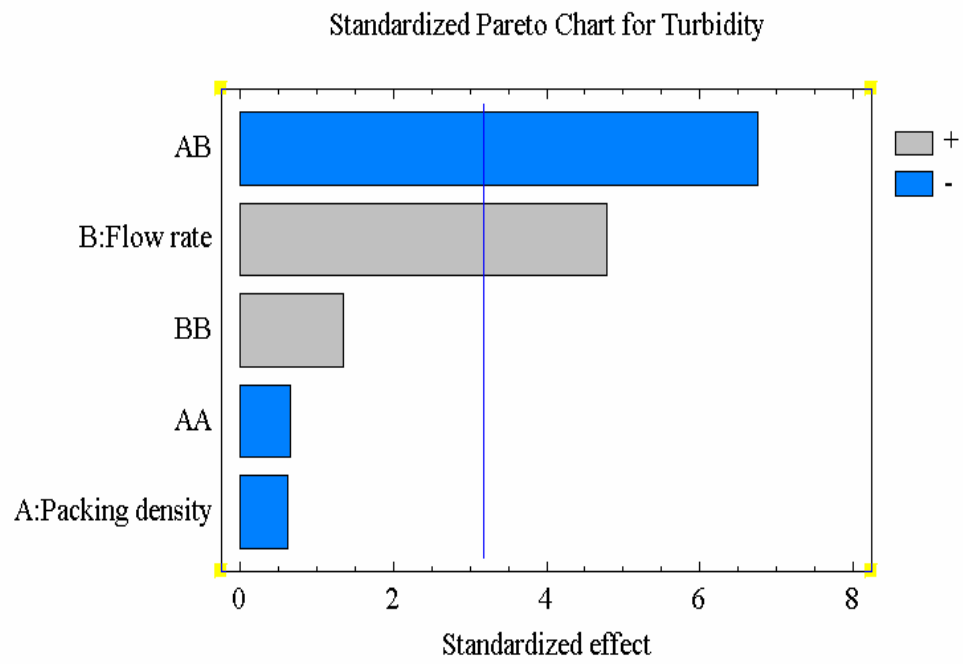


(a)

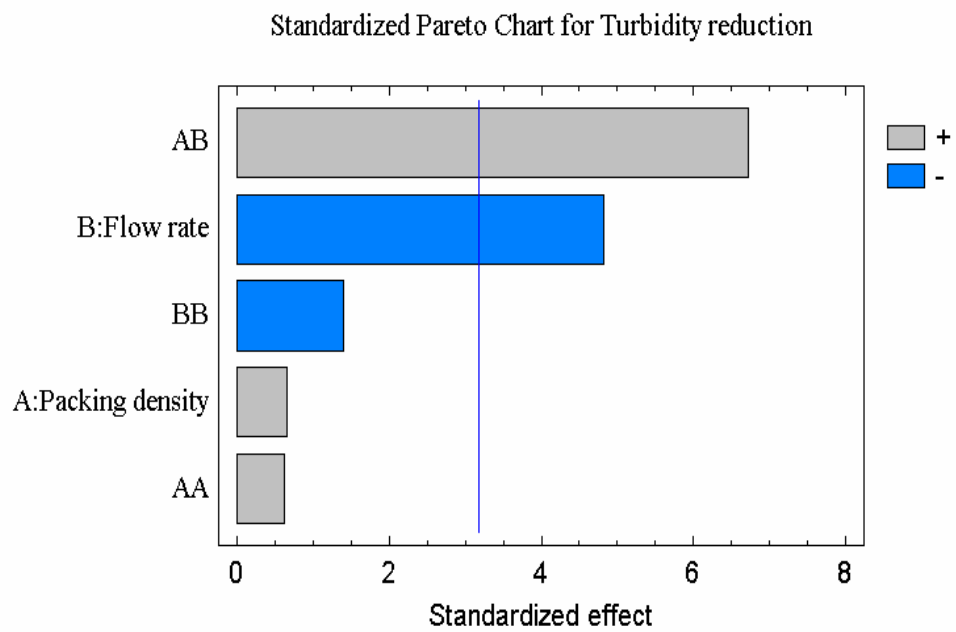


(b)

Figure 5.5 Pareto charts for standardized effects of (a) COD and (b) COD reduction



(a)



(b)

Figure 5.6 Pareto charts for standardized effects of (a) turbidity and (b) turbidity reduction

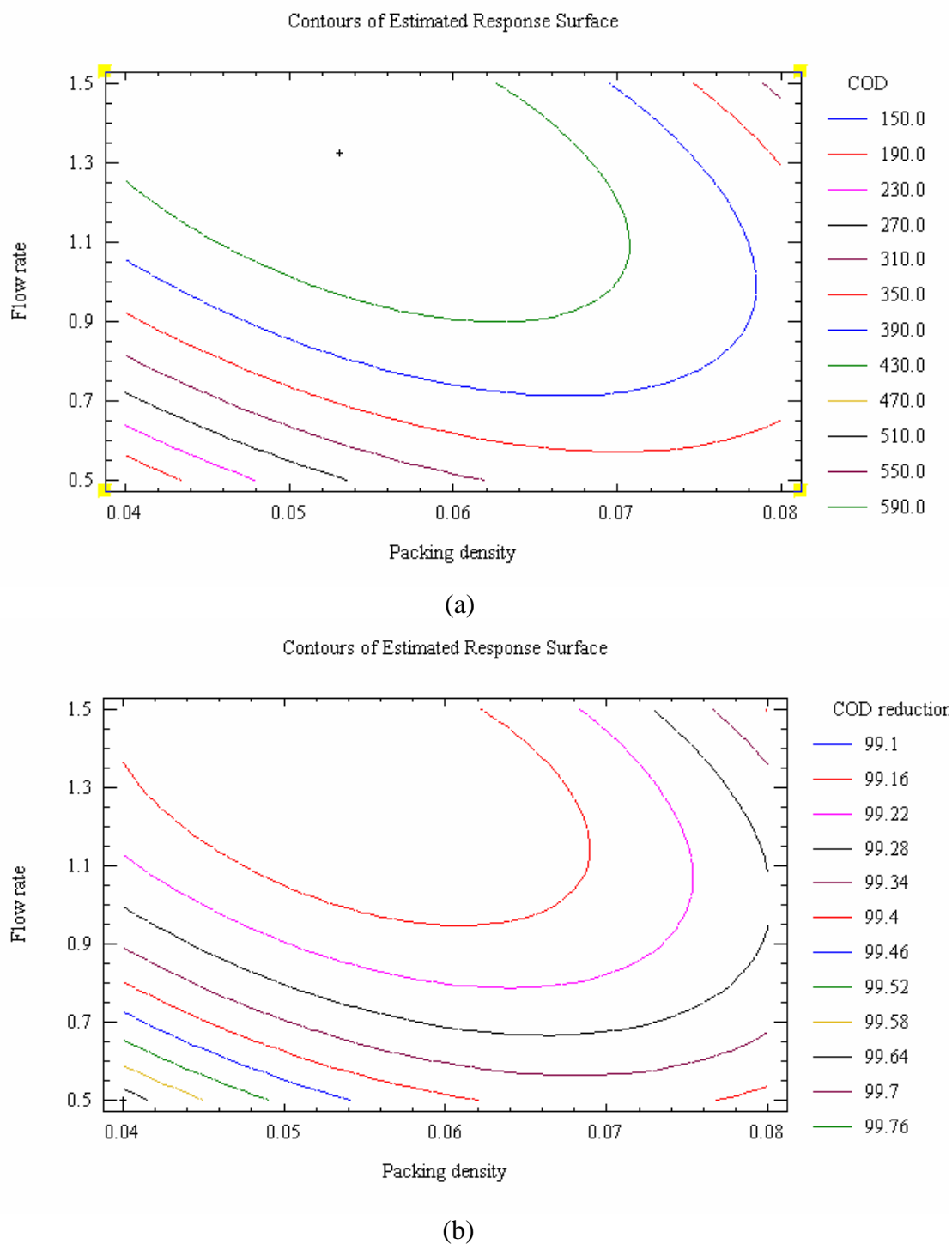


Figure 5.7 Response surface contour plot with packing density and flow rate as independent variables for (a) COD and (b) COD reduction

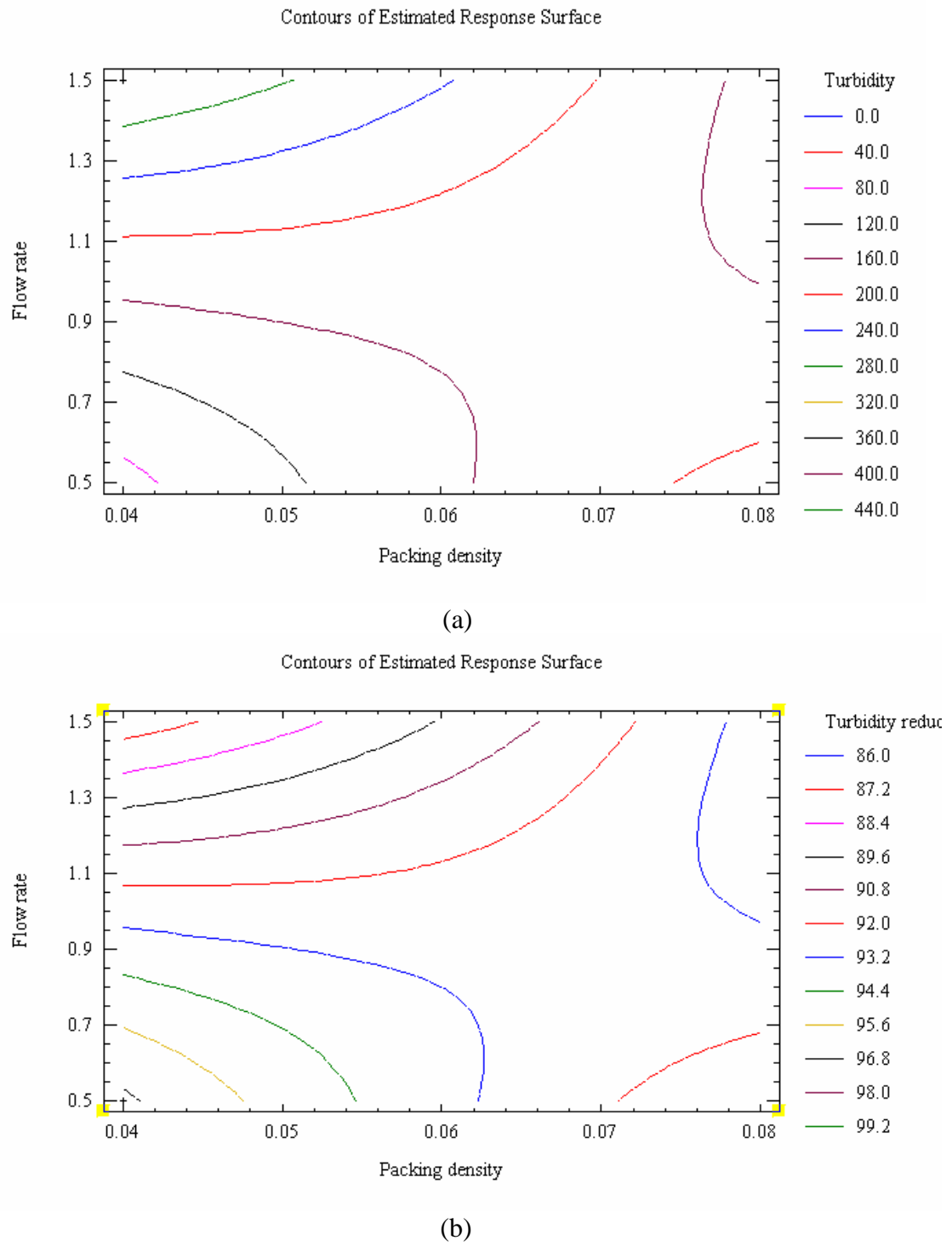


Figure 5.8 Response surface contour plot with packing density and flow rate as independent variables for (a) turbidity and (b) turbidity reduction

5.3 Factorial Experimental Design and Statistical Analyses

Full factorial design of 9 experimental runs were carried out, with all possible combination of values of each experimental factor (k), namely packing density and flow rate (Table 3.1). Statistical approach of analyses estimates the effect of the interaction strength of each experimental factor on the process performance. Pareto charts describe the relative importance of the factor and also the effect of factor setting adjustment, by displaying the most influencing factor followed by the least one. Three levels were applied for each factor:- low, medium and high. Regression analysis data on COD, COD reduction, turbidity and turbidity reduction following a second-order polynomial equation are described by Equation (4), and shown in Table 5.3. The correlation factor or R^2 describes the variability degree of the observed response and ranges between of 0 and 1. As a rule of thumb, R^2 value should be at least 0.75 or greater. Value above 0.9 indicates good agreement and accuracy of the response as predicted by the model [72]. This value is calculated by dividing the variation explained by the model (Regression of sum squares) by the total variation (Adjusted Total Sum of Squares). The location and surface shape of the curvature can be predicted by deriving contour plots from the given polynomial equation. The ideal position of the optimum point is located at the “bull’s eye” of the contour plots.

Figure 5.5 and 5.6 shows the Pareto charts of the standardized effects of the interaction between each factor affecting the COD, COD reduction, turbidity and turbidity reduction. None of the factors affected significantly the COD values. However, the interaction between flow rate and packing density was the main factor reducing the turbidity, whilst flow rate as a single factor increased turbidity. The other factors do not affect turbidity significantly. The contour of the estimated response plotted in Figure 5.7 suggests that the effluent will have the COD values at 0.053 g/cm³ packing density and 1.3 L/h flow rate. Based on the regression analyses of COD and COD reduction data of effluent (Table 5.3), the R^2 values of about 0.80 and 0.81 correlation factor implied a good agreement between the experimental and calculated data. Figure 5.8 suggests that the highest turbidity reduction can be obtained at 0.04 g/cm³ packing density and 0.5 L/h flow rate. The R^2 values of experimental data of 0.96 for turbidity not only implied a good agreement between the

experimental data and calculated data, but also a better fitness than the model for COD values. It was however not clear as to the reason for different turbidity reduction where turbidity was predicted at 0.04 g/cm^3 but at a flow rate of 1.5 L/h . Similar result has been reported in a study with kapok fiber packed inside a column to perform a lab scale cleanup for diesel-water mixture [2]. Three types of packing densities are used: 0.07 , 0.08 and 0.09 g/cm^3 , at fixed flow rate, and the filtration efficiency all exceed 99.9% removal.

At low flow rate and longer residence time, the oil droplet could coalesce and becomes large enough to be entrapped. As the packing density increases, higher inlet pressure is needed to maintain a certain flow rate of the emulsion feed, and this may be followed by the reduction of void porosity and velocity increment [5]. The COD reduction is therefore should be highly affected by the combination of flow rate and packing density. As discussed in previous Chapter, the interfiber distance inside kapok structure at low packing density is higher, which increases the size of the effective flow channels as compared to higher packing density. All of the three packing densities have high percentage of void fractions- 96.9, 95.4 and 93.9% for 0.04 , 0.06 and 0.08 g/cm^3 packing density, respectively. The high percentage of void fraction may be the main factor behind the insignificant effect of packing density and flow rate COD and COD reduction. Apparently in our study, regardless of higher or lower packing density and flow rate, the COD values will be affected. This may suggest other important factors such as kapok chemical composition and structural make-up itself that could influence significantly the COD reduction. The COD method quantifies whatever substances oxidized by dichromate under the conditions of the test. The results may be greater or less than the true theoretical oxygen demand of all organics present in the sample [11]. Based on the model and contour plot, the flow rate at 1.3 L/h and 0.05 g/cm^3 packing density for optimum COD removal, could support this postulation as both are moderately high values.

The highest percentage of turbidity reduction was achieved at the lowest flow rate (0.5 L/h) and the highest packing density (0.08 g/cm^3). This flow rate increases the residence time, resulting in higher degree of interaction between kapok sorbent and the oil inside the mixtures. This explains the significant effect on the

turbidity reduction. Unlike COD which requires the presence of chemical species to be oxidized, the turbid mixtures resulted from the emulsion formation between oil and water which may be comparable in sizes to be filtered out or broken down. By breaking down the emulsion, no coalescence between oil and water would occur and this will result in a more reduced turbidity in the liquid at the column outlet. At certain flow rate, the void spaces are progressively clogged by the retained oil, followed by the increment of the local velocity of the liquid phase. This could weaken the interaction forces and drive the disperse phase droplets to penetrate deeper into the kapok bed. This entrainment ensures optimum usage and more durable filtration process [5]. Other study has shown that higher value of turbidity could result from lower packing density where about 9.77, 9.67 and 7.12 NTU are reported for 0.07, 0.08 and 0.09 g/cm³ packing density [2]. However, this study is actually carried out under constant applied pressure which therefore makes packing density an important factor.

5.4 Conclusions

Deep-bed filtration column with simple setup had been constructed in this study to evaluate the performance of kapok filter for oily water separation under different packing densities and flow rate. Four stages of liquid movement involved in kapok filtration column: infiltration, separation, displacement and equilibrium, were observed. Based on the statistical analyses, none of the factors play significant role in reducing the percentage of COD. This may suggest important role of kapok chemical composition and structural make-up. Above 99% COD reductions were observed for all kapok filters at different packing densities and flow rate, and about 97% reduction was observed for kapok at 0.08 g/cm³ and 0.5 L/h flow rate. However the interaction of packing density and flow rate played significant role in turbidity reduction. The excellent turbidity reduction could be due to the stronger interaction of kapok with oil which can break down oil-water emulsion.

CHAPTER SIX

CHLOROFORM AND ALKALI TREATMENT OF KAPOK

The physicochemical characteristics could affect the oil sorption capacity of sorbent. Chemical nature of sorbents include the amount of surface wax, molecular arrangement, physical configuration of fiber such as hollow lumen, twist, and crimp, surface roughness, porosity and fineness. For kapok, its oleophilic-hydrophobic characteristic is attributed to the presence of large, non-collapsing hollow lumens as well as high waxy content. Physicochemical properties of plant wax determine the plant wettability, optical appearance, water repellency and the solubility among organics and polar solvents. Wax content of kapok (about 3%) which is also higher than cotton (0.4-0.8 %), and high acetyl content (13%) may be responsible for its high hydrophobicity [6]. Higher waxy content promotes stronger interaction between the oil and kapok by lowering the surface tension between kapok surface and sorbed oil. Once the surface tension is lowered, no energy barrier exists to prevent the liquid from penetrating the solid structure and thereby enhancing the oil sorption capacity and water repellent capacity [14].

Chemical treatment to modify the surface properties of natural fibres could improve the desired properties of the sorbents. Several chemical modifications have been proposed such as ethanol and chloroform treatments [2], acetylation using 4-dimethylaminopyridine (DMAP) [67] or N-bromosuccinimide (NBS) as catalysts. The NaOH treatment on kapok fibre is applied to produce fibre with better mechanical properties for the polymer reinforcement material, rather than just as oil sorption-active material. In a study where kapok is soaked in chloroform and ethanol for 1 hour, and undergoes alkalization using NaOH at 20°C for 48 hours, the chemically-treated kapok have shown premature oil breakthrough and lower oil retention capacity [2, 25, 26].

The objectives of this study were to investigate the stability of kapok hollow structure and waxy layer on the kapok surface. Treatment duration and solvent types used were varied in this experiment. There has yet to be any report on the effect of

alkali treatment on the oil sorption characteristics of kapok fibre. From these experiments, major factors that determine the kapok hydrophobic-oleophilic properties could be identified.

6.1 Comparison between Chloroform and Alkali Treatment on Chemical Constituent and Kapok Microstructure

6.1.1 Infrared spectra

Extraction using soxhlet was used to study the effect of chloroform treatment for two different durations - 4 and 8 hours. Chloroform was chosen as one of the extracting solvent due to its hydrophobicity, similar to kapok waxy surface. Chloroform regeneration is likely to occur inside the soxhlet chamber, allowing for a continued extraction of kapok wax surface. Alkali treatment was carried out by boiling the kapok fibre inside the reflux apparatus using 1% NaOH at pH 13. Figure 6.1 shows FTIR spectrum of untreated and treated kapok using chloroform. As discussed earlier in Chapter 4, a well-pronounced trough observed at 2918 cm^{-1} corresponds to the asymmetric and symmetric aliphatic CH_2 and CH_3 stretching. The band is associated with the presence of plant wax, generally consisting of n-alkanes, smaller portion of alcohols, fatty acids, aldehydes, ketones and n-alkyl esters [2]. With chloroform extraction, transmittance at 2918 cm^{-1} increased significantly. The transmittance trough at 1425 and 1375 cm^{-1} , corresponding to the presence of wax surface, also showed increasing values. The transmittance increment was similarly observed for band positioned around 1750 and 1250 cm^{-1} correlating to the presence of carbonyl group (C=O) in the ester bonds [2]. These increments suggest the possibility of wax removal from the kapok surface, but the difference between 4 and 8 hours extraction was not significant. Infact 8 hour extraction only showed slightly higher band height than 4 hours extraction suggesting only slightly higher percentage of wax removal. Others have reported that kapok immersed in chloroform after 1 hour had absorbance value reduced, to indicate wax removal. However, absorbance reductions observed for both kapok soaked in chloroform and alcohol have the same band positions [2] as observed in our study, albeit with transmittance increment.

Figure 6.2 shows the infrared spectrum of alkali-treated kapok using 1%(w/w) NaOH. The duration of 4 and 8 hours treatment were also employed. After alkalization, washing with water was applied to remove any waxy debris from the fibre. After drying at 60°C for 24 hours, the kapok fibre became pulp-like and hardened. The dried material was ground by using blender to form fine fibre. This was used for the determination of oil sorption and retention capacity. The profile was significantly different from the chloroform-treated profile where there are increments or reductions in transmittance as compared to raw profile. With NaOH treatment, the hydrogen bonding inside kapok fibre could have been reduced via the hydroxyl group reduction. This can be observed from the transmittance increment of $-OH$ bands at 3361 cm^{-1} . The hydroxyl groups facilitate the hydrogen bonding with the carboxyl groups, such as fatty acids on the surface of the natural fiber. Similar to chloroform-treated kapok, transmittance increments around 2918 , 1750 and 1250 cm^{-1} are attributed to the wax removal. However, the effect at 1750 cm^{-1} corresponding to the presence of the carbonyl group ($C=O$) in the ester bonds were most significant where no sharp transmittance trough was observed after 4 and 8 h alkali treatment. This phenomenon is termed “deesterification” [26]. Transmittance increment at 1651 cm^{-1} suggests greater water removal, and at around 1604 cm^{-1} implies the removal of unsaturated carbon chain ($C=C$ stretching) inside the traces of oil. Comparing between Figure 6.1 and 6.2, other than the peak at 1750 cm^{-1} flattened out, the disappearance of sharp transmittance trough around 1247 cm^{-1} can also be observed which indicates the removal $C-O$ stretching of acetyl group [26]. In addition, new troughs were observed at 2380 cm^{-1} and the greater separation between untreated and alkali treated kapok at 898 cm^{-1} . The latter suggests the increased removal of β -glucosidic linkage between sugar units in hemicelluloses and celluloses.

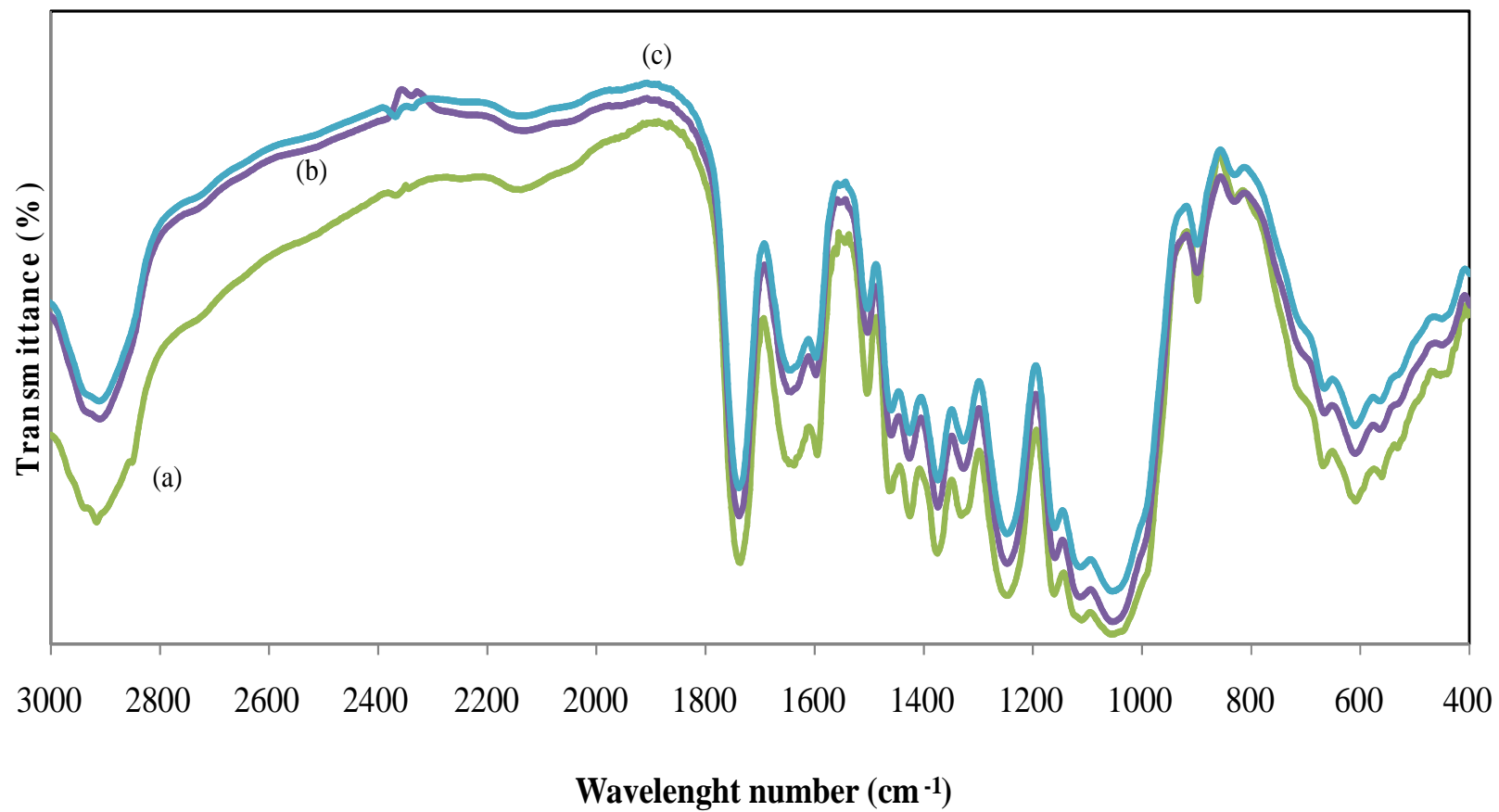


Figure 6.1 FTIR spectrum of kapok (a) before, (b) after 4 hours, and (c) 8 hours of chloroform treatment

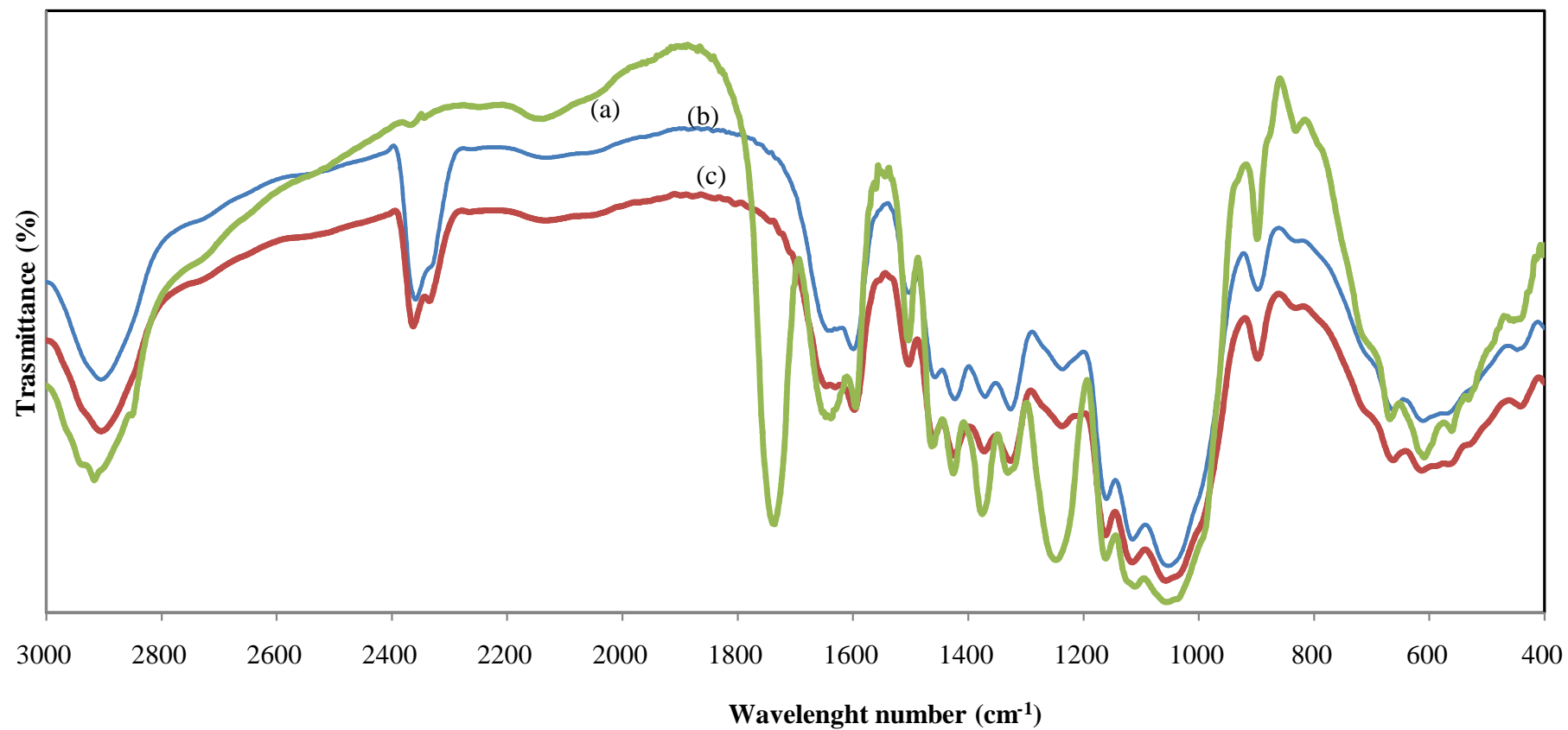
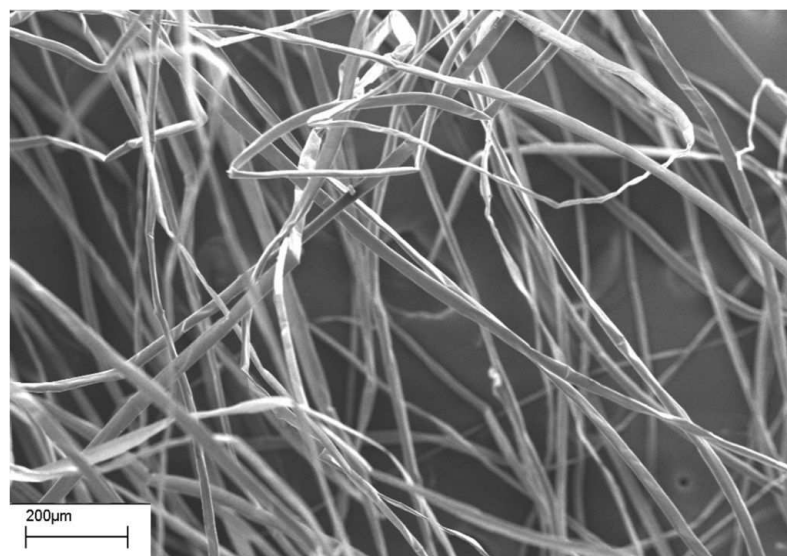
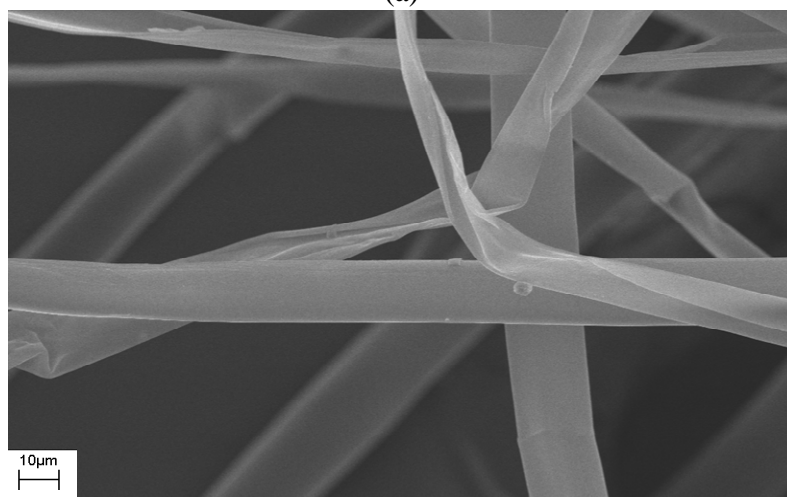


Figure 6.2 FTIR spectra of kapok (a) before, after (b) 4 hours and (c) 8 hours of alkali treatment



(a)



(b)

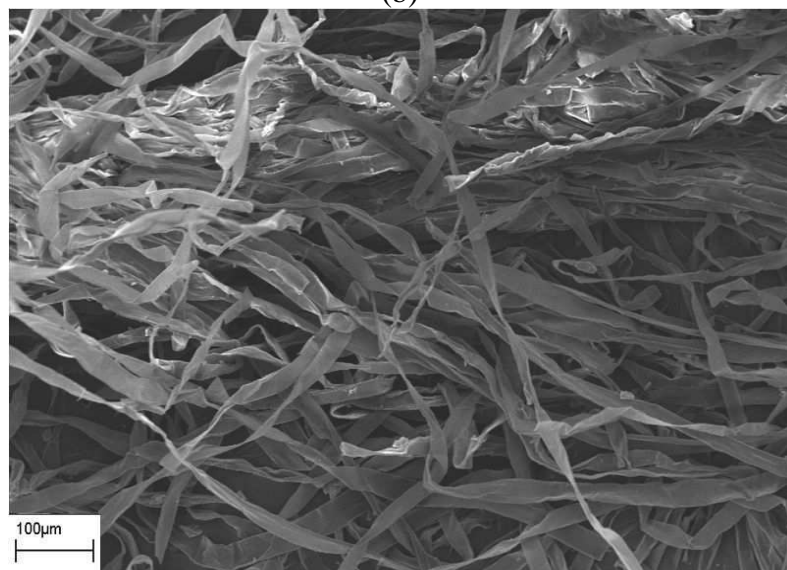


Figure 6.3 SEM image of (a) untreated and (b) chloroform-treated and (c) alkali-treated kapok



(a)



(b)



(c)



(d)



(e)

Figure 6.4 Kapok appearance (a) before and after (b) 4 hours and (c) 8 hours chloroform treatment, (d) 4 hours and (e) 8 hours alkali treatment

6.1.2 Kapok microstructures and morphology

Based on SEM analysis (Figure 6.3b), chloroform-treated kapok was not significantly different from untreated one. The tubular structure remained intact with scattered white spots observed on the kapok surface possibly indicating the wax removal. Nevertheless, some parts of the fibre were flattened. The high buoyancy is due to the air entrapment inside the tubular structure and together with the presence of wax prevents water from penetrating the structure. With alkali treatment (Figure 6.3c) there was almost total disappearance of air entrapment inside kapok fiber and the structure became completely flattened similar to flat ribbon-like structure with increased density. Physically, chloroform-treated kapok was not significantly different from untreated one. Although the silky appearance of chloroform treated-kapok was reduced, the buoyancy and fluffiness was retained (Figure 6.4b,c). Similar observation has been reported about the reduction of silky cluster of kapok after soaking for 1 hour in chloroform [2]. As shown by Figure 6.4d and 6.4.e, the color of alkali treated-kapok fiber was changed into dark from originally fluffy white. The silky and smooth structure had also changed into hardened structure. This could be due to excessive removal of hemicellulose and lignin [73]. The material needs grinding as a pretreatment for oil sorption applications

6.2 Comparison between Chloroform and Alkali Treatment on Oil Sorption Characteristics

6.2.1 Oil sorption capacity

Oil sorption capacity and percentage of dynamic oil retention were monitored to evaluate the kapok performance after being treated with chloroform and alkali. As shown in Table 6.1, no significant difference in oil sorption capacity was observed between chloroform-extracted kapok and untreated kapok. On the other hand, the oil sorption capacities of alkali-treated kapok were reduced by 14.9 % and 26.3 % after 4 and 8 hours treatments, respectively. The oil sorption capacity after 8 hours treatment was 11.4 % lower than 4 hours treatment. Waxy content appears not

to be the primary factor affecting the sorption capacity of oil. If the tubular structure of kapok remained intact, higher oil uptake could still be observed as in the case with chloroform-treated sample. With alkali treatment, the whole kapok structure could have been disrupted and higher amount of wax may have also been removed. With more compact density, the air entrapment inside kapok structure was significantly decreased, followed by oil sorption capacity reduction. The flattened structure also did not provide ample interstitial volume for oil entrapment.

It has been argued that although viscose rayon (VR) is a hydrophilic polymer based on its structure, the presence of physical configurations such as twist and crimp, provide sufficient space for oil entrapment. The VR has high oil sorption capacity, 19 g oil/g fiber (Table 2.1) which supports our earlier suggestion that oil sorption capacity of chloroform-treated kapok remains high due to the conserved hollow structure of treated-kapok. The extraction of milkweed and cotton fiber using 1,1,2-trichloroethane also result in significant reduction of oil sorption capacities for diesel and light crude oil samples [13, 59]. However the reduction of oil sorption capacity of cotton and wool after alkali treatment using 2 % Na_2CO_3 and NaOH solutions are even more significant [13]. As shown in Figure 2.11, about 44.6 and 22.6 % of the oil sorption of cotton and milkweed, respectively, have been reduced after alkali treatment. The higher oil sorption reduction is attributed to the higher concentration of Na_2CO_3 and NaOH solutions used.

NaOH is known as a bleaching chemical. Generally, natural fibers are chemically treated using NaOH to remove the lignin-containing component, such as pectin, waxy substances and oil layer that cover the external surface of fibre cell wall. This treatment removes the fibrils (Figure 6.5) and produces rough surface plant fibres [26]. Cellulose structure changes from type I to type II structure upon NaOH treatment, commonly known as mercerization or alkalization. The reaction of NaOH with the cellulose can be summarized as below [25]:

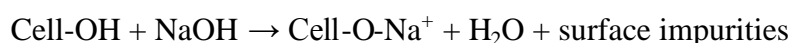


Table 6.1 Oil sorption capacity of chloroform and alkali-treated kapok at 0.04 g/cm³ packing density

Oil sorption capacity (g oil/g fiber)				
Untreated	Chloroform-treated		Alkali-treated	
	4H	8H	4H	8H
20.8	20.5	20.4	17.7	15.4

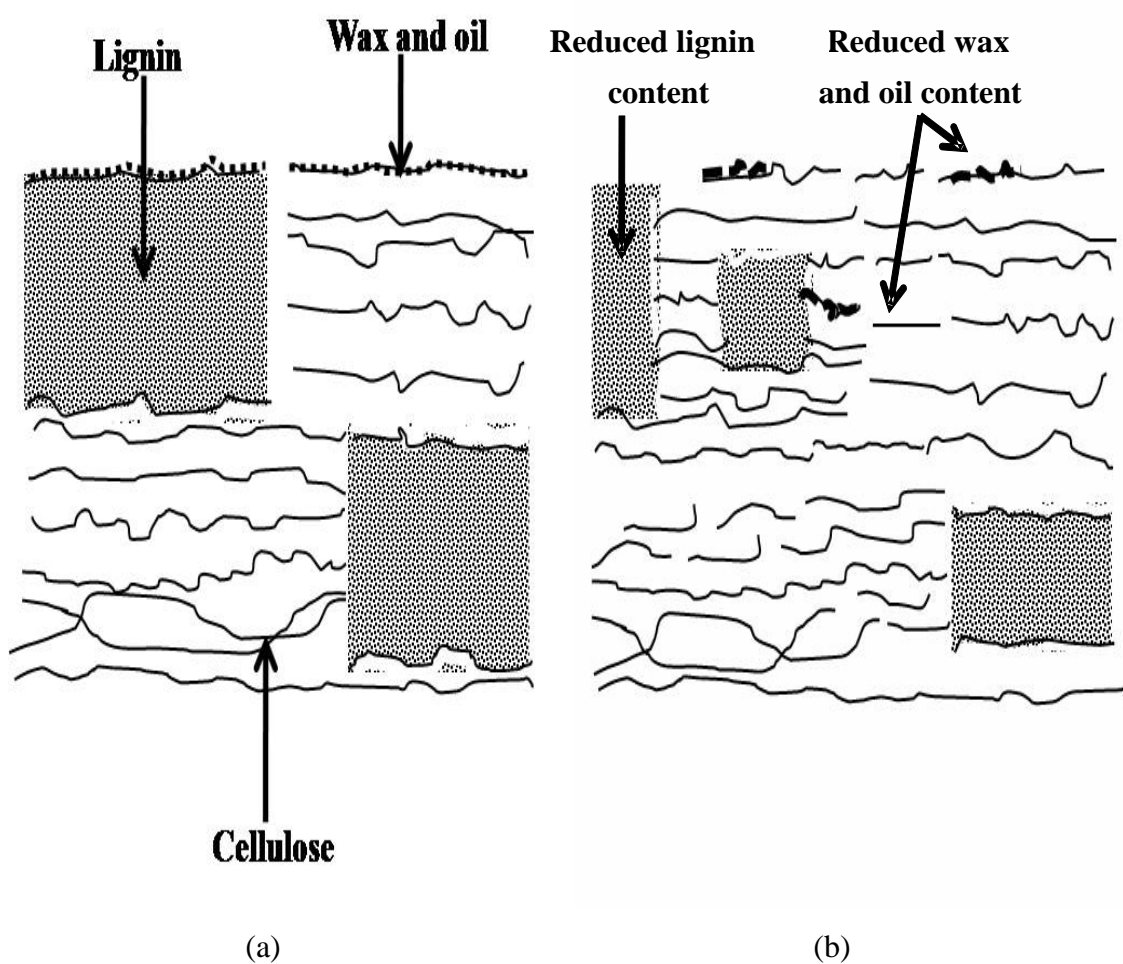
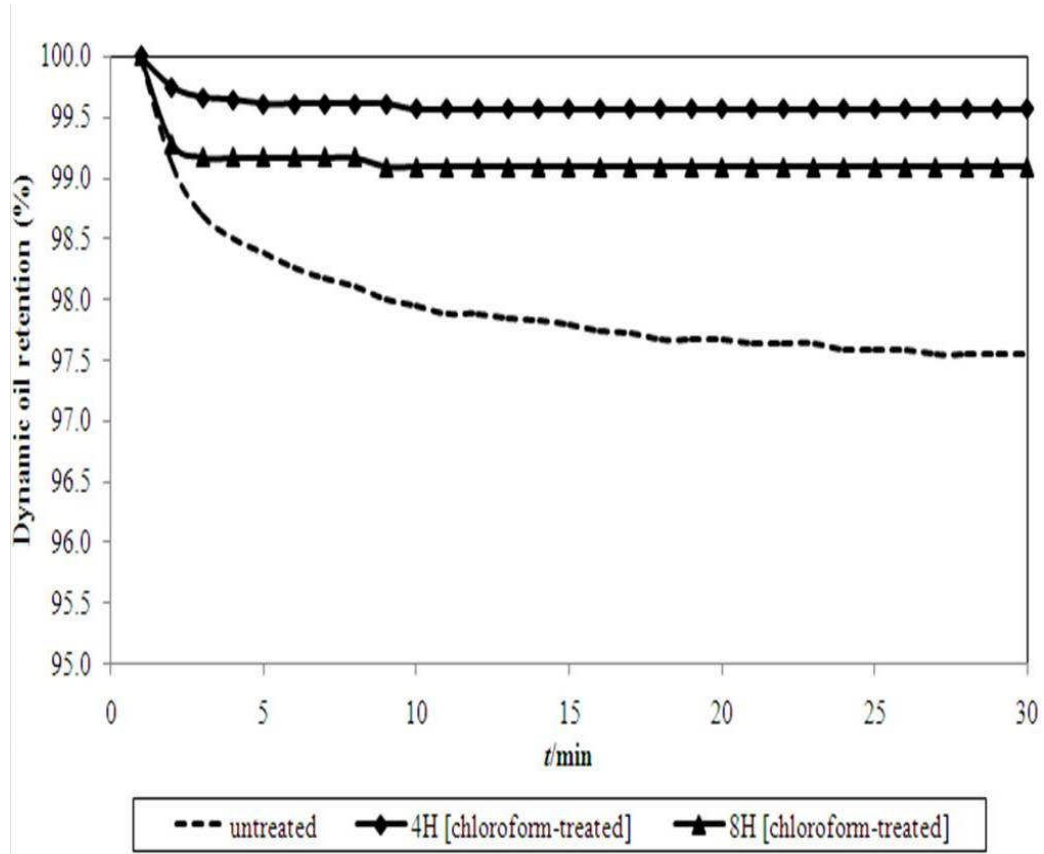


Figure 6.5 Typical structure of (a) untreated and (b) alkalinized cellulosic fiber

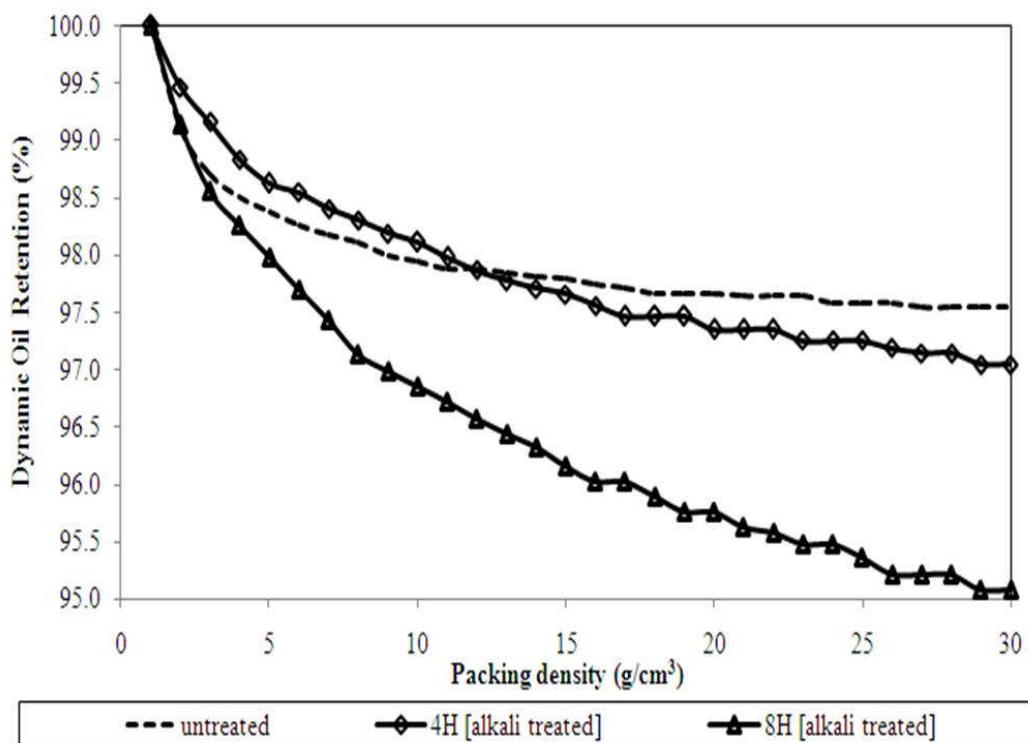
6.2.2 Percentage of dynamic oil retention

Figure 6.6a shows that after chloroform treatment, the oil retention capacity was increased slightly by 2 and 1.5 % after 4 and 8 hours extraction, respectively. The oil draining out from the extra-lumen liquids is lesser possibly due to the reduced amount of wax surface. Other study has reported the reduction of oil and water retention capacity by 48.9 and 9.1 % [2], respectively. However the study is for the use of kapok for oily water mixture and not applied on pure oil bath. Wax removal causes the kapok fibre to become more hydrophilic, thus creating a more competitive condition for water and oil to penetrate inside kapok structure from oily water mixture. Hence in this study for kapok as deep filter media for treating 2.5% diesel-water mixture, the oil retention capacity of chloroform treated kapok is reduced significantly [2].

The oil retention capacity for 4 hours alkali-treatment was not significantly different from untreated kapok, but was reduced with 8 hours treatment. For alkali-treated kapok, most of the wax could have been removed from its surface resulting in lower oil retention capacity. The presence of wax on the kapok surface caused the tubular structure to provide sufficient capillary pressure that can hold up the absorbed oil. Once most of the wax removed, the capillary pressure inside the tubular structure is reduced. This could cause higher amount of oil dripping out from the kapok assembly and oil retention capacity reduced. About 0.5 and 2.5 % of oil retention capacity reduction was obtained, for kapok treated at 4 and 8 hours respectively (Figure 6.6b)



(a)



(b)

Figure 6.6 Oil retention profile kapok after (a) chloroform and (b) alkali treatment

6.3 Conclusions

Chloroform and alkali treatments were applied for 4 and 8 hours duration to study the effect on kapok oil sorption characteristics. The infrared spectra of chloroform and alkali-treated kapok showed the increment of percentage transmittance band which correlated well with the wax removal from the kapok surface. SEM and morphological analyses suggest no significant difference of kapok microstructure after and before chloroform treatment. However, for alkali treatment, almost complete structural disruption of kapok microstructure was observed. The brown appearance of alkali-treated kapok possibly indicated the removal of hemicellulose and lignin. Significantly lower oil sorption capacity of 26.5 % reduction was observed for 8 hours alkali treatment as compared to the untreated-kapok.

The physical configuration, such as the presence of hollow structure appears to play more significant role in the performance of kapok as oil sorbent rather than the wax layer per se that covers the fiber surface. As long as the hollow structures of kapok remain intact throughout the experiment, kapok has retained its excellent capability as oil sorbent. However, increased removal of wax together with the collapse of rigid, hollow structure could reduce the oil sorption capability and on the other hand may increase kapok hydrophilicity. These results suggest that extreme conditions must be applied to remove most of the wax attached on the kapok surface and to disrupt the kapok hollow structure implying their rigid structure and high stability for prolonged use.

CHAPTER SEVEN

CONCLUSION AND RECOMMENDATION

7.1 Conclusions

The potential of *Ceiba pentandra* (L.) Gaertn. as an oil removal has been investigated based on the physicochemical properties and the process design parameters. Kapok surface has low contact angle and surface tension values with the experimental oils which suggest oil as wetting liquid for kapok. Diesel has the lowest density and viscosity, followed by new engine oil and used engine oil.

Higher packing density has lower sorption capacity but higher percentage of dynamic oil retention. The percentage of dynamic oil retention was in the decreasing order of: used engine oil, new engine oil and diesel. At higher oil viscosity and packing density, higher saturation time and lower bed height reduction were observed. After fifteen cycles of reuse, kapok only lost 30% of its initial oil sorption capacity. At 0.08 g/cm³ packing density, more than 90% of oil still retained inside the kapok assembly. These results imply the excellent properties of Malaysian kapok as oil sorbent that has high oil sorption and oil retention capacity which also stable for prolonged use.

Infrared spectrum shows that raw kapok is a lignocellulosic material with hydrophobic waxy coating. After chloroform and alkali treatment, the increment of several transmittance bands that correlated with the removal of plant wax, were observed. No significance difference was observed from the SEM and micrographic analyses of chloroform-treated kapok. However, alkali-treated kapok experienced almost complete the structural disruption of kapok microstructure. About 26.5 % reduction of oil sorption capacity of kapok was resulted after 8 hours of alkali treatment. Insignificant of oil sorption and oil retention capacity differences were observed for kapok after chloroform treatment. These studies confirmed that kapok fibre hollow structure and wax surface would be conserved during the entire oil sorption process.

The performance of kapok fiber for oily water filtration was investigated using a custom-made deep-bed filtration column by varying packing densities and flow rate. The liquid front movement stages during the oily water filtration process can be divided into infiltration, separation, displacement and equilibrium stage. For all packing densities and flow rates, the COD reductions were above 99 %. About 97% turbidity reduction was observed at 0.08 g/cm^3 and 0.5 mL/h flow rate suggesting the capability of kapok to break down oil-water emulsion and at the end reduced the turbidity. The statistical analyses using two way factorial design suggested that the interaction of packing density and flow rate played significant role in turbidity reduction. While none of the factors play significant role in reducing the percentage of COD which may suggest other reason, the kapok chemical composition and structure interfere the final COD value. The excellent turbidity reduction could be due to the stronger interaction of kapok with oil which can break down oil-water emulsion.

7.2 Recommendations

Our study has proven the performance of kapok as a natural sorbent for oil removal and as a packed-bed system for oily water filtration. The conditions for large scale application of kapok filter need to be investigated further. These include the study on the engineering parameter, such as mixing, column height, column diameter and temperature to achieve the optimum condition for pilot plant scale. The study on field application should include the feasibility for both on-shore and off-shore remediation. The parameters include the optimum configuration such as mat, pad, booms and skimmer, and also the reusability for several cycles and prolonged use and versatile use for filtration of storm-water.

The results from the chloroform and alkali treatment of kapok gave preliminary insight the possible application of kapok fibre other than as an oil sorbent. With suitable chemical treatment, kapok fibre surfaces can be modified to further regulate the hydrophobicity and hydrophilicity. This could lead to the possibility of kapok as both the oil and heavy metal sorbent. The development in biomaterials science and engineering can be exploited to explore the potential of chemically-

modified kapok as composite material for application in car manufacturing, or as a scaffold in tissue engineering or as a receptor of elastase to enhance wound healing.

REFERENCES

1. Fingas, M., *Basics of oil spill cleanup*. 2000, New York: CRC Press.
2. Lim, T.T., and Huang, X., *Evaluation of hydrophobicity/oleophilicity of kapok and its performance in oily water filtration: Comparison of raw and solvent-treated fibers*. *Industrial Crops and Products*, 2007. **26**(2): p. 125-134.
3. Liu, D.H.F., and Liptak, B. G., *Wastewater Treatment*. Nature of Wastewater. 2000, USA: CRC Press.
4. Adebajo, M.O., Frost, R.L., Kloropogge, J.T., Carmody, S. and Kokot, S., *Porous materials for oil spill cleanup: a review synthesis and absorbing properties*. *Journal of Porous Materials*, 2003. **10**: p. 159-170.
5. Cambiella, A., Ortea, E., Rios, G., Benito, J. M., Pazos, C., and Coca, J., *Treatment of oil-water emulsions: Performance of a sawdust bed filter*. *Journal of Hazardous Materials*, 2006. **131**: p. 195-199.
6. Hori, K., Flavier, M.E., Kuga, S., Lam, T.B.T., and Iiyama, K., *Excellent oil absorbent kapok [Ceiba pentandra (L.) Gaertn.] fiber: fiber structure, chemical characteristics and applications*. *Journal of Wood Science*, 2000. **46**: p. 401-404.
7. Lim, T.T., and Huang, X., *In situ oil/water separation using hydrophobic-oleophilic fibrous wall: A lab-scale feasibility study for groundwater cleanup*. *Journal of Hazardous Materials*, 2006. **137**(2): p. 820-826.
8. Lim, T.T., and Huang, X., *Evaluation of kapok [Ceiba pentandra (L.) Gaertn.] as a natural hollow hydrophobic-oleophilic fibrous sorbent for oil spill cleanup*. *Chemosphere*, 2007. **66**(5): p. 955-963.
9. Mueller, J., Chen, Y., and Davis, R. H., *Crossflow microfiltration of oily water*. *Journal of Membrane Science*, 1997. **129**: p. 221-235.
10. *Environmental Quality (Sewage and Industrial Effluents) Regulations*, T.a.E. Ministry of Science, Editor. 1979: Kuala Lumpur.
11. Droste, R.J., *Theory and practice of water and wastewater treatment*. 1996, New York: John Wiley and Sons, Inc.
12. Pasila, A., *A biological oil adsorption filter*. *Marine Pollution Bulletin*, 2004. **49**: p. 1006-1012.
13. Johnson, R.F., Manjrekar, T. G., and Halligan, J. E. , *Removal of oil from water surfaces by sorption on unstructured fibers*. *Environmental Science and Technology*, 1973. **7**(5): p. 439-443.
14. Choi, H.M., and Moreau, J.P., *Oil sorption behavior of various sorbents studied by sorption capacity measurement and environmental scanning electron microscopy*. *Microscopy Research and Techniques*, 1993. **25**: p. 447-455.
15. Deschamps, G., Caruel, H., Borredon, M. E., Albasi, C., Riba, J. P., Bonnin, C., and Vignoles, C., *Oil removal from water by selective sorption on hydrophobic cotton fibers.2. Study of sorption parameters in dynamic mode*. *Environmental Science and Technology*, 2003. **37**: p. 5034-5039.
16. Deschamps, G., Caruel, H., Borredon, M. E., Albasi, C., Riba, J. P., Bonnin, C., and Vignoles, C., *Oil removal from water by selective sorption on hydrophobic cotton fibers.1. study of sorption properties and comparison with other cotton fiber-based sorbents*. *Environmental Science and Technology*, 2003. **37**: p. 1013-1015.

17. Huang, X., and Lim, T. T., *Perfomance and mechanism of hydrophobic-oleophilic kapok filter for oil/water separation*. Desalination, 2006. **190**: p. 295-307.
18. Khan, E., Virojnagud, W., and Ratpukdi, T., *Use of biomass sorbents for oil removal from gas station runoff*. Chemosphere, 2004. **57**: p. 681-689.
19. Kobayashi, Y., Matsuo, R., and Nishiyama, M., *Method for adsorption of oils*. 1977, Agency of Industrial Science & Technology (Tokyo, JA) Japanese Patent.
20. Lee, B., Han, J. S., and Rowell, R. M., *Oil sorption by lignocellulosic fibers*, in *Kenaf Properties, Processing and Products*, N.A. Reichart, and Sellers, T., Editor. 1999, Mississippi State University-Agro and Bio Engineering: Mississippi. p. 423-433.
21. Suni, S., Kosunen, A.-L., Hautala, M., Pasila, A., and Romantshuck, M., *Use a by-product of peat excavation, cotton grass fiber as a sorbent for oil-spills*. Marine Pollution Bulletin, 2004. **49**: p. 916-921.
22. Viraraghavan, T., and Mathavan, G. N., *Treatment of oil-in-water emulsions using peat*. Oil and Chemical Pollution, 1988. **4**: p. 261-280.
23. *Kapok*, in *The New Encyclopaedia Britannica*. 2002, Encyclopaedia Britannica, Inc.: Chicago. p. 732.
24. Environmental Technology, C. *Environment Canada 1999-2004 Sorbent Test Program*. 2004 September, 4, 2008 [cited 2008 August, 27]; Available from: <http://www.etc-cte.ec.gc.ca/databases/Sorbent/Default.aspx>.
25. Mwaikambo, L.Y., and Ansell, M. P., *The effect of chemical treatment on the properties of hemp, sisal, jute and kapok for composite reinforcement*. Die Angewandte Makromolekulare Chemie, 1999. **272**: p. 108-116.
26. Mwaikambo, L.Y., and Ansell, M. P., *Chemical modification of hemp, sisal, jute and kapok fibers by alkalization*. Journal of Applied Polymer Science, 2002. **84**: p. 2222-2234.
27. Doerr, J.W., *Oil spill response in the marine environment*. 1st ed. 1992, United Kingdom: Pergamon Press.
28. Schrader, E.L., *Remediation of floating, open water oil spills: comparative efficacy of commercially available polypropylene sorbent booms*. Environmental Geological and Water Science, 1991. **17**(2): p. 157-166.
29. Ahmad, A.L., Bathia, S., Ibrahim, N., and Sumathi, S., *Adsorption of residual oil from palm oil mill effluent using rubber powder*. Brazillian Journal of Chemical Engineering, 2005. **22**: p. 371-379.
30. Annuciado, T.R., Sydenstricker, T. H. D., and Amico, S. C., *Experimental investigation of various vegetable fibers as sorbent materials for oil spill*. Marine Pollution Bulletin, 2005. **50**(1340-1346).
31. Banerjee, S.B., Joshi, M. V., and Jayaram, R. V., *Treatment of oil spills using organo fly-ash*. Desalination, 2006. **195**: p. 32-39.
32. Bastani, D., Safekordi, A. A., Alihosseini, A., and Taghikhani, V., *Study of oil sorption by expanded perlite at 298.15K*. Separation and Purification Technology, 2006. **52**: p. 295-300.
33. Carmody, O., Frost, R., Xi, Y., and Kokot, S., *Adsorption hydrocarbon on organo-clays. Implication for oil spill remediation*. Journal of Colloid and Interface Science, 2007. **305**: p. 17-24.

34. Inagaki, M., Shibata, K., Setou, S., Toyoda, M., and Aizawa, J., *Sorption and recovery of heavy oils by expholiated graphite part III: Trials for practical applications*. Desalination, 2000. **128**: p. 219-222.
35. Inagaki, M., Konno, H., Toyoda, M., Moriya, K., and Kihara, T., *Sorption and recovery of heavy oils by using expholiated graphite part II: Recovery of heavy oils and recycling of expholiated graphite*. Desalination, 2002. **128**: p. 213-218.
36. Kumagai, S., Noguchi, Y., Kurimoto, Y., and Takeda, K., *Oil adsorbent produced by the carbonization of rice husks*. Waste Management, 2007. **27**(4): p. 554-561.
37. Rajakovic-Ognjagovic, V., Aleksic, G., and Rajakovic Lj., *Governing factors for motor oil removal from water with different sorption materials*. Journal of Hazardous Materials, 2007.
38. Teas, C., Kalligeros, S., Zanikos, F., Stournas S., Lois, E., and Anastopoulos G., *Investigation of the effectiveness of absorbent materials in oil spills clean up*. Desalination, 2001. **140**(3): p. 259-264.
39. Toyoda, M., Moriya, K., Aizawa, J., Konno, H., and Inagaki, M., *Sorption and recovery of heavy oils by using expholiated graphite part I: Maximum sorption capacity* Desalination, 2000. **128**: p. 205-211.
40. Toyoda, M., Nishi, Y., Iwashita, N., and Inagaki, M., *Sorption and recovery of heavy oils by expholiated graphite part IV: Discussion of high oil sorption of expholiated grahite*. Desalination, 2002. **151**: p. 139-144.
41. Lee, B., Han, J.S., and Rowell, R.M., *Oil sorption by lignocellulosic fibers*, in *Kenaf Propersties, Processing and Products*, S.T. Reichart N.A., Editor. 1999, Mississippi State University-Agro and Bio Engineering: Mississippi. p. 423-433.
42. Sayed, S.A., and Zayed, A.M., *Investigation of the effectiveness of some adsorbent materials in oil spill clean-ups*. Desalination, 2000. **194**: p. 90-100.
43. Carmody, O., Frost, R., Xi, Y., and Kokot S., *Adsorption hydrocarbon on organo-clays. Implication for oil spill remediation* Journal of Colloid and Interface Science, 2007. **305**: p. 17-24.
44. Carmody, O., Frost, R., Xi, Y., and Kokot S., *Surface characterisation of selected sorbent materials for common hydrocarbon fuels*. Surface Science, 2007. **601**(2066-2076).
45. Wei, Q., Mather, R. R., Fortheringham, A. F., and Yang, R. D., *Evaluation of non woven polypropylene oil sorbents in marine oil-spill recovery* Marine Pollution Bulletin, 2003. **46**: p. 780-783.
46. Duong, H.T.T., and Burford, R. P., *Effect of Foam Density, Oil Viscosity, and Temperature on Oil Sorption Behavior of Polyurethane*. Journal of Applied Polymer Science, 2006. **99**: p. 360-367.
47. Kwon, O-J., Yang, S-R., Kim, D-H., and Park, J-S., *Characterization of polyurethanefoam prepared by using starch as polyol*. Jounal of Applied Polymer Science, 2006. **103**: p. 1544-1553.
48. Toyoda, M., Aizawa, J., and Inagaki, M., *Sorption and recovery of heavy oil by using exfoliated graphite*. Desalination, 1998. **115**: p. 199-201.
49. Zheng, Y.-P., Wang, H-N., Kang, F-Y., Wang, L-N., and Inagaki M., *Sorption capacity of exfoliated graphite for oils-sorption in and among worm-like particles*. Carbon, 2004. **42**: p. 2603-2607.
50. Payra, P., and Dutta, P.K., *Handbook of zeolite science and technology*. 2003, New York: Marcel Dekker Inc.

51. Sun, X.F., Sun, R. C., and Sun, J. X., *Acetylation of sugarcane bagasse using NBS as a catalyst under mild reaction conditions for the production of oil sorption-active mechanism*. Bioresource Technology, 2004. **95**: p. 90-100.
52. Mueller, J., and Riederer, M., *Plant surface properties in the chemical ecology*. Journal of Chemical Ecology, 2005. **31**: p. 2621-2651.
53. Wakelyn, P.J., and French, A.D., *Chemical composition of cotton*, in *Cotton Fiber, Chemistry and Technology*. 2007, CRC Press: New York.
54. Cohen, A.D., Rollins, M. S., Zunic, W. M., and Durig, J. R., *Effects of chemical and physical differences in peats on their ability to extract hydrocarbons from water*. Water Research, 1991. **25**(9): p. 1047-1060.
55. Smith, E.F., and Mark, H. B. Jr., *The use of modified forms of peat as an oil coalescer*. Journal of Environmental Science and Health, 1976. **12**: p. 727-734.
56. Mathavan, G.N., and Viraraghavan, T., *Coalescence/filtration of an oil-in-water emulsion in a peat bed*. Water Research, 1992. **26**(1): p. 91-98.
57. *Milkweed floss*, in *The Encyclopaedia Britannica*. 2003, Encyclopaedia Britannica, Inc.: Chicago. p. 130.
58. Rowell, R.M., Pettersen, R., Han, J.S., Rowell, J.S., and Tshabalala, M.A., *Cell wall chemistry*, in *Handbook of Wood Chemistry and Wood Composites*, R.M. Rowell, Editor. 2005, CRC Press: Florida.
59. Choi, H.M., and Cloud, R.M., *Natural sorbents for oil spill cleanup*. Environmental Science and Technology, 1992. **26**: p. 772-776.
60. Viswanath, D.S., Ghosh, T.K., Prasad, D.L., Dutt, N.K., and Rani, K.Y., *Viscosity of Liquid: Theory, Estimation, Experiment and Data*. 2007, Dordrecht, Nederland: Springer Verlag.
61. Noble, R.D., and Terry, P.A., *Principles of Chemical Separations with Environmental Application*. Cambridge Series in Chemical Engineering ed. A. Varma. 2004, Cambridge: Cambridge University Press.
62. ASTM1998c, *F726-99: Standard test method for sorbent performance of adsorbents*, in *Annual Book of ASTM Standards*. 1998, ASTM Committee on Standards: West Conshohocken, PA.
63. Boyles, W., *The science of chemical oxygen demand*, in *Technical Information Series*. 1997, Hach Company: USA.
64. Sincero, A.P., and Sincero, G.A., *Physical-chemical treatment of water and wastewater*. 2003, New York: CRC Press.
65. Sawyer, C.N., McCarty, P.L., and Parkin, G.F., *Chemistry for Environmental Engineering and Science*. 5th Edition ed. 2003, New York: McGraw Hill.
66. Choi H.M., M.J.P., *Oil sorption behavior of various sorbents studied by sorption capacity measurement and environmental scanning electron microscopy*. Microscopy Research and Techniques, 1993. **25**: p. 447-455.
67. Adebajo, M.O., and Frost, R. L., *Infrared and ¹³C MAS nuclear magnetic resonance spectroscopic study of acetylation cotton*. Spectrochimica Acta Part A, 2004. **60**(449-453).
68. Tserki, V., Zafeiropoulos, N. E., Simon, F., and Panayiotou, C., *A study the effect of acetylation and propionylation surface treatments on natural fibers*. Composites Part A: Applied Science and Manufacturing, 2005. **36**: p. 1110-1118.

69. Kaewprasit, C., Hequet, E., Abidi, N., and Gurlot, J.P., *Application of methylene blue adsorption to cotton fiber surface area measurement: Part I. Methodology*. The Journal of Cotton Science, 1998. **2**: p. 164-173.
70. Carmody, O., Frost, R., Xi, Y., and Kokot, S., *Surface characterisation of selected sorbent materials for common hydrocarbon fuels*. Surface Science, 2007. **601**: p. 2066-2076.
71. Schatzberg, P., *U.S.Coast Guard Report* U.S.C.G. Headquarters, Editor. 1971: Washington DC.
72. Haaland, P.D., *Experimental Design in Biotechnology*. 1989, New York: CRC Press.
73. Zhu, S., Wu, Y., Yu, Z., Liao, J., and Zhang, Y., *Pretreatment by microwave/alkali of rice straw and its enzymic hydrolysis*. Process Biochemistry, 2005. **40**: p. 3082-3086.